

Optimal control of geometric partial differential equations

Michael Hintermüller, Tobias Keil

submitted: August 2, 2019

Weierstrass Institute
Mohrenstr. 39
10117 Berlin
Germany
E-Mail: michael.hintermueller@wias-berlin.de,
tobias.keil@wias-berlin.de

No. 2612
Berlin 2019



2010 *Mathematics Subject Classification.* 49J20, 49K20, 35J87, 35Q93, 35Q35, 35R35, 90C33, 90C46, 76D45, 76T10, 65K10, 65K15.

Key words and phrases. Adaptive discretization, constraint degeneracy, diffuse interface model, electro-wetting on dielectric, geometric evolution, mathematical program with equilibrium constraints, multiphase fluids, numerical method, optimal control, sharp interface model, C stationarity conditions.

Edited by
Weierstraß-Institut für Angewandte Analysis und Stochastik (WIAS)
Leibniz-Institut im Forschungsverbund Berlin e. V.
Mohrenstraße 39
10117 Berlin
Germany

Fax: +49 30 20372-303
E-Mail: preprint@wias-berlin.de
World Wide Web: <http://www.wias-berlin.de/>

Optimal control of geometric partial differential equations

Michael Hintermüller, Tobias Keil

Abstract

Optimal control problems for geometric (evolutionary) partial differential inclusions are considered. The focus is on problems which, in addition to the nonlinearity due to geometric evolution, contain optimization theoretic challenges because of non-smoothness. The latter might stem from energies containing non-smooth constituents such as obstacle-type potentials or terms modeling, e.g., pinning phenomena in microfluidics. Several techniques to remedy the resulting constraint degeneracy when deriving stationarity conditions are presented. A particular focus is on Yosida-type mollifications approximating the original degenerate problem by a sequence of non-degenerate nonconvex optimal control problems. This technique is also the starting point for the development of numerical solution schemes. In this context, also dual-weighted residual based error estimates are addressed to facilitate an adaptive mesh refinement. Concerning the underlying state model, sharp and diffuse interface formulations are discussed. While the former always allows for accurately tracing interfacial motion, the latter model may be dictated by the underlying physical phenomenon, where near the interface mixed phases may exist, but it may also be used as an approximate model for (sharp) interface motion. In view of the latter, (sharp interface) limits of diffuse interface models are addressed. For the sake of presentation, this exposition confines itself to phase field type diffuse interface models and, moreover, develops the optimal control of either of the two interface models along model applications. More precisely, electro-wetting on dielectric is used in the sharp interface context, and the control of multiphase fluids involving spinodal decomposition highlights the phase field technique. Mathematically, the former leads to a Hele-Shaw flow with geometric boundary conditions involving a complementarity system due to contact line pinning, and the latter gives rise to a Cahn-Hilliard Navier-Stokes model including a non-smooth obstacle type potential leading to a variational inequality constraint.

Contents

1	Introduction	2
2	The sharp interface approach	5
2.1	Finite horizon model predictive control	7
2.1.1	Existence of solutions	7
2.1.2	Stationarity conditions	9
2.2	Numerical solution methods	10
2.2.1	Numerical solution algorithm	11
2.2.2	Numerical examples	12
3	The phase field approach	14
3.1	Phase field models	14
3.1.1	The free energy density and spinodal decomposition	18
3.1.2	The sharp interface limit and geometric flows	19
3.1.3	Incorporating hydrodynamic or surface effects	20
3.2	Existence of solutions	22

3.2.1	Discretization in time	23
3.2.2	Regularity of solutions	25
3.3	Optimal control of a phase field model	26
3.3.1	Stationarity conditions	27
3.4	Numerical solution methods	35
3.4.1	Adaptive mesh refinement techniques	35
3.4.2	Numerical solution algorithms	36
3.4.3	Numerical examples	37

1 Introduction

The interaction between partial differential equations and geometric analysis gives rise to a variety of challenging problems. In various application fields such as, e.g., materials science, biology, image processing or astrophysics, there are specific phenomena modeled by partial differential equations, where the behavior or the underlying domain is governed by some geometric quantities of interest. At the same time, the theory of partial differential equations has shown to be a powerful analytical tool for studying geometric and even topological properties, in particular, in situations, where the geometry is variable.

In many cases geometric partial differential equations describe the behavior of two or more coexisting immiscible phases (of underlying substances). This particularly requires a precise identification of the associated contact area, where the phases meet. This contact region is also called the phase boundary, boundary surface or interface. In general, the phase boundary is unknown and needs to be determined as a part of the solution of the system. Thus, the problem falls into the class of free boundary problems, cf. e.g. [31, 56, 141]. If the system depends on time, it is also referred to as moving boundary problem.

The motion of the phase boundary can be dictated 'implicitly' by a (system of) partial differential equation(s) on the bulk domains associated with the different phases (see e.g. [123]) and/or by requirements on or properties of the surface itself. The latter includes the important case of so-called surface partial differential equations, where additional partial differential equations have to be satisfied on the boundary surface. Since these partial differential equations have to be treated on an unknown domain, the analytical and numerical solution of these problems is quite challenging and has received a significant amount of research recently. On the other hand, if the evolution of the phase boundary depends on its geometry, we call the corresponding equation, which characterizes the geometric flow, a geometric evolution equation or surface evolution equation, cf. e.g. [64].

Traditionally, but not restrictively, these problems arise in material science, where the different phases correspond to different materials or different physical states of the same material. A typical example is the evolution of a solid-liquid configuration like melting or solidification processes, where we consider a domain $\Omega \subset \mathbb{R}^n$, with boundary $\partial\Omega$, filled with a material that is either in a solid state (on Ω^s) or a liquid state (on Ω^l). Starting from a given initial configuration Ω_0^s, Ω_0^l with the temperature profile $u_0 : \Omega \rightarrow \mathbb{R}$, one is interested in the evolution of the configuration over a time interval $(0, T)$.

In this example, depending on the temperature $u(x, t)$ at a point $x \in \Omega$ and time $t \in (0, T)$, the material might change its state (e.g. if the temperature drops below the freezing point), which causes a shift of the separation surface Γ between the solid phase and the liquid phase. Within the phases the temperature obeys some type of diffusion equation, e.g., the heat equation

$$u_t - \Delta u = f, \text{ on } \Omega \setminus \Gamma(t), \quad (1)$$

where $f : \Omega \times (0, T) \rightarrow \mathbb{R}$ represents a possible external heat source. However, the diffusion equation does not hold at the interface Γ . Instead, an additional condition determines the speed of

the solid-liquid interface based on the temperature evaluated at both sides of the phase boundary, which is typically derived from a conservation law, such as, e.g., the conservation of energy. The so-called Stefan condition

$$V - [\nabla u]_s^l \cdot \nu = 0, \text{ on } \Gamma(t) \quad (2)$$

relates the normal velocity V of the interface Γ to the jump of the temperature gradient ∇u from the solid towards the liquid phase denoted by $[\nabla u]_s^l$ and the unit normal ν of the interface pointing into the liquid phase. In combination with the initial data and suitable boundary conditions for the temperature, e.g.,

$$u = g, \text{ on } \partial\Omega \times (0, T), \quad (3)$$

with $g : \partial\Omega \times (0, T) \rightarrow \mathbb{R}$, problem (1)-(3) is called the Stefan problem, which is a classical model for phase transition processes, cf. e.g. [41, 123].

In practical applications it might be desirable to control the temperature profile of the configuration, for instance, by prescribing a specific temperature at the boundary, in order to achieve a desired distribution of the solid and liquid phases. In this context, g (boundary control) and/or f (distributed control) can be interpreted as controls of the system.

In the presence of undercooling or superheating effects, the model needs to be supplemented by the so-called Gibbs-Thomson law

$$u + V = H_\gamma, \text{ on } \Gamma(t), \quad (4)$$

which is derived from a thermodynamical equilibrium condition and acknowledges the effects of the surface tension of Γ . The latter may cause the temperature at the interface Γ to differ from the melting/freezing temperature. In (4), H_γ is an anisotropic mean curvature, which is a modification of the standard mean curvature - defined as the sum of the principal curvatures of γ - depending on the surface energy density γ , cf., e.g., [8].

In summary, the motion of the phase boundary Γ depends on its current geometry (i.e. its mean curvature) as well as the current temperature profile u , which relates to the solution of a partial differential equation on the complement of Γ . Note that the motion of Γ is uniquely determined by the normal velocity V . The strong correlation of the partial differential equation and the surface evolution equation complicates the analytical and numerical treatment of these types of problems. In general, classical solutions, where Γ and u (on each phase) are smooth, do not exist. However, various different methods have emerged to secure the existence of weak solutions, which can be shown to coincide with smooth hypersurfaces up to a precisely determined singular set. This is achieved by relying on variational methods, suitable time-discretization schemes, and/or the theory of minimal surfaces, where weak solutions are constructed as the boundary of sets with finite perimeters and measures supported on a countable union of Lipschitz graphs, see, e.g., [74].

Numerical solution algorithms are confronted with the demanding task to efficiently generate suitable meshes, which accurately track the motion of the interface Γ over time and capture possible topological changes, as the system is usually very sensitive with respect to the interface.

In the context of optimal control, these aspects become even more relevant, since we typically rely on some sensitivity and differentiability results for the associated control-to-state operator to characterize optimal solutions, e.g., by necessary first-order optimality conditions, and/or compute their finite-dimensional approximations. Since different controls usually lead to different evolutions of the interface, this motivates the task to derive qualitative statements on the change of the interface with respect to varying controls by, e.g., using topological derivatives.

In general, the choice of analytical and numerical tools depends primarily on the underlying representation of the interface. Here we mainly distinguish two different approaches: the sharp interface approach and the phase field (or diffuse interface) approach.

The sharp interface approach relies on a precise characterization of the hypersurface Γ as an object of lower dimension. The most common way is to describe the evolution of Γ with the help of a parametrization over a reference manifold $\hat{\Gamma}$.

For a vector field $\mathbf{u} : \hat{\Gamma} \rightarrow \mathbb{R}^n$ and a mapping $\mathbf{X}(\tau; \mathbf{u})(\cdot) : \hat{\Gamma} \rightarrow \mathbb{R}^n$ we characterize the interface at the time $\tau \geq 0$ by

$$\Gamma(\tau) = \mathbf{X}(\tau; \mathbf{u})(\hat{\Gamma}), \quad (5)$$

where the equation is evaluated for each $x \in \hat{\Gamma}$. Possible choices for the base manifold $\hat{\Gamma}$ can be the given surface Γ_0 of the initial configuration or a suitable topological object, e.g. a sphere, of the corresponding dimension. Moreover, u often times relates to a velocity field for the interface motion like

$$u = Vv, \quad (6)$$

such that \mathbf{X} is given by

$$\mathbf{X}(\tau; \mathbf{u})(\Gamma_0) = \Gamma_0 + \tau \mathbf{u}(\Gamma_0), \quad (7)$$

where '+' is understood in the sense that for $x \in \Gamma_0$, $\mathbf{X}(\tau; \mathbf{u})(x) = x + \tau \mathbf{u}(x)$.

Employing equation (5), we can relate geometrical quantities such as the mean curvature to the derivatives of the parametrization. As a consequence, the corresponding geometric evolution equations (e.g. (4)) can be transformed into nonlinear parabolic systems of partial differential equations for \mathbf{X} .

A special case of this approach is met when $\hat{\Gamma}$ denotes a subset of a hyperplane and the parametrization can be expressed by means of a smooth height function $\chi : \hat{\Gamma} \times [0, T) \rightarrow \mathbb{R}$ over $\hat{\Gamma}$. Then, we can represent the surface as a graph of the height function as follows

$$\Gamma(\tau) = \{(x, \chi(x, \tau)) \mid x \in \hat{\Gamma}\}, \quad (8)$$

and reformulate the surface evolution equation (4) as a nonlinear parabolic partial differential equation for χ .

In contrast to the general parametrization approach, where $\Gamma(\tau)$ does not necessarily correspond to the boundary of an open set and involve a more precise characterization of the associated bulk phases (e.g. Ω_s and Ω_l), the height function χ naturally divides the infinite cylinder $\hat{\Gamma} \times \mathbb{R}$ into the regions above and below the interface $\Gamma(\tau)$. As a consequence, the general approach can handle topological changes such as self-intersection of the interface Γ without producing singularities, whereas the graph representation strongly restricts the topology of the interface, which rules out many important applications.

Another method, the so-called level-set method, describes the interface implicitly as a zero level set of a higher dimensional function $\gamma : \mathbb{R}^{n+1} \times [0, T) \rightarrow \mathbb{R}$, i.e.

$$\Gamma(\tau) = \{x \in \mathbb{R}^{n+1} \mid \gamma(x, \tau) = 0\}, \quad (9)$$

see, e.g., [129]. In this setting, (4) translates to a nonlinear, degenerate and singular partial differential equation and the different phases (Ω_s and Ω_l) can be associated with the regions $\{x \in \mathbb{R}^{n+1} \mid \gamma(x, \tau) > 0\}$ and $\{x \in \mathbb{R}^{n+1} \mid \gamma(x, \tau) < 0\}$ in a natural way. In contrast to the graph representation, the level-set method can also model topological changes such as a split up of phases, which are usually related to local extrema of the level-set function γ .

The phase field approach differs from the previous methods in the sense that the interface is replaced by a interfacial band of arbitrarily small width. Similar to the level-set method, we rely on an auxiliary function $\varphi : \mathbb{R}^{n+1} \times [0, T) \rightarrow \mathbb{R}$ and identify the interface with the following region

$$\Gamma(\tau) = \{x \in \mathbb{R}^{n+1} \mid \psi_1 < \varphi(x, \tau) < \psi_2\}. \quad (10)$$

Accordingly, the bulk phases are represented by the sets

$$\{x \in \mathbb{R}^{n+1} | \varphi(x, \tau) = \psi_1\} \quad \text{and} \quad \{x \in \mathbb{R}^{n+1} | \varphi(x, \tau) = \psi_2\}.$$

However, instead of (4), the evolution of the phase boundaries is modeled with the help of a homogeneous energy function, which has local minima at ψ_1 and ψ_2 .

In this article, we discuss the advantages and disadvantages of both approaches, the sharp interface approach and the phase field approach, with respect to the optimal control of geometric partial differential equations at the hands of two examples. In Section 2, we study different approaches to the optimal control of sharp interface models, and elaborate on the existence of solutions and stationarity conditions in the context of electrowetting on dielectric. Moreover, we investigate corresponding numerical solution methods with respect to four different control objectives in Subsection 2.2. Section 3 is concerned with the optimal control of phase field models. We start with a short outline of the historical and physical background of these models and discuss the relation to sharp interface models. Then, we describe the analytical approaches to proof the existence and regularity of feasible and optimal points, followed by an investigation of stationarity concepts for the optimal control problems. Finally, Subsection 3.4 comments on numerical challenges and solvers, and provides some illustrating numerical examples.

2 The sharp interface approach

In this section, we discuss sharp interface models and the associated optimal control problems. These problems emerge in various situations, e.g., if one aims to eliminate the distortions connected to a thermal treatment of a workpiece during the manufacturing chain [134], control the solid-state dewetting of thin films on a flat substrate, [149], minimize the effects of the ramified growth of the electrode surface due to morphological instabilities during electrodeposition [111], or control melting and/or solidification processes such as lava evolution, casting and energy storage, see e.g. [103]

As mentioned above, sharp interface models usually describe the interface as a suitable manifold Γ . Typically, Γ corresponds to the boundary of an open set Ω , which constitutes the domain of a partial differential equation. In the presence of additional effects on the surface, the model is supplemented with (partial differential) equations which hold on the interface Γ .

In the following we exemplify the control of geometric evolution in the sharp interface context by means of an example application. The associated problem is interesting as it not only represents an optimal control problem for a geometric PDE (with control on the interface), but it also contains an additional non-smooth component in the interface condition. The latter gives rise to an optimization theoretic degeneracy which spoils the straight forward application of well-known optimization theory of Karush-Kuhn-Tucker (KKT) type as all available constraint qualifications for multiplier existence notoriously fail. Rather one is required to develop an approach which is capable of handling the degeneracy while still yielding sharp stationarity characterizations which may then serve as the starting point for the design of (numerical) solution algorithms. In case the reader wishes to understand the control of a geometric PDE without this degeneracy, then the nonsmooth term and the associated analytical treatment in our example application may be ignored. As a result, KKT theory becomes directly applicable for characterizing first-order optimality. The corresponding mathematical realization will, however, be left to the reader, but can be inferred from our more complex context.

Indeed, an important application which includes surface effects is the manipulation of fluids in digital microfluidic devices, e.g. via electrowetting on dielectric (EWOD), which is used, e.g., in lab-on-a-chip devices [66, 126], mass spectrometry [146], and electrofluidic displays [72]. Hereby, one influences the contact angle of a single droplet between two narrowly separated parallel plates where one of the plates contains an embedded grid of electrodes by applying voltages to the

electrodes on the grid, compare [37, 130]. Besides the partial differential equations, which ensure the conservation of momentum and the conservation of mass within the droplet, a proper EWOD model has to include a so-called “pressure boundary condition”, cf. [144], which describes the impact that boundary effects such as curvature of the droplet, the electrowetting force, or contact line pinning have on the pressure inside the droplet. Without these effects, the model fails to accurately capture the behavior of the droplet. In particular, numerical simulations of the droplets disregarding the pinning effect predict motions that are up to ten times faster than observed in the laboratory, cf. [144] and the references therein.

In [143, 144], the authors proposed the following time-discrete spatially-continuous sharp interface model for electrowetting on dielectric

$$\alpha \frac{\mathbf{u}^{i+1} - \mathbf{u}^i}{\delta t_{i+1}} + \beta \mathbf{u}^{i+1} + \nabla p^{i+1} = 0 \quad \text{in } \Omega^i, \quad (11a)$$

$$\operatorname{div} \mathbf{u}^{i+1} = 0 \quad \text{in } \Omega^i, \quad (11b)$$

$$p^{i+1} \mathbf{v}^i - \kappa^{i+1} \mathbf{v}^i - E^i \mathbf{v}^i - \lambda^{i+1} \mathbf{v}^i - D_{\text{visc}}(\mathbf{u}^{i+1} \cdot \mathbf{v}^i) \mathbf{v}^i = 0 \quad \text{on } \Gamma^i, \quad (11c)$$

$$\lambda^{i+1} - P_{\text{pin}} \partial \left(\|\cdot\|_{L^1(\Gamma^i)} \right) (\mathbf{u}^{i+1} \cdot \mathbf{v}^i) \ni 0 \quad \text{on } \Gamma^i. \quad (11d)$$

Here, the time interval $(0, T)$ is partitioned into intervals of length $\delta t_i > 0$. Moreover \mathbf{u}^i and p^i denote the fluid velocity and the pressure, and the constants $\alpha \ll \beta$ are non-dimensional material and geometry constants associated with the underlying device and $D_{\text{visc}}, P_{\text{pin}} > 0$ are contact-line friction coefficients.

The flow within the droplet domain Ω^i at time t^i is based on the classical conservation laws (11a) and (11b). In addition, the pressure at the boundary $\Gamma^i := \partial\Omega^i$ of the droplet is affected by the curvature κ^i , the electrowetting forcing term E^i , the pinning variable λ^i , and viscosity via (11c) and (11d). More precisely, the inclusion (11d) results from differentiating (in the sense of convex analysis) the non-smooth term $\|\cdot\|_{L^1(\Gamma^i)}$ and, physically, it relates to the fact that a certain resistance threshold must be overcome in order for the droplet to move. Otherwise, the molecular adhesion at the solid-liquid-air interface of the droplet and contact angle hysteresis hold the droplet in place, which leads to the aforementioned deceleration of the motion of the droplet, cf. [122, 144]. The approximate curvature term κ^{i+1} is defined by

$$\kappa^{i+1} \cdot \mathbf{v}^i(\cdot) := -\Delta_{\Gamma^i} \operatorname{id}(\cdot) - \delta t_{i+1} \Delta_{\Gamma^i} \mathbf{u}^{i+1}(\cdot), \quad (12)$$

where id represents the identity mapping and Δ_{Γ^i} denotes the Laplace-Beltrami operator on Γ^i ; see, e.g., [47] for a definition.

The system (11) is coupled with the subsequent interface evolution equation of type (7)

$$\Gamma^{i+1} := \mathbf{X}^{i+1}(\delta t_{i+1})(\Gamma^i) := \Gamma^i + \delta t_{i+1} \mathbf{u}^{i+1}(\Gamma^i), \quad (13)$$

which involves the velocity \mathbf{u}^{i+1} (defined on Γ^i) at time t_{i+1} . Ideally, one would like to prescribe the motion of the droplet by adjusting the electrowetting forcing terms E^i , $i = 1, \dots, K$, over the entire time interval $(0, T)$ accordingly.

Unfortunately, the optimal control of sharp interface models such as given by the system (11)-(13) becomes very challenging, due to the dependencies of the operators, the underlying spaces, and the solutions on the interfaces. Without further restrictive assumptions or additional constraints, one might not even be able to prove the existence of an optimal control $\mathbf{E} := (E^1, \dots, E^K)$. Furthermore, from a numerical standpoint, this comprehensive constraint system would imply substantial computational effort, assuming the problem is even tractable.

There are various approaches to handle these difficulties. If the free boundary allows for a graph representation, e.g., of the form (8), the optimal control problem can be simplified by appropriately reformulating it, see, e.g., [10, 11, 45, 94, 95]. Another way is to treat the free boundary implicitly, compare [13, 125]. A shape optimization perspective to (geometric) complementarity

problems has been investigated in [86, 87, 89]. Recently, a parameter identification problem in the study of cell motility with both sharp and diffuse interface formulations was considered in [42] and droplet footprint control via surface tension in [102]. We also mention [110], in which shape sensitivity analysis and control for time-dependent shapes with PDE-constraints is considered.

2.1 Finite horizon model predictive control

Complementing the aforementioned techniques, in this subsection we present a more tractable approach inspired by finite horizon model predictive control [60] to deal with the analytical and numerical challenges. To the best of our knowledge, this is the only method for the (suboptimal) control of a geometric partial differential equation (PDE) coupled with an equilibrium or complementarity condition (such as the pinning constraint (11d)), which has been investigated in the literature up to this point.

In order to describe the basic idea behind model predictive control in the current setting, we denote the control space at time t_i by \mathcal{E}^i and the remaining variables $z = (\mathbf{u}, p, \lambda)$ lie in the space \mathcal{Z}^i . Moreover, \mathcal{J}^i represents a compatible objective function, $\mathcal{E}_{ad}^i \subset \mathcal{E}^i$ is the constraint set for the controls and Ω^i is the given droplet domain at time t_i with sufficiently smooth boundary Γ^i . In addition, the current velocity field \mathbf{u}^i and the time step size δt_{i+1} are known.

Then, we compute the optimal control E^i at the given time step by (approximately) solving the minimization problem

$$\min \mathcal{J}^i(E, z) \text{ over } (E, z) \times \mathcal{E}_{ad}^i \times \mathcal{Z}^i : (E, z) \text{ satisfies (11), (12)} \quad (\text{P})$$

by a descent method. After successfully computing an approximate solution of (P), the boundary Γ^i is evolved according to the new velocity field via (13) and we proceed to the next time step.

The optimal control problem (P) is a challenging problem in its own right. In particular, the presence of the subdifferential inclusion (11d) means that we are still tasked with solving a so called mathematical program with equilibrium constraints (MPEC) in function space; see [84] for more on this problem class in a non-geometric context. In the following, we briefly outline the theory and numerics for one time step before passing to the evolution in time.

We point out that a more detailed discussion of mathematical programs with equilibrium constraints and the associated difficulties in the context of the optimal control of phase field models can be found in the subsequent Section 3.

2.1.1 Existence of solutions

We start by formulating the distributional form of (11),(12). For this purpose, we subsequently introduce the relevant notation and function spaces. For the sake of readability, we henceforth leave off the superscripts i . Given an (open bounded) droplet domain Ω with smooth boundary Γ , we let \mathbb{V} be the closure of $C^\infty(\overline{\Omega}; \mathbb{R}^n)$ with respect to the norm

$$\|\mathbf{v}\|_{\mathbb{V}} := \left(\|\mathbf{v}\|_{H(\text{div}; \Omega)}^2 + \delta t_i \|\nabla_{\Gamma} \mathbf{v}\|_{L^2(\Gamma; \mathbb{R}^n)}^2 \right)^{\frac{1}{2}}.$$

Then we define the subspace space \mathbb{V}_{sol} of solenoidal functions as follows

$$\mathbb{V}_{\text{sol}} := \{ \mathbf{v} \in \mathbb{V} \mid \mathbf{B}\mathbf{v} = 0 \}.$$

Moreover, we let \mathcal{E}_{ad} be a non-empty, closed, convex subset of $\mathcal{E} := L^2(\Gamma)$, and define the bounded linear operators $A : \mathbb{V}_{\text{sol}} \rightarrow \mathbb{V}_{\text{sol}}^*$, $C : \mathbb{V}_{\text{sol}} \rightarrow L^2(\Gamma)$, $F_0 : \mathcal{E} \rightarrow \mathbb{V}_{\text{sol}}^*$ and the continuous

affine mapping $F : \mathcal{E} \rightarrow \mathbb{V}_{\text{sol}}^*$ by

$$\begin{aligned} \langle A\mathbf{u}, \mathbf{v} \rangle &:= \left(\frac{\alpha}{\delta t_{i+1}} + \beta \right) (\mathbf{u}, \mathbf{v})_{L^2(\Omega; \mathbb{R}^n)} + D_{\text{visc}}(\mathbf{u} \cdot \mathbf{v}, \mathbf{v} \cdot \mathbf{v})_{L^2(\Gamma)} \\ &\quad + \delta t_{i+1} (\nabla_{\Gamma} \mathbf{u}, \nabla_{\Gamma} \mathbf{v})_{L^2(\Gamma; \mathbb{R}^n)}, \\ \langle C\mathbf{u}, \boldsymbol{\mu} \rangle &:= (\mathbf{u} \cdot \mathbf{v}, \boldsymbol{\mu})_{L^2(\Gamma)}, \quad \langle F_0(E), \mathbf{v} \rangle := -(E, \mathbf{v} \cdot \mathbf{v})_{L^2(\Gamma)}, \\ \langle F(E), \mathbf{v} \rangle &:= \frac{\alpha}{\delta t_{i+1}} (\mathbf{u}, \mathbf{v})_{L^2(\Omega; \mathbb{R}^n)} + \langle F_0(E), \mathbf{v} \rangle - (\nabla_{\Gamma} \mathbf{X}^{i+1}(0), \nabla_{\Gamma} \mathbf{v})_{L^2(\Gamma; \mathbb{R}^n)}. \end{aligned}$$

Here, the definitions of $\langle \cdot, \cdot \rangle$ and the test functions should be clear in context. In addition, we introduce $\varphi : \mathbb{V}_{\text{sol}} \rightarrow \mathbb{R}$ by

$$\varphi(\mathbf{u}) := P_{\text{pin}}(\|\cdot\|_{L^1(\Gamma)} \circ C)(\mathbf{u}), \quad \mathbf{u} \in \mathbb{V}_{\text{sol}}.$$

Using these operators and function spaces, the weak form of (11),(12) can be stated as follows, cf. [9],

$$A\mathbf{u} + \partial\varphi(\mathbf{u}) \ni F(E). \quad (14)$$

Hence, we can reformulate the control problem (P) as follows

$$\begin{aligned} \min \quad & \widehat{\mathcal{J}}(E, \mathbf{u}) \text{ over } (E, \mathbf{u}) \in \mathcal{E} \times \mathbb{V}_{\text{sol}} \\ \text{s.t.} \quad & A\mathbf{u} + \partial\varphi(\mathbf{u}) \ni F(E), \quad E \in \mathcal{E}_{\text{ad}}. \end{aligned} \quad (15)$$

Note that, due to (14), both the pressure variable p and the pinning variable λ become implicit. Therefore, we henceforth consider the reduced objective functional $\widehat{\mathcal{J}}(E, \mathbf{u})$ rather than $\mathcal{J}(E, z)$. Unless otherwise noted, we assume that the objective $\widehat{\mathcal{J}} : \mathcal{E} \times \mathbb{V}_{\text{sol}} \rightarrow \mathbb{R}$ is continuously Fréchet differentiable and the set of admissible controls \mathcal{E}_{ad} is nonempty, closed, convex and bounded.

In order to provide a basic existence theorem for (15), we additionally assume that $\widehat{\mathcal{J}}$ satisfies the usual assumptions needed to obtain the existence of a minimizer.

Theorem 1 (Existence of solutions) *Let $\widehat{\mathcal{J}} : \mathcal{E} \times \mathbb{V}_{\text{sol}} \rightarrow \overline{\mathbb{R}}$ be bounded from below, weakly lower-semicontinuous in \mathcal{E} /strongly lower-semicontinuous in \mathbb{V}_{sol} , and either \mathcal{E}_{ad} is bounded or $\widehat{\mathcal{J}}$ is partially coercive with respect to \mathcal{E}_{ad} , i.e., for every sequence $(E_k, \mathbf{u}_k) \in \mathcal{E} \times \mathbb{V}_{\text{sol}}$ with $\|E_k\|_{\mathcal{E}} \rightarrow \infty$ it holds that $\widehat{\mathcal{J}}(E_k, \mathbf{u}_k) \rightarrow \infty$.*

Then there exists a minimizer $(E, \mathbf{u}) \in \mathcal{E}_{\text{ad}} \times \mathbb{V}_{\text{sol}}$ of (15).

Since A is a coercive symmetric bounded linear operator, and therefore strongly monotone, and $\partial\varphi$ is a maximal monotone operator defined on the real Hilbert space \mathbb{V}_{sol} , the operator $A + \partial\varphi$ is surjective, see e.g., [29, Theorems 2, 2'] or [120, 121]. Moreover, one can either apply a classical result of Minty [108], see e.g., [148, Theorem 26.A], or standard arguments from variational inequalities, see e.g., the well-known monograph [100], to demonstrate that the solution operator $\widehat{\Phi} := (A + \partial\varphi)^{-1}$, with $\widehat{\Phi} : \mathbb{V}_{\text{sol}}^* \rightarrow \mathbb{V}_{\text{sol}}$, is Lipschitz continuous. Furthermore, as F is a continuous affine operator, the mapping $\Phi := \widehat{\Phi} \circ F$ is Lipschitz continuous from \mathcal{E} into \mathbb{V}_{sol} . Therefore, the reduced objective $\mathcal{J}(E) := \widehat{\mathcal{J}}(E, \Phi(E))$ is weakly lower-semicontinuous in E . This allows us to rewrite the MPEC (15) in reduced form as

$$\min \mathcal{J}(E) \text{ over } E \in \mathcal{E}_{\text{ad}}. \quad (16)$$

Then the existence of optimal points follows via a standard application of the direct method of calculus of variations.

2.1.2 Stationarity conditions

In this subsection, we present primal-dual stationarity conditions for (15). In order to cope with the constraint degeneracy, caused by the pinning condition, a regularization procedure is applied, exploiting techniques from PDE-constrained optimization. More precisely, the derivation is based on several approaches found in the optimal control of elliptic variational inequalities, i.e., another class of MPECs in function space. In particular, we mention the monograph by Barbu [13] for regularization approaches and [84, 85] for efficient numerical methods and relevant stationarity concepts.

For the formulation of stationarity conditions we define the “strongly active sets” $\mathcal{A}^+, \mathcal{A}^- \subset \Gamma$ and the “weakly active/biactive sets” $\mathcal{B}^+, \mathcal{B}^- \subset \Gamma$ at \mathbf{u} (with associated λ as in (11d)) by

$$\begin{aligned}\mathcal{A}^+ &:= \{s \in \Gamma \mid \lambda(s) = P_{\text{pin}}, (\mathbf{C}\mathbf{u})(s) > 0\}, \\ \mathcal{B}^+ &:= \{s \in \Gamma \mid \lambda(s) = P_{\text{pin}}, (\mathbf{C}\mathbf{u})(s) = 0\}, \\ \mathcal{A}^- &:= \{s \in \Gamma \mid \lambda(s) = -P_{\text{pin}}, (\mathbf{C}\mathbf{u})(s) < 0\}, \\ \mathcal{B}^- &:= \{s \in \Gamma \mid \lambda(s) = -P_{\text{pin}}, (\mathbf{C}\mathbf{u})(s) = 0\}.\end{aligned}$$

Then the “inactive set” is given by $\mathcal{I} := \Gamma \setminus (\mathcal{A}^+ \cup \mathcal{A}^- \cup \mathcal{B}^+ \cup \mathcal{B}^-)$.

Theorem 2 (Stationary Points) *Assume that $\partial \widehat{\mathcal{J}} : \mathcal{E} \times \mathbb{V}_{\text{sol}} \rightarrow \mathcal{E}^* \times \mathbb{V}_{\text{sol}}^*$, where $\partial \widehat{\mathcal{J}} = (\partial_E \widehat{\mathcal{J}}, \partial_{\mathbf{u}} \widehat{\mathcal{J}})$, is bounded. Let (E^*, \mathbf{u}^*) be a (locally) optimal solution of (15). Furthermore, let $\mathcal{A}_* := \mathcal{A}_*^+ \cup \mathcal{A}_*^-$ denote the strongly active set associated with (E^*, \mathbf{u}^*) .*

Then there exists an adjoint state $\mathbf{w}^ \in \mathbb{V}_{\text{sol}}$, and $m^*, \mathcal{J}_{\mathbf{u}}^* \in \mathbb{V}_{\text{sol}}^*$, and some sequences*

$$E_k \xrightarrow{\mathcal{E}} E^*, \quad \mathbf{u}_k \xrightarrow{\mathbb{V}_{\text{sol}}} \mathbf{u}^*, \quad \mathbf{w}_k \xrightarrow{\mathbb{V}_{\text{sol}}} \mathbf{w}^*, \quad m_k \xrightarrow{\mathbb{V}_{\text{sol}}^*} m^*, \quad \text{as } k \rightarrow +\infty,$$

such that $\partial_{\mathbf{u}} \mathcal{J}(E_{k_l}, \mathbf{u}_{k_l}) \xrightarrow{\mathbb{V}_{\text{sol}}^*} \mathcal{J}_{\mathbf{u}}^*$ and

$$A^* \mathbf{w}^* + P_{\text{pin}} m^* = -\mathcal{J}_{\mathbf{u}}^*, \quad (17)$$

$$\liminf_{k \rightarrow +\infty} \langle m_k, \mathbf{w}_k \rangle \geq 0, \quad (18)$$

$$\liminf_{k \rightarrow +\infty} \langle \partial_E \mathcal{J}(E_k, \mathbf{u}_k) - F_0^* \mathbf{w}_k, E - E_k \rangle \geq 0, \quad \forall E \in \mathcal{E}_{\text{ad}}, \quad (19)$$

$$\lim_{k \rightarrow +\infty} \int_{\{s \in \Gamma \mid (\mathbf{C}\mathbf{u}_k)(s) = 0\}} |(\mathbf{C}\mathbf{w}_k)(s)|^2 ds = 0. \quad (20)$$

Moreover, for all $\varepsilon > 0$, there exists a Lebesgue measurable set $\mathcal{A}_*^\varepsilon \subset \mathcal{A}_*$ with $|\mathcal{A}_*^\varepsilon| \leq \varepsilon$ such that

$$0 = \langle m^*, \mathbf{v} \rangle, \quad \forall \mathbf{v} \in \mathbb{V}_{\text{sol}} : \mathbf{C}\mathbf{v} = 0, \quad \text{a.e. on } \{s \in \Gamma \mid (\mathbf{C}\mathbf{u}^*)(s) = 0\} \cup \mathcal{A}_*^\varepsilon. \quad (21)$$

Condition (21) is the infinite-dimensional analog of the finite-dimensional condition where the multiplier $m^* = 0$ on the inactive set. Together with (17)-(20), the entire system constitutes a weak form of limiting ε -almost C -stationarity, see [91, 92]. In the case when there exists some function μ^* such that $m^* = C^* \mu^*$, then it would result in limiting ε -almost C -stationarity.

For a rigorous derivation of the above theorem we refer to [9].

Under additional compactness assumptions on the gradient of the objective functional $\widehat{\mathcal{J}}$ or if the control space \mathcal{E} is not finite dimensional, the system (17)-(19) can be further refined. For instance, let H be a Hilbert space, let $L : \mathbb{V}_{\text{sol}} \rightarrow H$ be a compact bounded linear operator, and let $\widehat{\mathcal{J}} : \mathcal{E} \times \mathbb{V}_{\text{sol}} \rightarrow \mathbb{R}$ be given by

$$\widehat{\mathcal{J}}(E, \mathbf{u}) := \frac{1}{2} \|\mathbf{L}\mathbf{u} - u_b\|_H^2 + \frac{\mathbf{v}}{2} \|E\|_{\mathcal{E}}^2,$$

where $\mathbf{v} > 0$ and $u_b \in H$.

Then the system (17)-(19) can be transformed into

$$A^* \mathbf{w}^* + P_{\text{pin}} m^* = L^*(u_b - L\mathbf{u}^*), \quad (22a)$$

$$\langle m^*, \mathbf{w}^* \rangle \geq 0 \quad (22b)$$

$$\langle \nu E^* - F_0^* \mathbf{w}^*, E - E^* \rangle \geq 0, \forall E \in \mathcal{E}_{ad}. \quad (22c)$$

This concludes our analytical investigations of the control problem (15). In the sequel, we discuss an algorithm for the numerical realization of a strategy for (suboptimally) solving the optimal control of the EWOD model (11).

2.2 Numerical solution methods

Similar to the analysis, there are various approaches to solve optimal control problems associated with sharp interface models numerically, e.g. depending on the chosen representation of the interface. Whether a method is preferable over others strongly depends on the actual application and the corresponding model, e.g., the (system of) partial differential equations, the underlying domain, etc.

Another important factor is the objective functional of interest. Here, we present four possible choices in the context of the control problem of the previous subsection following the finite horizon model predictive control approach.

1 Barycenter Matching:

$$\mathcal{J}^{i+1}(\mathbf{u}, E) = \frac{1}{2} \left\| \frac{1}{|\Omega^i|} \int_{\Omega^i} (x + \delta t_{i+1} \mathbf{u}(x)) dx - \mathbf{b}_d \right\|_{\mathbb{R}^2}^2 + \frac{\zeta}{2} \|E\|_{\mathcal{E}}^2$$

The integral expression is applied componentwise, which yields a vector in \mathbb{R}^2 . Moreover, \mathbf{b}_d represents the coordinates of the desired barycenter at the final time step. Hence, \mathbf{b}_d does not change at each time step.

The objective additionally includes a penalization of the cost of the control E with parameter $\zeta > 0$. In the numerical experiments presented below, the Tikhonov parameter was set to $\zeta := 1e-8$.

2 Barycenter Tracking: The only difference to the previous functional is that \mathbf{b}_d is replaced by a \mathbf{b}_d^{i+1} , where $(\mathbf{b}_d^1, \dots, \mathbf{b}_d^T)$ represents a trajectory of desired barycenters.

The barycenter functionals have the advantage of not relying on information concerning the specific shape of the interface Γ . For droplets that are slightly larger than the size of the individual electrodes on the surface of the EWOD device, these are useful objectives. In this case the effect of the surface tension on the droplet should somewhat inhibit topological changes.

3 Matching the Shape of an Ideal Droplet

$$\mathcal{J}^{i+1}(\mathbf{u}, E) = \frac{1}{2} \|\text{id}(\cdot) + \delta t \mathbf{u}(\cdot) - \mathbf{X}_d^{i+1}(\cdot)\|_{L^2(\Gamma^i)}^2 + \frac{\zeta}{2} \|E\|_{\mathcal{E}}^2$$

Hereby, $\mathbf{X}_d^{i+1}(\cdot)$ is a closed curve in \mathbb{R}^2 that represents a desired droplet shape at time i . For this purpose, one assumes that \mathbf{X}_d^{i+1} have parameterizations of the form $(x_1(s), x_2(s))$ and $(x_1^d(s), x_2^d(s))$ $s \in [0, 1]$, respectively, and one considers the first term in the objective as follows:

$$\frac{1}{2} \sum_{j=1}^2 \int_0^1 (x_j(s) + \delta t_{i+1} (\mathbf{u} \circ (x_1, x_2))(s) \cdot \mathbf{e}_j - x_j^d(s))^2 ds,$$

where $\mathbf{e}_1, \mathbf{e}_2$ are the standard basis vectors of \mathbb{R}^2 . In the experiments highlighted below $\mathbf{X}_d^{i+1} := \mathbf{X}_d$, where \mathbf{X}_d is some ideal droplet shape.

Here, one relies on information concerning the current and the next free boundary Γ , which requires one to provide substantial information on the ideal trajectory of a droplet. However, by providing the path of a droplet whose topology does not change over the time interval, it is possible to obtain a sequences of controls that keep the original droplet's topology intact.

4 Minimal velocity and Barycenter Matching

$$\mathcal{J}^{i+1}(\mathbf{u}, E) = \frac{1}{2} \|\mathbf{u}(\cdot)\|_{L^2(\Gamma^i)}^2 + \frac{1}{2} \left\| \frac{1}{|\Omega^i|} \int_{\Omega^i} (x + \delta t_{i+1} \mathbf{u}(x)) dx - \mathbf{b}_d \right\|_{\mathbb{R}^2}^2 + \frac{\zeta}{2} \|E\|_{\mathcal{E}}^2.$$

Given an ideal droplet shape $\mathbf{X}_d^{i+1}(\cdot)$ with barycenter \mathbf{b}_d , the first term in \mathcal{J}^{i+1} enforces a minimal velocity (stationary configuration). The second term positions the droplet at a desired location by enforcing barycenter matching. In contrast to the previous examples, in the numerical computations depicted below $\zeta := 1e-10$.

Besides the objective functional, one also needs to specify the control action E respecting the physical limitations of the EWOD device and realistic opportunities for the control action. Following [144], the control of a Glycerin droplet on a square is shown, containing a 3×3 EWOD device. Thus, 9 domains Ω_j , $j = 1, \dots, 9$ and 9 controls/control spaces $E_j^i \in \mathcal{E}_j^i$ are defined, respectively. Empirical data provided in [144, Table II] motivate box constraints on the control E , i.e.,

$$\mathcal{E}_{ad} = \{E \in L^2(\Gamma) : -11.0145 \leq E(s) \leq 8.9462, \text{ a.e. } s \in \Gamma\}.$$

2.2.1 Numerical solution algorithm

As in the theoretical analysis of the control problem, the multivalued subdifferential mapping becomes an issue when solving the problem numerically. This can be circumvented by employing a similar smoothing approach as for the derivation of Theorem 2, cf. [9]. As a consequence, one has to solve the following problem at each step of the algorithm

$$\mathbf{A}\mathbf{u} + \mathbf{B}^*p + P_{\text{pin}}\mathbf{C}^*\lambda = F(E), \quad (23a)$$

$$\mathbf{B}\mathbf{u} = 0, \quad (23b)$$

$$\lambda = \Psi'_\alpha(\mathbf{C}\mathbf{u}), \quad (23c)$$

where (23c) is understood for pointwise almost every $s \in \Gamma$ as

$$\lambda(s) = \tilde{\Psi}'(\alpha^{-1}(\mathbf{C}\mathbf{u})(s)).$$

In the numerical experiments depicted below, α was initialized at $1e-2$ and reduced to the order of $1e-6$. Moreover, the following (convex C^2) form for $\tilde{\Psi}$

$$\tilde{\Psi}(r) := \begin{cases} r - 1/2, & r \geq 1, \\ r^3 - r^4/2, & r \in (0, 1), \\ -r^3 - r^4/2, & r \in (-1, 0], \\ -r - 1/2, & r \leq -1. \end{cases}$$

was employed, but other smoothed versions of Ψ are possible as well.

The system (23) is solved via an exact solver in combination with a regularization approach by adding a small amount of compressibility, i.e., the perturbation εp , to the left side of (23b). Hereby, the problem is discretized using $\mathcal{P}_2 - \mathcal{P}_1$ -Taylor-Hood finite elements, see e.g., [53]. For each fixed $\alpha > 0$ and $\varepsilon > 0$, one can solve the resulting system with the standard Newton's method with a backtracking line search as a globalization scheme. The stopping criteria is based on the discrete \mathbb{V} -norm of the Riesz representation in \mathbb{V} of the residual of the system (23) with an absolute tolerance of $1e-10$; ε was set to $1e-16$. The method exhibited fast/superlinear convergence,

e.g., averaging 3-4 iterations until convergence, throughout the experiments. The performance was slightly worsened for cases involving large deformations of the droplet.

Note that a typical problem for the numerical solution of sharp interface models is that the mesh may become severely distorted or thin neck regions may appear after each time step. This can be dealt with by a so-called harmonic lifting in which the current velocity $\mathbf{u}|_{\Gamma}$ is used as the boundary data for a harmonic equation, which yields a vector field that smoothly updates the mesh node positions at each time step and preserves the shape of the boundary, cf. [144].

2.2.2 Numerical examples

In this subsection, we present the results obtained by the numerical solution algorithm described above for four examples, one for each objective functional. The parameters were $T = 3s$ and $\delta t = 1e-3$. We note that larger time steps typically led to larger mesh deformations and failure of Newton's method.

The initial droplet is a circle of diameter 0.1125 mm and is centered at the point (0.05625, 0.05625) mm. For each of the experiments, the behavior of the droplets over nine points in time is shown in the figures below. The values of the nine separate controls are printed inside their respective electrodes at those points in time. Recall as mentioned above, that $E = 8.9462$ corresponds to 0V and $E = -11.0145$ to 50V.

- 1 Barycenter matching: For this example, the desired barycenter was set to $\mathbf{b}_d = (-0.105, -0.105)$. The results of this experiment can be seen in Figures 3.
- 2 Barycenter tracking: Here, the ideal barycenters follow the semicircle starting at (0.05625, 0.05625) and following the path described by $\mathbf{b}_d(t)$ where $\mathbf{b}_d(t) := (\mathbf{b}_{d,1}(t), \mathbf{b}_{d,2}(t))$ is given by

$$\mathbf{b}_{d,1}(t) = 0.09 \cos(\phi(t)) + 0.05625, \quad \mathbf{b}_{d,2}(t) = 0.09 \sin(\phi(t)) - 0.02813$$

with $\phi(t) := (3 - t)\pi/6 + t\pi/2$, $t \in [0, 3]$; compare Figures 1 and 2. The results of this experiment can be seen in Figure 4

- 3 Matching the Shape of an Ideal Droplet: In this example the ideal droplet is taken to be $\mathbf{X}^{i+1}(0)(\cdot) - 0.1350$. The initial droplet is as in the previous two examples. The results of this experiment can be seen in Figure 5.
- 4 Minimal velocity and Barycenter Matching: The initial droplet is an ellipse (●) and the ideal (desired) droplet is a circle (○) of the same size as in Figure 1. Furthermore to increase the impact of the controls the size of electrodes is reduced by half. The results of this experiment can be seen in Figure 6.

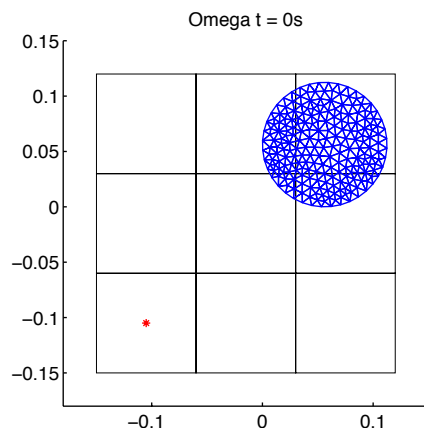


Figure 1: Initial configuration for barycenter matching: Initial droplet (top right) and desired barycenter (bottom left).

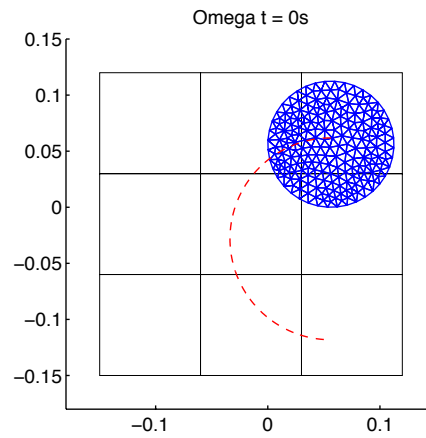


Figure 2: Initial configuration for barycenter tracking: Initial droplet (top right) and desired trajectory (dotted semicircle).

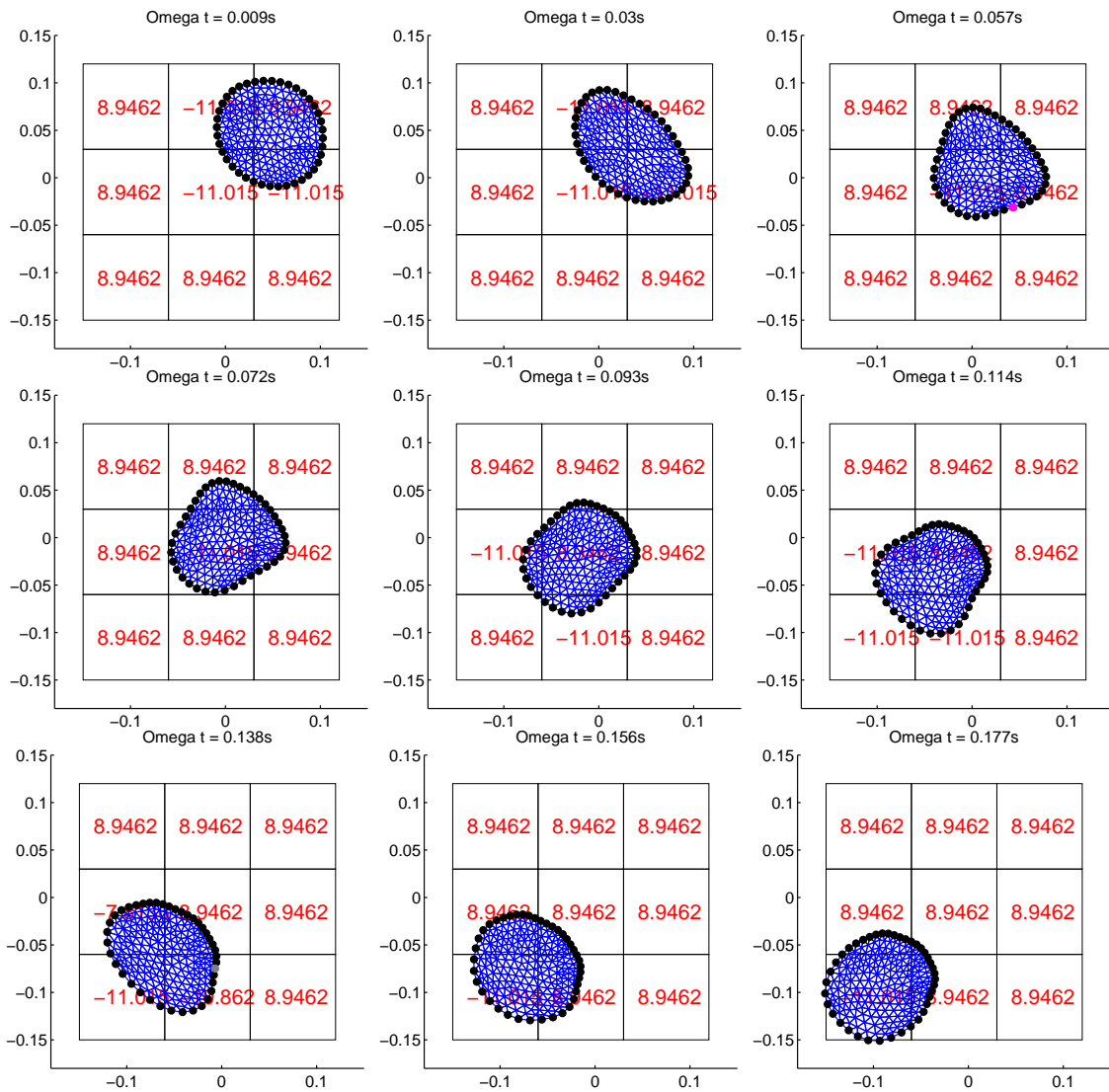


Figure 3: Barycenter matching: The 9 panels show the mesh modification at different times (in sec). The control E , shown in the background, is piecewise constant on each electrode. $E = 8.9462$ implies that a voltage of $0V$ is applied to that electrode and $E = -11.015$ correspond to $50V$. The active/inactive sets on the boundary are denoted by **Black ●**: strongly active, **Magenta ●**: biactive, **Grey ●**: inactive. Note the biactivity at time $t = 0.057s$

3 The phase field approach

3.1 Phase field models

Besides being a powerful mathematical tool to analyze flows driven by geometric quantities, the phase field approach was first developed as a physical model to describe the behavior of mixed liquids. In the following, we exemplarily discuss phase field models along with their physical meaning with respect to binary fluids, but phase field approaches enjoy a wide array of applications. Also, multiphase (as opposed to binary phase) problems are of relevance. The essential features, however, are already present with two phases. As the evolution of such fluids is strongly intertwined with the geometric properties of the system, this contributes to our understanding of geometric partial differential equations in general.

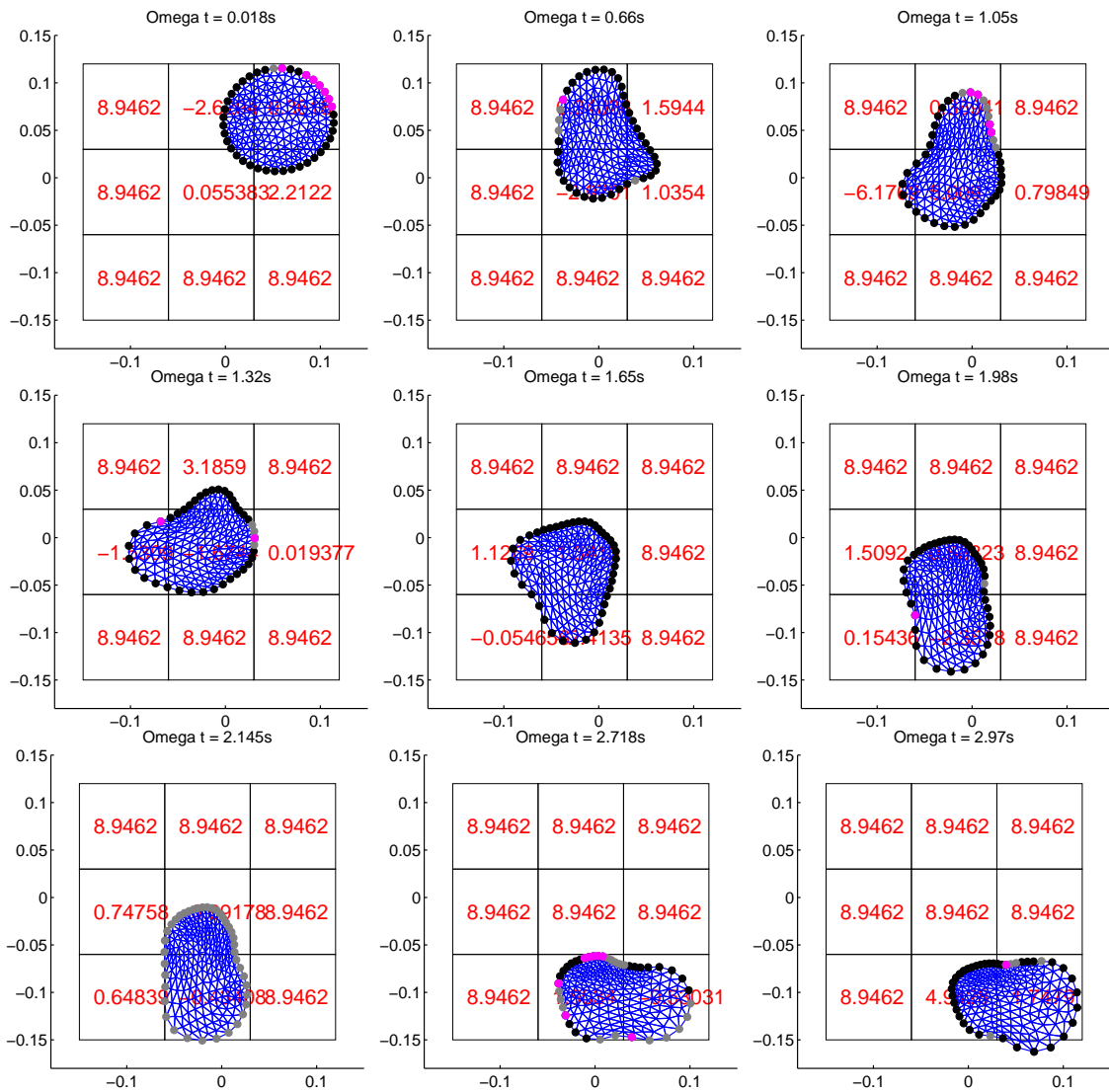


Figure 4: Barycenter tracking: The 9 panels show the mesh modification at different times (in sec). The control E , shown in the background, is piecewise constant on each electrode. $E = 8.9462$ implies that a voltage of $0V$ is applied to that electrode and $E = -11.015$ correspond to $50V$. The active/inactive sets on the boundary are denoted by **Black** \bullet : strongly active, **Magenta** \bullet : biactive, **Grey** \bullet : inactive. Note the biactivity at times $t = 0.018s, 0.66s, 1.05s, 1.32s, 1.98s, 2.718s, 2.97s$.

Originally, the interface between two fluids was considered to be a surface with zero thickness which possesses certain physical properties such as, e.g., a surface tension. As in the sharp interface approach, it was presumed that physical quantities are discontinuous across the interface and the respecting physical processes were represented by boundary conditions acting on the interface, which led to the formulation of free-boundary problems.

The first ones to attribute a finite width to the interface were J. W. Strutt and J. D. van der Waals, who assumed that the physical quantities instead perform a gradual smooth transition on the interface between the two phases. This lead to gradient theories for the interface based on thermodynamic principles such as van der Waals equation of state.

Expanding on these investigations J. W. Cahn and J. E. Hilliard presented their well-known phase-field model for binary fluids undergoing spinodal decomposition under isothermal and isochoric conditions in 1958; see [32].

In this context, spinodal decomposition denotes the process, where two components, which

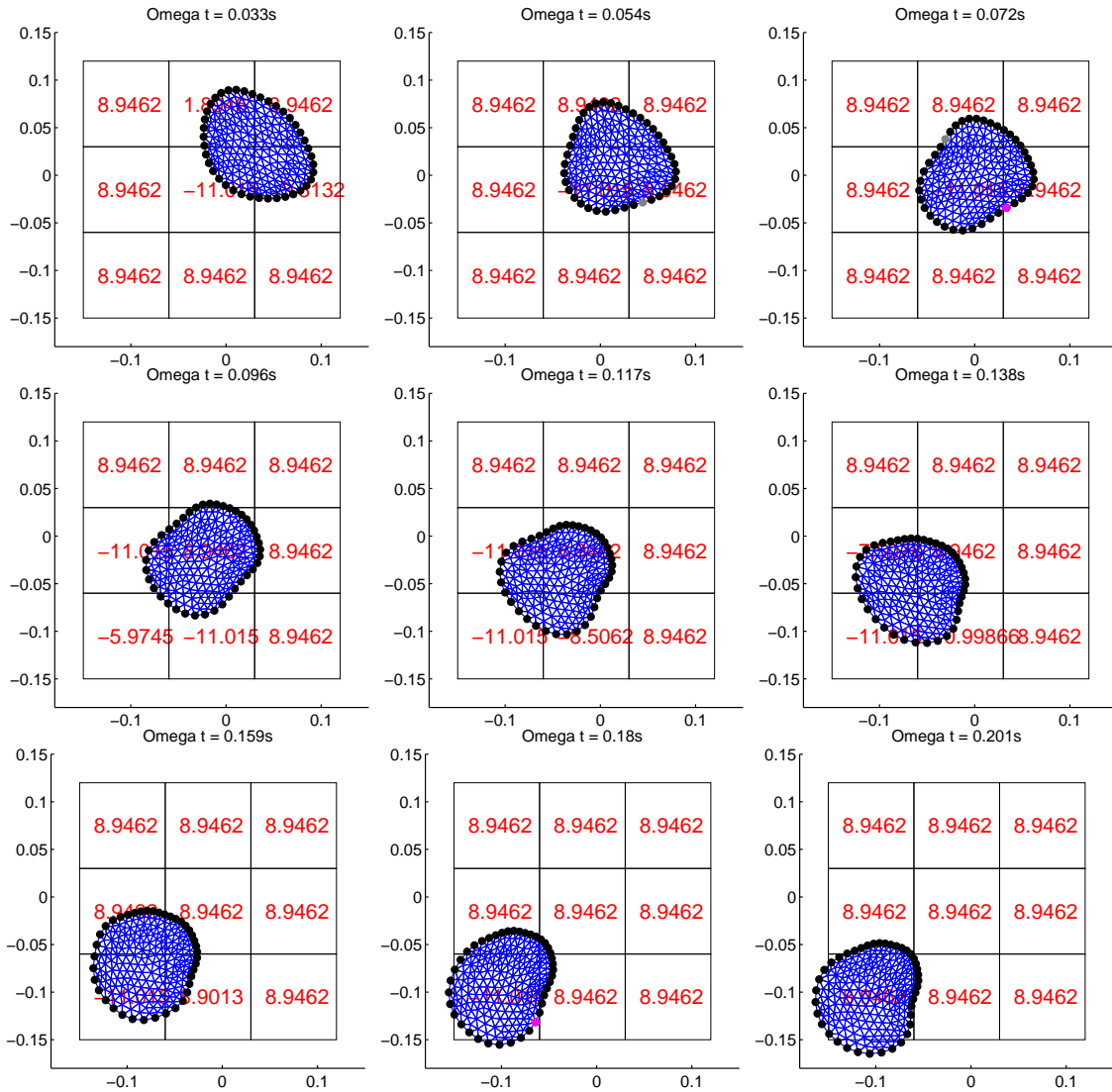


Figure 5: Matching an Ideal Droplet: The 9 panels show the mesh modification at different times (in sec). The control E , shown in the background, is piecewise constant on each electrode. $E = 8.9462$ implies that a voltage of $0V$ is applied to that electrode and $E = -11.015$ correspond to $50V$. The active/inactive sets on the boundary are denoted by **Black** ●: strongly active, **Magenta** ●: biactive, **Grey** ●: inactive. Note the biactivity at times $t = 0.072s$.

were mixed to form a single substance, rapidly decompose into two coexisting phases. In contrast to nucleation, in which sufficiently large nuclei of one phase appear randomly and grow, spinodal decomposition does not involve a free energy barrier and therefore the whole solution appears to nucleate at once, and periodic or semi-periodic structures can be observed.

The model is based on a generalized mass diffusion equation in terms of the local diffusion mass flux F and an order parameter φ , which represents the composition of the two phases

$$\partial_t \varphi = \nabla \cdot F, \quad (24)$$

where the mass flux F satisfies the boundary condition

$$F \cdot \vec{n}|_{\partial\Omega} = 0. \quad (25)$$

Following Fick's law, the mass flux is proportional to the gradient of the chemical potential μ , i.e.,

$$F = m(\varphi) \nabla \mu, \quad (26)$$

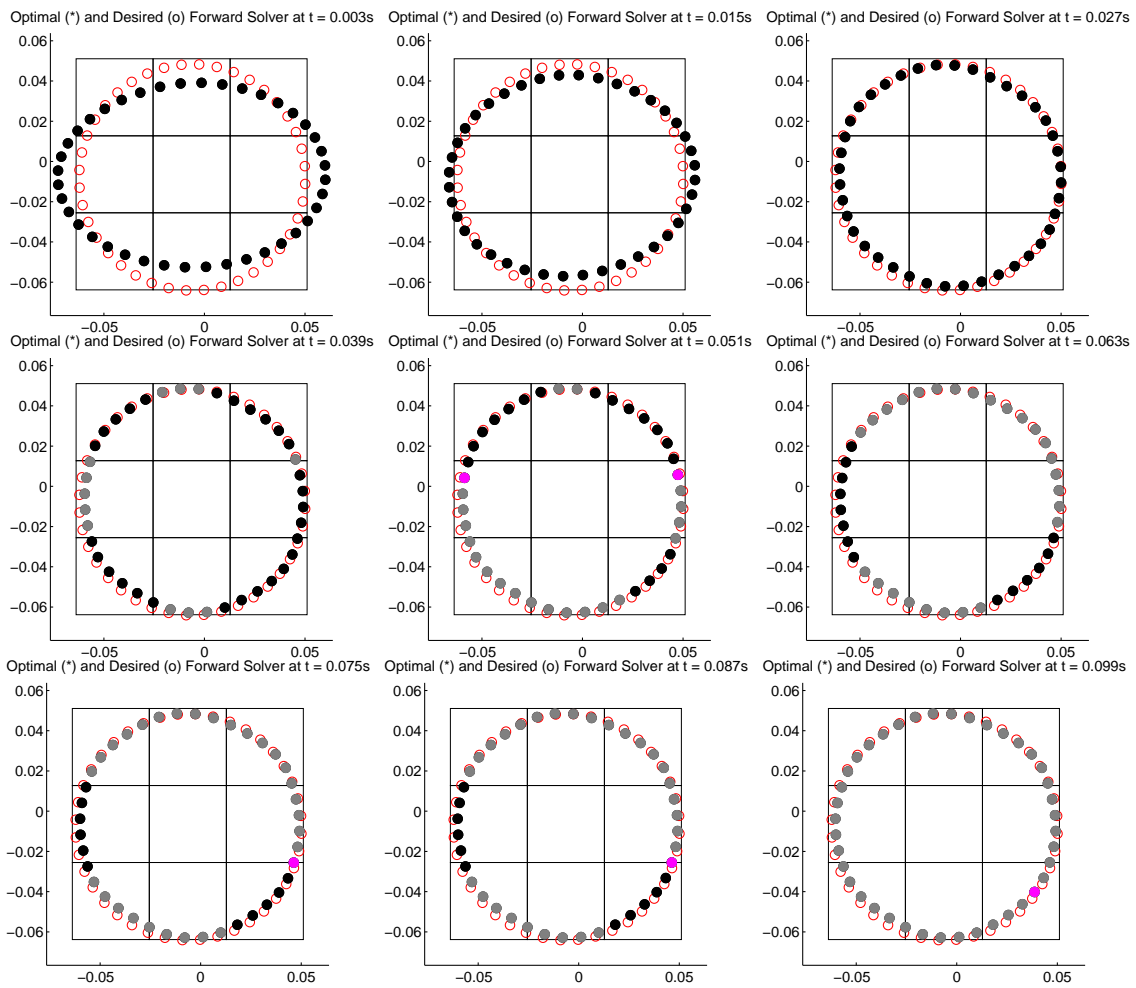


Figure 6: Minimal velocity and Barycenter Matching: The 9 panels show the optimal shape (●) and the desired shape (○) at different times (in sec). The active/inactive sets on the boundary are denoted by **Black ●**: strongly active, **Magenta ●**: biactive, **Grey ●**: inactive.

where $m(\varphi) \geq 0$ depicts the non-negative mobility depending on the concentration. Hereby, the (degenerate) case $m(\varphi) = 0$ corresponds to a pure transport of the components without diffusion. Following the Ginzburg-Landau theory the chemical potential is defined as the variational derivative of the free energy E given by

$$E(\varphi) = \int_{\Omega} \frac{\sigma \varepsilon}{2} |\nabla \varphi|^2 + \frac{\sigma}{\varepsilon} \Psi(\varphi) dx. \quad (27)$$

The first term of the right-hand side represents the surface tension of the interface, whereas $\Psi(\varphi)$ originates from the Helmholtz free energy density per molecule of the homogeneous system with composition φ . The parameters σ and ε are related to the interfacial energy, and the thickness of the interfacial region, respectively. The specific form of E (and Ψ) is crucial for the relation of the phase field models and geometric flows, as we will see below.

As a result, the Cahn-Hilliard system reads as follows

$$\partial_t \varphi - \operatorname{div}(m(\varphi) \nabla \mu) = 0, \quad (28)$$

$$-\frac{\sigma \varepsilon}{2} \Delta \varphi + \frac{\sigma}{\varepsilon} \partial \Psi(\varphi) - \mu = 0, \quad (29)$$

which corresponds to the H^{-1} -gradient flow of the Ginzburg-Landau energy in (27), cf. [55].

Another classical phase field model is the Allen-Cahn equation

$$\partial_t \varphi + m(\varphi) \left(-\frac{\sigma \varepsilon}{2} \Delta \varphi + \frac{\sigma}{\varepsilon} \partial \Psi(\varphi) \right) = 0, \quad (30)$$

which relates to the L^2 -gradient flow of the Ginzburg-Landau energy. It is often applied in materials science for solid-liquid phase changes such as, e.g., crystal growth. The main difference between these phase separation models is that the order parameter φ is not conserved for the Allen-Cahn equation, whereas for the Cahn-Hilliard equation it is.

In the past decades, the Cahn-Hilliard equation has been shown to be a qualitatively meaningful model for various diffusive processes, such as, e.g., growth and dispersal in population or phase transitions in binary alloys or polymer solutions [38, 118, 131, 136].

Although, the free-boundary description has been successful for a variety of applications, the diffuse interface approach has two main advantages. Namely, if the width of the interface is comparable to the length scale of the phenomena being examined, e.g., the motion of a contact line along a solid surface which requires a precise modeling of the fluid motion in the vicinity of the contact line, the representation of the interface as a boundary of zero thickness may not be adequate. Secondly, the diffuse interface approach naturally incorporates topological changes of the interface such as the break-up of liquid droplets or the coalescence of interfaces, which lead to serious difficulties, both, analytically and numerically, if the interface is described by a moving possibly self-intersecting boundary.

3.1.1 The free energy density and spinodal decomposition

An important part of the phase field model is the potential Ψ . According to Ginzburg and Landau the free energy can be obtained by integrating a homogeneous free energy density over a given volume fraction. Then the first term of the Ginzburg-Landau energy (27) emerges from the inclusion of spatial inhomogeneities, which is important to guarantee the conservation of the order parameter, whereas the second part is directly related to the free energy density, cf., e.g., [114]. We point out that this is a phenomenological modelling approach and can not be derived from a more microscopic description of the system. As a consequence, the choice of the free energy density can not be uniquely specified.

However, regardless of the specific choice, the free energy density usually possesses two local minima near -1 and 1 , which support the formation of the bulk phases associated with the sets $\{x \in \Omega \mid \varphi(x) = -1\}$ and $\{x \in \Omega \mid \varphi(x) = 1\}$, respectively. In their original work, Cahn and Hilliard considered a logarithmic barrier function

$$\Psi_{\text{In}}(\varphi) = (\ln(\varphi)\varphi + \ln(1-\varphi)(1-\varphi)) - \frac{\kappa}{2}\varphi^2. \quad (31)$$

Another important choice is the double-well potential given by

$$\Psi_{\text{W}}(\varphi) = \frac{\kappa}{2}\varphi^2(1-\varphi^2), \quad (32)$$

which is considered, e.g., in [25, 119]. A discussion on the inclusion of higher than quadratic order terms and other variants can be found in [132].

However, in [115, 116], Oono and Puri model the phase separation process utilizing cell dynamical systems, which are space-time discrete dynamical systems with a variable defined on each lattice point and updated in discrete time steps. The state of the lattice at a given time step is usually a function of the state at previous time steps

$$\varphi(t+1, n) = \psi(\varphi(t, n)) + D(g(\varphi(t, n)) - \varphi(t, n)), \quad (33)$$

where $\varphi(t, n)$ is the value of the order parameter in the cell n at time t , ψ describes the local dynamics of each cell (without any constraints) and D is a positive constant proportional to

the phenomenological diffusion constant. Furthermore, g corresponds to the isotropized discrete Laplacian and can be defined by

$$g(\varphi(t, n)) = \frac{1}{6} \sum (\varphi \text{ in the nearest-neighbor cells}) + \frac{1}{12} \sum (\varphi \text{ in the next-nearest-neighbor cells}). \quad (34)$$

The resulting cell dynamical system can be related to the Cahn-Hilliard system (28)-(29) by utilizing a specific discretization of the partial differential equations.

In this context, the first term of (27) reflects the relationship between different molecules or cells, which, e.g., causes the surface tension. In contrast, the second term models the properties of an isolated cell which is driven by a relaxational mechanism associated to a local free-energy functional.

Comparing different choices for the free energy, Oono and Puri found that short-time simulations based on (31) and (32) lead to solutions associated to the so-called “soft-wall” regime, in which the thickness of the boundary is appreciable relative to the representative pattern size. In order to obtain “hard-wall” behavior, i.e. sharp domain walls, whose thickness is negligible compared to the pattern size, simulations over a longer time period are necessary. In contrast, for the double-obstacle potential

$$\Psi(\varphi) = i_{[-1,1]}(\varphi) - \frac{\kappa}{2} \varphi^2, \quad (35)$$

where $i_{[-1,1]}$ represents the indicator function of the interval $[-1, 1]$, the “hard-wall” scenario was observed already after very short time spans. This can be related to the fact that for binary alloys without any vacancies, the order parameter should be always contained in the physically relevant interval $[-1, 1]$, which requires vertical potential walls. Furthermore, since the disordered phase is unstable the functional should be concave on $[-1, 1]$. Thus, in many cases, including, e.g., deep quenches of binary alloys or polymeric membrane formation under rapid wall hardening, the double-obstacle potential appears to be the best choice for modelling the phase separation process.

We point out that, due to the non-differentiability of the indicator function, the double-obstacle potential leads to the presence of a variational inequality of fourth order in (29), which highly complicates the analytical and numerical treatment of these systems, especially in the context of optimal control.

Nevertheless, we point out that the potentials (31),(32),(35) share the important characteristics of a single hyperbolic unstable fixed point, corresponding to the disordered state before quenching, and two hyperbolic stable fixed points, corresponding to the ordered states after quenching, symmetrically placed on each of its sides. As a consequence, a large part of the cells, which are not situated near the phase boundaries, have order parameter values close to those of the hyperbolic stable fixed points and the behavior of the cells near the phase boundaries is governed by the cells in the bulk phase. Thus, the global behavior is determined by the hyperbolicity of the sinks, which ensures the structural stability of the model. More precisely, most solutions to the associated Cahn-Hilliard equations that start with initial data near a fixed constant in the spinodal region, i.e., the interval where $\Psi'' < 0$, exhibit fine-grained decomposition. This is called the principle of spinodal decomposition.

3.1.2 The sharp interface limit and geometric flows

As discussed above, the solutions of the Cahn-Hilliard system or the Allen-Cahn equation will form large connected areas of each phase over time. These bulk regions are separated by a small interfacial band in which the order parameter performs a smooth transition from one value (-1 or 1) to the other. Hereby, the regularizing effect of the penalization of the gradient $\nabla \varphi$, i.e.

the first term in (27), ensures that the order parameter does not make too rapid changes such as jumps.

As a consequence, the phase field models can be used, e.g., to approximate the solution of a surface evolution equation by identifying the surface with the small interfacial layer. In fact, Modica has shown that the interfacial region, i.e. the set

$$\{x \in \Omega \mid -1 < \varphi(x) < 1\}$$

vanishes almost everywhere, if the interface width ε tends to zero; compare [109]. As a part of that, he additionally proved that the Ginzburg Landau energy in (27) Γ -converges in $L^1(\Omega)$ to a multiple of the perimeter functional given by

$$E_{\text{lim}}(\varphi) := \begin{cases} \int_{-1}^1 \sqrt{2\Psi(y)} dy \int_{\Omega} |\nabla \chi_{\{\varphi=1\}}(x)| dx & \text{if } \varphi \in BV(\Omega, \{-1, 1\}) \\ \infty & \text{if } \varphi \in BV(\Omega, \{-1, 1\}) \end{cases}, \quad (36)$$

if ε goes to zero. For convenience, we briefly recall the definition of Γ -convergence at this point, cf., e.g., [43].

Definition 1 *Let X be a reflexive Banach space. A family of functionals $f_\alpha : X \rightarrow [-\infty, \infty]$ is said to Γ -converge to $f : X \rightarrow [-\infty, \infty]$ for $\alpha \rightarrow 0$ if and only if the following statements are satisfied.*

- 1 *For every convergent sequence $\{x_\alpha\}_{\alpha>0} \subset X$ and the associated limit point \bar{x} , it holds that*

$$f(\bar{x}) \leq \liminf_{\alpha \rightarrow 0} f_\alpha(x_\alpha). \quad (37)$$

- 2 *For every $\bar{x} \in X$ there exists a sequence $\{x_\alpha\}_{\alpha>0} \subset X$ which converges to \bar{x} such that*

$$f(\bar{x}) \geq \limsup_{\alpha \rightarrow 0} f_\alpha(x_\alpha). \quad (38)$$

Furthermore, it has been shown that mean curvature flow is approximated by the Allen-Cahn equation (30) if ε is driven to zero, see, e.g., [28, 44, 54, 124] for a rigorous interface asymptotic analysis for double-well potentials and [36] for the corresponding convergence result for the double-obstacle potential. More precisely, the Hausdorff distance between the zero-level set of the phase field solution associated to the Allen-Cahn equation and the corresponding surface solution of the mean curvature flow is bounded by ε , cf., e.g., [19, 34] (double-well potential) and [112] (double-obstacle potential). Moreover, the zero-level set of the phase field solution converges to the viscosity solution of the level-set formulation of the mean curvature flow, see e.g. [54] for the double-well potential and [113] for the double-obstacle potential.

In case of the Cahn-Hilliard system the resulting sharp interface model is the so-called Mullins-Sekerka problem

$$\Delta \mu = 0 \quad \text{on } \Omega \setminus \Gamma_t, \quad (39)$$

$$2V = -[\nabla \mu]_\pm^\pm \cdot \nu \quad \text{on } \Gamma_t, \quad (40)$$

$$2\mu = CH \quad \text{on } \Gamma_t, \quad (41)$$

where $[\nabla \mu]_\pm^\pm$ represents the jump of a μ across the interface from Ω^+ to Ω^- . In this case, similar convergence results can be derived. For more information on the subject, we refer the reader to [7, 35, 118, 133] and the references therein.

3.1.3 Incorporating hydrodynamic or surface effects

An important advantage of the phase field approach is that the model can be easily extended to include other effects such as hydrodynamic effects. In particular, it also allows for the inclusion of surface effects. Hereby, the interface is indicated by the gradient $\nabla \varphi$ of the order parameter.

A first basic model which combined the phase field model with hydrodynamical properties was given by Pierre Claude Hohenberg and Bertrand I. Halperin in [96]. The so-called 'model H' for two incompressible, viscous Newtonian fluids with matched densities led to the following Cahn-Hilliard-Navier-Stokes system

$$\partial_t \varphi + v \nabla \varphi - \operatorname{div}(m(\varphi) \nabla \mu) = 0, \quad (42)$$

$$-\frac{\sigma \varepsilon}{2} \Delta \varphi + \frac{\sigma}{\varepsilon} \partial \Psi(\varphi) - \mu = 0, \quad (43)$$

$$\rho \partial_t(v) + \rho \operatorname{div}(v \otimes v) - \operatorname{div}(2\eta(\varphi)\varepsilon(v)) + \nabla \Pi + \sigma \varepsilon \operatorname{div}(\nabla \varphi \otimes \nabla \varphi) = 0, \quad (44)$$

$$\operatorname{div} v = 0. \quad (45)$$

The model describes the two-phase flow in terms of the order parameter φ , the chemical potential μ and the mean velocity v . Moreover, Π denotes the pressure acting on the system and $\eta(\varphi)$ symbolizes the viscosity of the composition.

It can be verified that the model is thermodynamically consistent in the sense that it obeys a local dissipation inequality and satisfies the second law of thermodynamics, respectively, cf. [71].

Following the publication of Hohenberg and Halperin, we have seen different approaches to develop a similar model for the case of non-matched densities. In [104], Lowengrub and Truskinovsky introduce a mass averaged/barycentric velocity and derive a thermodynamically consistent generalization of model H for non-matched densities. Unfortunately, the proposed model involves velocity fields with non-zero divergence. In addition, the fact that the pressure enters the Cahn-Hilliard equation further complicates the introduction of suitable discretization schemes.

In contrast, Boyer [26] and Ding [48] considered a volume averaged velocity field which led them to slightly different models, where the solenoidality of the velocity field is guaranteed. However, neither global nor local energy estimates could be derived for these models up to now.

In [4], Abels, Garcke and Grün came up with the following Cahn-Hilliard-Navier-Stokes system

$$\partial_t \varphi + v \nabla \varphi - \operatorname{div}(m(\varphi) \nabla \mu) = 0, \quad (46a)$$

$$-\Delta \varphi + \partial \Psi_0(\varphi) - \mu - \kappa \varphi \ni 0, \quad (46b)$$

$$\begin{aligned} \partial_t(\rho(\varphi)v) + \operatorname{div}(v \otimes \rho(\varphi)v) - \operatorname{div}(2\eta(\varphi)\varepsilon(v)) + \nabla p \\ + \operatorname{div}(v \otimes J) - \mu \nabla \varphi = 0, \end{aligned} \quad (46c)$$

$$\operatorname{div} v = 0, \quad (46d)$$

$$v|_{\partial\Omega} = 0, \quad (46e)$$

$$\partial_n \varphi|_{\partial\Omega} = \partial_n \mu|_{\partial\Omega} = 0, \quad (46f)$$

$$(v, \varphi)|_{t=0} = (v_{in}, \varphi_{in}), \quad (46g)$$

based on a volume averaged velocity, which is supposed to hold in the space-time cylinder $\Omega \times (0, \infty)$. Here, the density ρ of the mixture of the fluids depends affinely on the order parameter φ via

$$\rho(\varphi) = \frac{\rho_1 + \rho_2}{2} + \frac{\rho_2 - \rho_1}{2} \varphi, \quad (47)$$

where $0 < \rho_1 \leq \rho_2$ are the given densities of the two fluids under consideration. The relative flux $J := -\frac{\rho_2 - \rho_1}{2} m(\varphi) \nabla \mu$ corresponds to the diffusion of the two phases. The initial states are given by v_{in} and φ_{in} , and $\kappa > 0$ is a positive constant.

As ensured by equation (46d), the model is based on divergence-free velocity fields and, at the same time, allows for the verification of global energy estimates. Furthermore, it reduces to the well-known 'model H' for matched densities, i.e. if $\rho_1 = \rho_2$.

In [4], three variants of this model are proposed that can also handle, e.g., non-Newtonian fluids or additional particles that are transported across the interface but do not interact with it.

The existence of a weak solution for the case of constant mobility is shown in [2] for the logarithmic free energy that guarantees a-priori bounds on the range of the phase field. In [3], the existence of weak solutions is established for general smooth free energies together with a degenerate mobility that also guarantees these bounds. The existence of a weak solution for non-Newtonian fluids is discussed in [1] for a polynomially bounded free energy and constant mobility. In the latter work, also an extension of the model of [4] is proposed that allows to use nonlinear but smooth relations between the phase field φ and the density field $\rho(\varphi)$ for the case where $|\varphi|$ is not bounded by one, which appears due to a smooth free energy.

In [67], the existence of generalized solutions is shown for the case of a polynomially bounded free energy. Depending on the densities of the individual fluids, indicated by the Atwood number, these generalized solutions are weak solutions over a small time horizon. The analysis is based on proceeding to the limit in a numerical scheme.

Another example for the inclusion of surfactants can be found in [63], where a thermodynamically consistent model for two-phase flow with different densities is proposed that can also handle additional surface active agents, so called surfactants. These particles adhere to the interface, following some advection-diffusion equation and some sorption laws. On the interface they lower locally the surface tension of the interface. Thus, this model especially contains a locally varying surface tension and a partial differential equation on a diffuse interface. This work also contains numerical results based primarily on the results of [50] on the simulation of partial differential equations on evolving interfaces.

Moreover, we note that phase field models can naturally be extended to situation of multi phase flows with more than two fluid components by using a vector-valued phase field equation, see e.g. [24, 27].

3.2 Existence of solutions

The existence of solutions to phase field models such as the Allen-Cahn equation or the Cahn-Hilliard system is typically based on the fact that these models relate to the gradient flow of the Ginzburg-Landau energy. It can be shown that the total energy associated with such solutions is bounded by the energy of the initial configuration at all times, which allows us to apply a Galerkin method and/or a fixed point type argument to secure the existence of solutions; see, e.g., [25, 52]. If the phase field model is coupled to another partial differential equation, the approach has to be modified accordingly.

In the following, we exemplarily present the derivation of the existence of weak solutions to the Cahn-Hilliard-Navier-Stokes system (46). It is based on an implicit discretization in time and a subsequent limiting analysis with respect to the time step size tending to zero, which is a well-known technique to verify the existence of weak solutions to the Navier-Stokes equation, see e.g. [137].

Incorporating the hydrodynamics of the two-phase composition, the total energy E of a solution to (46) is given as the sum of the kinetic energy and the potential energy, i.e.,

$$E(v, \varphi) = \int_{\Omega} \rho(\varphi) \frac{|v|^2}{2} dx + \int_{\Omega} \frac{|\nabla \varphi|^2}{2} dx + \Psi(\varphi). \quad (48)$$

Similar to the decoupled Cahn-Hilliard system, it is possible to derive a (dissipative) energy law by testing (46a), (46b), (46c) and (46d) with μ , $\partial_t \varphi$, v and Π , respectively, which leads to

$$\partial_t E(v, \varphi) + 2 \int_{\Omega} \eta(\varphi) |\varepsilon(v)|^2 dx + \int_{\Omega} m(\varphi) |\nabla \mu|^2 dx \leq 0. \quad (49)$$

Inequality (49) is related to the physical property that the total energy of a closed system is non-increasing and - at the same time - serves as a very valuable analytical tool, e.g., to secure the boundedness of solutions to (46).

For the reasons mentioned above, it is desirable to maintain the energy inequality on the time discrete level, which typically requires the preservation of the strong coupling of the Cahn–Hilliard system and the Navier–Stokes equation as seen in Definition 2 below. However, F. Guillén-González and G. Tierra recently proposed a numerical splitting scheme for the Cahn–Hilliard–Navier–Stokes system, which maintains the energy law via introducing a small correction term to the velocity field, cf. [69].

3.2.1 Discretization in time

Before presenting the chosen discretization in time of the system (46) in its weak formulation, we observe that, assuming integrability in time, from (46d), (46a), (46e), and (46f), it follows that the order parameter satisfies

$$\begin{aligned} \int_{\Omega} \partial_t \varphi dx &= - \int_{\Omega} v \nabla \varphi dx + \int_{\Omega} \operatorname{div}(m(\varphi) \nabla \mu) dx \\ &= \int_{\Omega} \operatorname{div}(v) \varphi dx - \int_{\partial\Omega} v \varphi \vec{n}_{\Omega} dx + \int_{\partial\Omega} m(\varphi) \nabla \mu \vec{n}_{\Omega} dx = 0. \end{aligned}$$

In other words, the integral mean of φ remains constant

$$\frac{1}{|\Omega|} \int_{\Omega} \varphi dx \equiv: \overline{\varphi}_a \in (-1, 1), \quad (50)$$

which reflects the conservation of mass within the system. Note that the inclusion (50) excludes the uninteresting case with only one phase being present, i.e., $|\overline{\varphi}_a| = 1$. This observation allows us to assume that the integral mean of the order parameter is zero without loss of generality, as the general case can easily be transferred to the case $\overline{\varphi}_a = 0$ by considering a shifted system (46), where the order parameter is replaced by its projection onto $\overline{L}^2(\Omega)$. This involves a shift in the variables and coefficients such as, e.g. $\Psi_0(\varphi + \overline{\varphi}_a)$ and $m(\varphi + \overline{\varphi}_a)$, which we again denote by $\Psi_0(\varphi)$ and $m(\varphi)$ in a slight misuse of notation. Consequently, the two hyperbolic stable fixed points of the free energy describing the pure phases are now associated with the points

$$\psi_1 := -1 - \overline{\varphi}_a, \quad \psi_2 := 1 - \overline{\varphi}_a. \quad (51)$$

We introduce the following spaces

$$\begin{aligned} H_{0,\sigma}^k(\Omega; \mathbb{R}^n) &:= \left\{ f \in H^k(\Omega; \mathbb{R}^n) \cap H_0^1(\Omega; \mathbb{R}^n) : \operatorname{div} f = 0, \text{ a.e. on } \Omega \right\}; \\ \overline{H}^k(\Omega) &:= H_{(0)}^k(\Omega) := \left\{ f \in H^k(\Omega) : \int_{\Omega} f dx = 0 \right\}; \\ \overline{H}_{\partial_n}^k(\Omega) &:= \left\{ f \in \overline{H}^k(\Omega) : \partial_n f|_{\partial\Omega} = 0 \text{ on } \partial\Omega \right\}, \quad k \geq 2; \end{aligned}$$

where the boundary condition is supposed to hold true in the trace sense. The subscript σ here is a common notation representing the solenoidality. Unless otherwise noted, $\langle \cdot, \cdot \rangle := \langle \cdot, \cdot \rangle_{\overline{H}^{-1}, \overline{H}^1}$ represents the duality pairing between $\overline{H}^1(\Omega)$ and its dual $\overline{H}^{-1}(\Omega)$.

The subsequent assumption rigorously introduces the given data such as the mobility and viscosity coefficients m, η , the density function ρ , the convex part Ψ_0 of the free energy density Ψ and the initial data v_a, φ_a along with some necessary regularity requirements.

Assumption 1 *1 The coefficient functions $m, \eta \in C^2(\mathbb{R})$ as well as their derivatives up to second order are bounded, i.e. there exist constants $0 < b_1 \leq b_2$ such that for every $x \in \mathbb{R}$, it holds that $b_1 \leq \min\{m(x), \eta(x)\}$ and*

$$\max\{m(x), \eta(x), |m'(x)|, |\eta'(x)|, |m''(x)|, |\eta''(x)|\} \leq b_2.$$

2 The initial state satisfies $(v_a, \varphi_a) \in H_{0,\sigma}^2(\Omega; \mathbb{R}^n) \times \left(\overline{H}_{\partial_n}^2(\Omega) \cap \mathbb{K} \right)$ where

$$\mathbb{K} := \left\{ v \in \overline{H}^1(\Omega) : \psi_1 \leq v \leq \psi_2 \text{ a.e. in } \Omega \right\},$$

with $-1 - \overline{\varphi_a} =: \psi_1 < 0 < \psi_2 := 1 - \overline{\varphi_a}$.

3 The density ρ depends on the order parameter φ via

$$\rho(\varphi) = \frac{\rho_1 + \rho_2}{2} + \frac{\rho_2 - \rho_1}{2}(\varphi + \overline{\varphi_a}). \quad (52)$$

4 The functional $\Psi_0 : \overline{H}^1(\Omega) \rightarrow \mathbb{R}$ is given by $\Psi_0(\varphi) := \int_{\Omega} i_{[\psi_1; \psi_2]}(\varphi(x)) dx$, where the indicator function $i_{[\psi_1; \psi_2]} : \mathbb{R} \rightarrow \overline{\mathbb{R}}$ is defined by

$$i_{[\psi_1; \psi_2]} := \begin{cases} +\infty & \text{if } z < \psi_1, \\ 0 & \text{if } \psi_1 \leq z \leq \psi_2, \\ +\infty & \text{if } z > \psi_2. \end{cases}$$

We point out that Assumption 1 excludes the case of degenerate mobilities, i.e. where $m(\varphi) = 0$. More information on two-phase flows with degenerate mobilities can be found, e.g., in [3, 51] and, more recently, in [58].

Note that since the double-obstacle potential restricts the order parameter to the physically relevant interval $[\psi_1, \psi_2]$, the density remains always positive which is important for deriving appropriate energy estimates.

With these assumptions we now present the semi-discrete Cahn–Hilliard Navier–Stokes system. At this point, we additionally introduce a distributed force on the right-hand side of the Navier–Stokes equation, which will later serve the purpose of a distributed control of the system. Hereby, it is natural to consider the control force u_i to be an element of $L^2(\Omega; \mathbb{R}^n)$, in order to permit a point-wise interpretation almost everywhere on Ω for actual applications.

Moreover, we already include the inherent regularity properties of φ and μ anticipating the results obtained in Lemma 2. In the sequel, $\tau > 0$ denotes the time step-size and $K \in \mathbb{N}$ the total number of time instants.

Definition 2 (Semi-discrete CHNS system) Fixing $(\varphi_{-1}, v_0) = (\varphi_a, v_a)$ we say that a triple

$$(\varphi, \mu, v) = ((\varphi_i)_{i=0}^{K-1}, (\mu_i)_{i=0}^{K-1}, (v_i)_{i=1}^{K-1})$$

in $\overline{H}_{\partial_n}^2(\Omega)^K \times \overline{H}_{\partial_n}^2(\Omega)^K \times H_{0,\sigma}^1(\Omega; \mathbb{R}^n)^{K-1}$ solves the semi-discrete CHNS system with respect to a given control $u = (u_i)_{i=1}^{K-1} \in L^2(\Omega; \mathbb{R}^n)^{K-1}$, denoted by $(\varphi, \mu, v) \in S_{\Psi}(u)$, if it holds for all $\phi \in \overline{H}^1(\Omega)$ and $\psi \in H_{0,\sigma}^1(\Omega; \mathbb{R}^n)$ that

$$\left\langle \frac{\varphi_{i+1} - \varphi_i}{\tau}, \phi \right\rangle + \langle v_{i+1} \nabla \varphi_i, \phi \rangle + (m(\varphi_i) \nabla \mu_{i+1}, \nabla \phi) = 0, \quad (53)$$

$$(\nabla \varphi_{i+1}, \nabla \phi) + \langle \partial \Psi_0(\varphi_{i+1}), \phi \rangle - \langle \mu_{i+1}, \phi \rangle - \langle \kappa \varphi_i, \phi \rangle \ni 0, \quad (54)$$

$$\begin{aligned} & \left\langle \frac{\rho(\varphi_i) v_{i+1} - \rho(\varphi_{i-1}) v_i}{\tau}, \psi \right\rangle_{H_{0,\sigma}^{-1}, H_{0,\sigma}^1} - (v_{i+1} \otimes \rho(\varphi_{i-1}) v_i, \nabla \psi) \\ & + \left(v_{i+1} \otimes \frac{\rho_2 - \rho_1}{2} m(\varphi_{i-1}) \nabla \mu_i, \nabla \psi \right) + (2\eta(\varphi_i) \varepsilon(v_{i+1}), \varepsilon(\psi)) \\ & - \langle \mu_{i+1} \nabla \varphi_i, \psi \rangle_{H_{0,\sigma}^{-1}, H_{0,\sigma}^1} = \langle u_{i+1}, \psi \rangle_{H_{0,\sigma}^{-1}, H_{0,\sigma}^1}. \end{aligned} \quad (55)$$

The first two equations are supposed to hold for every $0 \leq i+1 \leq K-1$ and the last equation holds for every $1 \leq i+1 \leq K-1$.

Here, the boundary conditions specified in (46d)–(46f) are incorporated in the respective function spaces of Definition 2.

Note that the subdifferential of a convex function Ψ_0 is in general a set-valued mapping, see, e.g., [49]. Furthermore, the semi-discretization of (46) in time involves three time instants $(i-1), i, (i+1)$. Equations (53) and (54), however, do not involve the velocity at the time instant $(i-1)$. As a consequence, (φ_0, μ_0) are characterized by the (decoupled) Cahn-Hilliard system only. Nevertheless, the coupling of the Cahn-Hilliard and the Navier-Stokes system is maintained in the subsequent time instances, which enables us to derive a discrete equivalent of the dissipative energy law (49). Here, the discrete energy functional $E : \bar{H}_{0,\sigma}^1(\Omega) \times \bar{H}^1(\Omega) \times \bar{H}^1(\Omega) \rightarrow \mathbb{R}$ is defined by

$$E_i := E(v_i, \varphi_i, \varphi_{i-1}) := \int_{\Omega} \frac{\rho(\varphi_{i-1}) |v_i|^2}{2} dx + \int_{\Omega} \frac{|\nabla \varphi_i|^2}{2} dx + \Psi(\varphi_i). \quad (56)$$

Lemma 1 (Energy estimate for a single time step) *Let $\varphi_i, \varphi_{i-1} \in \bar{H}^1(\Omega) \cap \mathbb{K}$, $\mu_i \in \bar{H}^1(\Omega)$, $v_i \in H_{0,\sigma}^1(\Omega; \mathbb{R}^n)$ be the state of the system at time step i and $u_{i+1} \in (H_{0,\sigma}^1(\Omega; \mathbb{R}^n))^*$ a given external force.*

Then, if $(\varphi_{i+1}, \mu_{i+1}, v_{i+1}) \in \bar{H}^1(\Omega) \times \bar{H}^1(\Omega) \times H_{0,\sigma}^1(\Omega; \mathbb{R}^n)$ solves the system (53)–(55) for one time step, the corresponding total energy is bounded by

$$\begin{aligned} E(v_{i+1}, \varphi_{i+1}, \varphi_i) &+ \int_{\Omega} \rho(\varphi_{i-1}) \frac{|v_{i+1} - v_i|^2}{2} dx + \int_{\Omega} \frac{|\nabla \varphi_{i+1} - \nabla \varphi_i|^2}{2} dx \\ &+ \tau \int_{\Omega} 2\eta(\varphi_i) |\varepsilon(v_{i+1})|^2 dx + \tau \int_{\Omega} m(\varphi_i) |\nabla \mu_{i+1}|^2 dx + \int_{\Omega} \kappa \frac{(\varphi_{i+1} - \varphi_i)^2}{2} \\ &\leq E(v_i, \varphi_i, \varphi_{i-1}) + \langle u_{i+1}, v_{i+1} \rangle_{H_{0,\sigma}^{-1}, H_{0,\sigma}^1}. \end{aligned} \quad (57)$$

For rigorous proofs of the results of this section we refer to [83].

Note that, due to the positivity of the density and the coefficients m, η , all the terms of the left-hand side of the inequality are always non-negative such that Lemma 1 indeed ensures that the energy of the next time step is non-increasing if the external force u_{i+1} is absent.

Next, the existence of feasible points for the semi-discrete Cahn-Hilliard Navier-Stokes system for single time steps can be established based on Schaefer's fixed point theorem, also called the Leray-Schauder principle. The associated boundedness constraint is verified with the help of the energy estimate (57). In addition, some arguments from monotone operator theory are employed. As a consequence, we arrive at the following result concerning the solvability of the semi-discrete system (53)–(55).

Theorem 3 (Existence of solutions to the CHNS system for a single time step) *Let the assumptions of Lemma 1 be satisfied. Then the system (53)–(55) admits a solution $(\varphi_{i+1}, \mu_{i+1}, v_{i+1}) \in \bar{H}^1(\Omega) \times \bar{H}^1(\Omega) \times H_{0,\sigma}^1(\Omega; \mathbb{R}^n)$ for one time step.*

3.2.2 Regularity of solutions

An important feature of phase field models is the increased regularity of the corresponding solutions. For instance, in case of the Cahn-Hilliard system, it can be easily seen that the order parameter is twice weakly differentiable in space, which is a direct consequence of equation (29) using regularity theory of elliptic partial differential equations. This holds true even if Ψ_0 represents the non-smooth double-obstacle potential and (29) relates to a variational inequality; see, e.g., [91, 100].

For the coupled system (53)–(55) one additionally relies on the well-established regularity for the Navier-Stokes equation [137]. This allows one to prove the following lemma via a bootstrap argument, if the initial data is sufficiently regular.

Lemma 2 (Regularity of solutions) *Let the assumptions of Lemma 1 be satisfied, and suppose additionally that $\varphi_i \in H^2(\Omega)$ and $u_{i+1} \in L^2(\Omega; \mathbb{R}^n)$. Moreover, let $(\varphi_{i+1}, \mu_{i+1}, v_{i+1}) \in \overline{H}^1(\Omega) \times \overline{H}^1(\Omega) \times H_{0,\sigma}^1(\Omega; \mathbb{R}^n)$ be a solution to the system (53)–(55)*

Then it holds that $\varphi_{i+1}, \mu_{i+1} \in \overline{H}_{\partial_n}^2(\Omega)$, $\varphi_{i+1} \in \mathbb{K}$ and $v_{i+1} \in H^2(\Omega; \mathbb{R}^n)$, and there exists a constant $C = C(N, \Omega, b_1, b_2, \tau, \kappa) > 0$ such that

$$\begin{aligned} & \|\varphi_{i+1}\|_{H^2} + \|\mu_{i+1}\|_{H^2} + \|v_{i+1}\|_{H^2} \\ & \leq C(\|\varphi_{i+1}\| + \|\mu_{i+1}\| + \|\varphi_i\| + \|v_{i+1}\|_{H^1} \|\varphi_i\|_{H^2}). \end{aligned} \quad (58)$$

This also ensures that the system (53)–(55) is well-posed for each subsequent time step. Thus, applying Theorem 3 and Lemma 2 repeatedly for each time step $i = 0, \dots, K-2$ directly verifies the existence of solutions to the semi-discrete Cahn–Hilliard–Navier–Stokes system given in Definition 2.

Proposition 1 (Existence of feasible points) *Let $u \in L^2(\Omega; \mathbb{R}^n)^{K-1}$ be given.*

Then the semi-discrete CHNS system admits a solution $(\varphi, \mu, v) \in \overline{H}_{\partial_n}^2(\Omega)^K \times \overline{H}_{\partial_n}^2(\Omega)^K \times H_{0,\sigma}^2(\Omega; \mathbb{R}^n)^{K-1}$.

From here onwards, the existence of solutions to the time-continuous CHNS system can be established via a limiting process with respect to the total number of time instances $K \rightarrow \infty$ and the time step size $\tau := \frac{T}{K} \rightarrow 0$. For this purpose, one considers certain step functions f_{step}^K with respect to the time t which are equal to the time discrete solutions $f_{step}^K(t) = f_i$ on each interval $t \in [(i-1)\tau, i\tau)$; $i = 1, \dots, K-1$ for $f \in \{v, \varphi, \mu\}$. Employing the energy estimate (57) these functions can be bounded in the spaces $v_{step}^K \in L^2(0, T, H^1(\Omega; \mathbb{R}^n))$, $\varphi_{step}^K \in L^\infty(0, T, H^1(\Omega))$, $\mu_{step}^K \in L^2(0, T, H^1(\Omega))$. Then, the limit point of an appropriate subsequence can be shown to satisfy the system (46). For more details, we refer to, e.g., [2], where this method has been successfully applied to a similar system where the free energy density is defined through the logarithmic potential $\Psi(\varphi) = (1 + \varphi) \ln(1 + \varphi) + (1 - \varphi) \ln(1 - \varphi) - \frac{\kappa}{2} \varphi^2$.

However, since the same arguments cannot be applied to the adjoint system associated with the optimal control problem later on, we subsequently focus on the semi-discrete (in time) system.

3.3 Optimal control of a phase field model

Let us now discuss the optimal control of phase field models and the associated difficulties. The general idea is to influence the system via a control force u in order to achieve some prescribed goal. For this purpose, we introduce an objective functional $\mathcal{J} : \mathcal{X} \rightarrow \mathbb{R}$ with

$$\mathcal{X} := \overline{H}^1(\Omega)^K \times \overline{H}^1(\Omega)^K \times H_{0,\sigma}^1(\Omega; \mathbb{R}^n)^{K-1} \times L^2(\Omega; \mathbb{R}^n)^{K-1}.$$

In many applications \mathcal{J} corresponds to a tracking-type functional

$$\mathcal{J}(\varphi, \mu, v, u) := \frac{1}{2} \|\varphi_{K-1} - \varphi_d\|^2 + \frac{\xi}{2} \|u\|_{(L^2)^{(K-1)}}^2, \quad \xi > 0, \quad (59)$$

where $\varphi_d \in L^2(\Omega)$ denotes the desired states and the control is penalized via the parameter ξ .

Then the optimal control problem is given by

$$\begin{aligned} & \min \mathcal{J}(\varphi, \mu, v, u) \text{ over } (\varphi, \mu, v, u) \in \mathcal{X} \\ & \text{s.t. } u \in U_{ad}, (\varphi, \mu, v) \in \mathcal{S}_\Psi(u). \end{aligned} \quad (P_\Psi)$$

Here, possible control constraints are represented by the constraint set $U_{ad} \subset L^2(\Omega; \mathbb{R}^n)^{K-1}$. Moreover, we assume that \mathcal{J} be a Fréchet differentiable. Further requirements on U_{ad} and \mathcal{J} are made explicit in connection with Theorem 4, below.

Since the feasible set of problem (P_Ψ) is non-empty due to the results from the previous section, the existence of globally optimal points can be verified via standard arguments from optimization theory. Hereby, some classical assumptions on the objective functional and the constraint set U_{ad} are imposed, cf. [83].

Theorem 4 (Existence of global solutions) *Suppose that the objective functional $\mathcal{J} : \overline{H}_{\partial_n}^2(\Omega)^K \times \overline{H}_{\partial_n}^2(\Omega)^K \times H_{0,\sigma}^1(\Omega; \mathbb{R}^n)^{K-1} \times L^2(\Omega; \mathbb{R}^n)^{K-1} \rightarrow \mathbb{R}$ is convex and weakly lower-semi-continuous and U_{ad} is non-empty, closed and convex. Assume that either U_{ad} is bounded or \mathcal{J} is partially coercive, i.e. for every sequence $\{(\varphi^{(k)}, \mu^{(k)}, \nu^{(k)}, u^{(k)})\}_{k \in \mathbb{N}}$ which satisfies $\lim_{k \rightarrow \infty} \|u^{(k)}\| = +\infty$ it holds true that $\lim_{k \rightarrow \infty} \mathcal{J}(\varphi^{(k)}, \mu^{(k)}, \nu^{(k)}, u^{(k)}) = +\infty$.*

Then the optimization problem (P_Ψ) admits a global solution.

The proof is based on a convergence analysis for the weak limit point of infimizing sequences for the optimal control problem (P_Ψ) .

The optimal control problem associated to the Cahn-Hilliard-Navier-Stokes system with matched densities and a non-smooth homogeneous free energy density (double-obstacle potential) has been previously studied in [92, 93]. We also mention the recent articles [59] (which treats the control of a nonlocal Cahn-Hilliard-Navier-Stokes system in two dimensions) and [135]. Apart from these contributions the literature on the optimal control of the coupled CHNS system with non-matched densities is - to the best of our knowledge - essentially void. Nevertheless, there are numerous publications concerning the optimal control of the phase separation process itself, i.e. the distinct Cahn-Hilliard system; see, e.g., [25, 39, 40, 52, 78, 91, 145, 147].

For some applications, a boundary control might be easier to realize than the distributed control. Hereby, the homogeneous boundary of the velocity field is omitted in favor of the boundary condition

$$v_{i+1}|_{\partial\Omega} = u_{i+1}. \quad (60)$$

In this case, the control u_{i+1} is an element of the space $H_{Tr} := Tr(H_\sigma^1(\Omega; \mathbb{R}^n))$, where Tr denotes the zero-order trace operator, cf., e.g., [5]. Due to the embedding properties of Sobolev spaces, H_{Tr} is contained in $H^{\frac{1}{2}}(\partial\Omega; \mathbb{R}^n)$. Moreover, it is a Hilbert space and the trace operator regarded from $H_\sigma^1(\Omega; \mathbb{R}^n)$ into H_{Tr} is a linear, bounded and surjective mapping between Hilbert spaces. Hence, there exists a right inverse operator $B_{Tr} : H_{Tr} \rightarrow H_\sigma^1(\Omega; \mathbb{R}^n)$ such that $Tr \circ B_{Tr}$ equals the identity operator on H_{Tr} , cf. [12, 73].

The operator can be employed to reduce the inhomogeneous Navier-Stokes system to the problem with homogeneous Dirichlet boundary conditions, which is used in [92], to derive the existence of solutions to the associated Cahn-Hilliard-Navier-Stokes system. In the aforementioned article, a boundary-control equivalent of the problem (P_Ψ) is studied with a tracking-type functional for matched densities. Furthermore, the constraint set U_{ad} is assumed to be a closed, linear subspace of H_{Tr} and an additional compatibility condition on the given data is imposed.

Though the involved trace spaces require a careful (embedding) analysis as sketched above, similar arguments as for the distributed control can be cited to derive an analogous stationarity system due to the linearity of the trace operator, cf. [92].

3.3.1 Stationarity conditions

One of the major challenges of optimal control theory is the derivation of meaningful optimality conditions. This is not only to provide a more precise characterization of globally and/or locally optimal points, but also facilitates the development of efficient numerical solution methods to approximate these solutions.

However, we recall that in the presence of the non-smooth double-obstacle potential the phase field model includes a variational inequality of the form

$$-\Delta\varphi_{i+1} + a_{i+1} - \mu_{i+1} - \kappa\varphi_i = 0, \quad (61)$$

with $a_{i+1} \in \partial\Psi_0(\varphi_{i+1})$, which can be reformulated as

$$\langle -\Delta\varphi_{i+1} + a_{i+1} - \mu_{i+1} - \kappa\varphi_i, \phi - \varphi_{i+1} \rangle \geq 0, \forall \phi \in \mathbb{K}. \quad (62)$$

As a result the associated optimal control problem falls into the realm of mathematical programs with equilibrium constraints (MPECs) in function space (see e.g. [83,92]), which, as already mentioned earlier in this exposition, is well-known for its constraint degeneracy even in finite dimensions; see, e.g., [105, 117].

In order to demonstrate the upcoming difficulties in the context of the optimal control problem (P_Ψ) , we point out that Lemma 2 ensures that the order parameter φ_{i+1} is an element of $H^2(\Omega)$. Although the subdifferential $\partial\Psi_0$ is in general only contained in the dual space $\overline{H}^1(\Omega)^*$, this allows us to deduce the following additional regularity for the subgradient a_{i+1}

$$a_{i+1} = \Delta\varphi_{i+1} + \mu_{i+1} + \kappa\varphi_i \in L^2(\Omega). \quad (63)$$

Consequently, the duality pairing in (62) can be equivalently defined as the inner product in $L^2(\Omega)$. Moreover, the following sets are well-defined.

Definition 3 For a solution φ_{i+1} of the variational inequality (62), we introduce the active sets

$$\mathcal{A}_{\varphi_{i+1},1} := \{x \in \Omega : \varphi_{i+1}(x) = \psi_1\}, \quad (64)$$

$$\mathcal{A}_{\varphi_{i+1},2} := \{x \in \Omega : \varphi_{i+1}(x) = \psi_2\}, \quad (65)$$

the strongly active sets

$$\mathcal{A}_{\varphi_{i+1},1}^+ := \{x \in \Omega : \varphi_{i+1}(x) = \psi_1 \wedge a_{i+1}^-(x) > 0\}, \quad (66)$$

$$\mathcal{A}_{\varphi_{i+1},2}^+ := \{x \in \Omega : \varphi_{i+1}(x) = \psi_2 \wedge a_{i+1}^+(x) > 0\}, \quad (67)$$

the biactive sets

$$\mathcal{A}_{\varphi_{i+1},1}^0 := \{x \in \Omega : \varphi_{i+1}(x) = \psi_1 \wedge a_{i+1}(x) = 0\}, \quad (68)$$

$$\mathcal{A}_{\varphi_{i+1},2}^0 := \{x \in \Omega : \varphi_{i+1}(x) = \psi_2 \wedge a_{i+1}(x) = 0\}, \quad (69)$$

and the inactive set

$$\mathcal{I}_{\varphi_{i+1}} := \{x \in \Omega : \psi_1 < \varphi_{i+1}(x) < \psi_2\} \quad (70)$$

Hereby, $a_{i+1}^+(x) := \max(0, a_{i+1}(x))$ and $a_{i+1}^-(x) := -\min(0, a_{i+1}(x))$ are defined pointwise almost everywhere on Ω such that $a_{i+1} = a_{i+1}^+ - a_{i+1}^-$.

Note that the variational inequality (62) corresponds to the necessary and sufficient first-order optimality condition of the convex optimization problem

$$\min_{\varphi_{i+1} \in \mathbb{K}} \frac{1}{2} \|\nabla\varphi_{i+1}\|^2 - (\mu_{i+1} + \kappa\varphi_i, \varphi_{i+1}). \quad (71)$$

In this setting, a_{i+1}^- and a_{i+1}^+ correspond to the Lagrange multipliers associated with the inequality constraints $\varphi_{i+1} \geq \psi_1$ and $\varphi_{i+1} \leq \psi_2$, respectively. The variational inequality can be further expressed as the subsequent complementarity system

$$-\Delta\varphi_{i+1} + a_{i+1} - \mu_{i+1} - \kappa\varphi_i = 0, \quad (72a)$$

$$\varphi_{i+1} \geq \psi_1, \quad a_{i+1}^- \geq 0, \quad (a_{i+1}^-, \varphi_{i+1} - \psi_1) = 0, \quad (72b)$$

$$\varphi_{i+1} \leq \psi_2, \quad a_{i+1}^+ \geq 0, \quad (a_{i+1}^+, \varphi_{i+1} - \psi_2) = 0. \quad (72c)$$

From the complementarity conditions (72b), (72c), we directly infer that

$$\mathcal{A}_{\varphi_{i+1},1} \cup \mathcal{A}_{\varphi_{i+1},2} \cup \mathcal{I}_{\varphi_{i+1}} = \Omega. \quad (73)$$

With the help of (72) the optimization problem (P_Ψ) can be equivalently reformulated as the following mathematical program with complementarity conditions (MPCC)

$$\min \mathcal{J}(\varphi, \mu, v, u) \text{ over } (\varphi, \mu, v, u) \in \mathcal{X} \quad (74a)$$

$$\text{s.t. } u \in U_{ad}, \quad (74b)$$

$$\left\langle \frac{\varphi_{i+1} - \varphi_i}{\tau}, \phi \right\rangle + \langle v_{i+1} \nabla \varphi_i, \phi \rangle + (m(\varphi_i) \nabla \mu_{i+1}, \nabla \phi) = 0, \quad (74c)$$

$$(\nabla \varphi_{i+1}, \nabla \phi) + \langle a_{i+1}, \phi \rangle - \langle \mu_{i+1}, \phi \rangle - \langle \kappa \varphi_i, \phi \rangle = 0, \quad (74d)$$

$$\varphi_{i+1} \geq \psi_1, \quad a_{i+1}^- \geq 0, \quad (a_{i+1}^-, \varphi_{i+1} - \psi_1) = 0, \quad (74e)$$

$$\varphi_{i+1} \leq \psi_2, \quad a_{i+1}^+ \geq 0, \quad (a_{i+1}^+, \varphi_{i+1} - \psi_2) = 0, \quad (74f)$$

$$\begin{aligned} & \left\langle \frac{\rho(\varphi_i) v_{i+1} - \rho(\varphi_{i-1}) v_i}{\tau}, \psi \right\rangle_{H_{0,\sigma}^{-1}, H_{0,\sigma}^1} - (v_{i+1} \otimes \rho(\varphi_{i-1}) v_i, \nabla \psi) \\ & + \left(v_{i+1} \otimes \frac{\rho_2 - \rho_1}{2} m(\varphi_{i-1}) \nabla \mu_i, \nabla \psi \right) + (2\eta(\varphi_i) \varepsilon(v_{i+1}), \varepsilon(\psi)) \\ & - \langle \mu_{i+1} \nabla \varphi_i, \psi \rangle_{H_{0,\sigma}^{-1}, H_{0,\sigma}^1} - \langle u_{i+1}, \psi \rangle_{H_{0,\sigma}^{-1}, H_{0,\sigma}^1} = 0, \end{aligned} \quad (74g)$$

where (74c)-(74f) hold for every $\phi \in \overline{H}^1(\Omega)$, $0 \leq i+1 \leq M-1$, and equation (74g) holds for every $\psi \in H_{0,\sigma}^1(\Omega; \mathbb{R}^N)$, $1 \leq i+1 \leq M-1$.

In general, the corresponding control-to-state operator S_Ψ is not Fréchet differentiable at u , if the biactive set $\mathcal{A}_{\varphi_i,1}^0 \cup \mathcal{A}_{\varphi_i,2}^0$ associated with the state $(\varphi, \mu, v) = S(u)$ is non-empty. Moreover, the feasible set

$$\mathcal{F} := \{(\varphi, \mu, v, u) \in \mathcal{X} : u \in U_{ad}, (\varphi, \mu, v) = S_\Psi(u)\} \quad (75)$$

is non-convex.

In the classical optimization theory, we usually argue that the contingent cone of the feasible set at a given solution has a suitable polyhedral convex form, if the problem satisfies a constraint qualification, e.g., the Slater condition or the Mangasarian-Fromovitz constraint qualification. This allows for the derivation of more explicit multiplier-based stationarity concepts. However, due to the inherent nonconvexity of the feasible set \mathcal{F} , the corresponding contingent cone is in general neither convex nor polyhedral. Hence, the problem (74) fails to satisfy any of the classical constraint qualifications, which prevents the application of Karush-Kuhn-Tucker theory for the first-order characterization of optimal solutions by (Lagrange) multipliers. Instead, we have to acknowledge the combinatorial nature of the complementarity constraints, which leads to a variety of different stationarity concepts.

In [127], the authors presented a hierarchy of stationarity conditions for finite-dimensional MPECs based on some auxiliary nonlinear programs. The nonlinear programs emerge from (74) by omitting the complementarity equation, i.e. the last equation in (74e) and (74f), but eventually forcing one or both of the factors (i.e. φ_{i+1} , a_{i+1}^+ or a_{i+1}^-) to be equal to zero. These auxiliary programs 'encase' the original problem (74) in some sense. By relating the stationarity conditions of (74) to the necessary first-order conditions of the auxiliary programs, the notions of weak-, C- and strong stationarity for MPECs are introduced, cf. [127].

In order to illustrate these concepts in the infinite dimensional case, we define the associated MPCC-Lagrangian of (74).

Definition 4 The MPCC-Lagrangian $L : \mathcal{Y} \rightarrow \mathbb{R}$ corresponding to (P_Ψ) defined on the product space

$$\begin{aligned} \mathcal{Y} := & \bar{H}^1(\Omega)^M \times \bar{H}^1(\Omega)^M \times H_{0,\sigma}^1(\Omega; \mathbb{R}^N)^{M-1} \times \bar{L}^2(\Omega)^M \times L^2(\Omega; \mathbb{R}^n)^{M-1} \\ & \times \bar{H}^1(\Omega)^M \times \bar{H}^1(\Omega)^M \times H_{0,\sigma}^1(\Omega; \mathbb{R}^N)^{M-1} \times \bar{H}^1(\Omega)^M \\ & \times \left(\bar{H}^1(\Omega)^*\right)^M \times \left(\bar{H}^1(\Omega)^*\right)^M \end{aligned}$$

is given by

$$\begin{aligned} L(\varphi, \mu, v, a, u, p, r, q, \pi, \lambda^+, \lambda^-) := & J(\varphi, \mu, v, u) \\ & + \sum_{i=-1}^{M-2} \left[\left\langle \frac{\varphi^{i+1} - \varphi^i}{\tau}, p^{i+1} \right\rangle + \langle v^{i+1} \nabla \varphi^i, p^{i+1} \rangle + \langle m(\varphi^i) \nabla \mu^{i+1}, \nabla p^{i+1} \rangle \right] \\ & + \sum_{i=-1}^{M-2} \left[\langle -\Delta \varphi^{i+1}, r^{i+1} \rangle + \langle a^{i+1}, r^{i+1} \rangle - \langle \mu^{i+1}, r^{i+1} \rangle - \langle \kappa \varphi^i, r^{i+1} \rangle \right] \\ & + \sum_{i=0}^{M-2} \left[\left\langle \frac{\rho(\varphi^i) v^{i+1} - \rho(\varphi^{i+1}) v^i}{\tau}, q^{i+1} \right\rangle - \langle v^{i+1} \otimes \rho(\varphi^{i+1}) v^i, \nabla q^{i+1} \rangle_{H^{-1}, H_0^1} \right. \\ & \left. + \left\langle v^{i+1} \otimes \frac{\rho_2 - \rho_1}{2} m(\varphi^{i+1}) \nabla \mu^i, \nabla q^{i+1} \right\rangle_{H^{-1}, H_0^1} - \langle \mu^{i+1} \nabla \varphi^i, q^{i+1} \rangle_{H^{-1}, H_0^1} \right. \\ & \left. + (2\eta(\varphi^i) D_{\text{sy}}(v^{i+1}), D_{\text{sy}}(q^{i+1})) - \langle Bu^{i+1}, q^{i+1} \rangle_{H^{-1}, H_0^1} \right] \\ & - \sum_{i=0}^{M-1} \langle a^i, \pi^i \rangle + \sum_{i=0}^{M-1} \langle (\lambda^i)^+, \varphi^i - \psi_2 \rangle - \sum_{i=0}^{M-1} \langle (\lambda^i)^-, \varphi^i - \psi_1 \rangle. \quad (76) \end{aligned}$$

In general, dual stationarity conditions for a feasible point (φ, μ, v, a, u) of the problem (74) are based on the existence of multipliers $(p, r, q, \pi, \lambda^+, \lambda^-)$ such that

$$\nabla_{(\varphi, \mu, v, a, u)} L[\varphi, \mu, v, a, u, p, r, q, \pi, \lambda^+, \lambda^-](\varphi^\delta, \mu^\delta, v^\delta, a^\delta, u^\delta) = 0, \quad (77)$$

for every direction $(\varphi^\delta, \mu^\delta, v^\delta, a^\delta, u^\delta)$. This leads to the system

$$\begin{aligned} & -\frac{1}{\tau}(p^{i+1} - p^i) + m'(\varphi^i) \nabla \mu^{i+1} \cdot \nabla p^{i+1} - \text{div}(p^{i+1} v^{i+1}) - \Delta r^i \\ & + (\lambda^i)^+ - (\lambda^i)^- - \kappa r^{i+2} - \frac{1}{\tau} \rho(\varphi^i)' v^{i+1} \cdot (q^{i+2} - q^{i+1}) \\ & - (\rho(\varphi^i)' v^{i+1} - \frac{\rho_2 - \rho_1}{2} m'(\varphi^i) \nabla \mu^{i+1})(Dq^{i+2})^\top v^{i+2} \\ & + 2\eta(\varphi^i)' D_{\text{sy}}(v^{i+1}) : Dq^{i+1} + \text{div}(\mu^{i+1} q^{i+1}) = \frac{\partial J}{\partial \varphi^i}(z), \quad (78a) \end{aligned}$$

$$\begin{aligned} & -r^i - \text{div}(m(\varphi^{i-1}) \nabla p^i) - \text{div}\left(\frac{\rho_2 - \rho_1}{2} m(\varphi^{i-1})(Dq^{i+1})^\top v^{i+1}\right) \\ & - q^i \cdot \nabla \varphi^{i-1} = \frac{\partial J}{\partial \mu^i}(z), \quad (78b) \end{aligned}$$

$$\begin{aligned} & -\frac{1}{\tau} \rho(\varphi^{i-1})(q^{i+1} - q^i) - \rho(\varphi^{i-1})(Dq^{i+1})^\top v^{i+1} \\ & - (Dq^i)(\rho(\varphi^{i-2}) v^{i-1} - \frac{\rho_2 - \rho_1}{2} m(\varphi^{i-2}) \nabla \mu^{i-1}) \\ & - \text{div}(2\eta(\varphi^{i-1}) D_{\text{sy}}(q^i)) + p^i \nabla \varphi^{i-1} = \frac{\partial J}{\partial v^i}(z), \quad (78c) \end{aligned}$$

$$B^* q^i = \frac{\partial J}{\partial u^i}(z), \quad (78d)$$

$$r^i - \pi^i = 0. \quad (78e)$$

Here, we assumed that $U_{ad} = L^2(\Omega; \mathbb{R}^n)^{M-1}$ for the sake of simplicity. A rigorous derivation of the system (78) is postponed to the subsequent chapter.

Following the notation of the optimal control of partial differential equations, we refer to the equations (78a)-(78c) as adjoint equations and call (p, r, q) the corresponding adjoint state. Moreover, the multiplier π can be replaced by the adjoint state r via (78e) without loss of information.

Hereby, the multiplier $r_i (= \pi_i)$ should vanish on the strongly active set $\mathcal{A}_{\varphi_i,1}^+ \cup \mathcal{A}_{\varphi_i,2}^+$. Since r_i is an element of $H^1(\Omega)$, the condition can be interpreted pointwise almost everywhere on Ω , i.e.

$$r_i = 0 \text{ a.e. on } \mathcal{A}_{\varphi_i,1}^+ \cup \mathcal{A}_{\varphi_i,2}^+. \quad (79)$$

By the definition of $\mathcal{A}_{\varphi_i,1}^+$, $\mathcal{A}_{\varphi_i,2}^+$, this yields

$$\langle a_i, \pi_i \rangle = 0. \quad (80)$$

Similarly, we expect the multiplier $\lambda^i := (\lambda^i)^+ - (\lambda^i)^-$ to vanish on the inactive sets \mathcal{I}_{φ_i} . However, λ_i is in general only contained in $\overline{H}^1(\Omega)^*$ and lacks a pointwise interpretation on Ω . Therefore, it is unclear how to translate the condition to the infinite dimensional setting. In the sequel, we present three possible interpretations, which are connected to different stationarity conditions for the problem (74).

Definition 5 A point $(\varphi, \mu, v, a, u, p, r, q, \pi, \lambda^+, \lambda^-) \in \mathcal{Y}$ is called *weakly stationary* for (74), if the following conditions are satisfied:

- (I) the point (φ, μ, v, a, u) is feasible, i.e. it fulfills (74b)-(74g);
- (II) the adjoint system (78a)-(78d) is satisfied;
- (III) the equality (79) holds true;
- (IV) for every $v \in \overline{H}^1(\Omega)$ with $v|_{\Omega \setminus \mathcal{I}_{\varphi_i}} = 0$ it holds that

$$\langle \lambda^i, v \rangle = 0. \quad (81)$$

It is further called *almost weakly stationary*, if conditions (I)-(III) are fulfilled and for every $v \in \overline{H}^1(\Omega)$ with $v|_{\Omega \setminus \mathcal{I}_{\varphi_i}} = 0$ and $v|_{\mathcal{I}_{\varphi_i}} \in H_0^1(\mathcal{I}_{\varphi_i})$ it holds that

$$\langle \lambda^i, v \rangle = 0, \quad (82)$$

$$\langle (\lambda^i)^+, \varphi^i - \psi_2 \rangle = \langle (\lambda^i)^-, \varphi^i - \psi_1 \rangle = 0. \quad (83)$$

It is called \mathcal{E} -almost weakly stationary, if conditions (I)-(III) are fulfilled and for every $c > 0$ there exist a measurable subset \mathcal{I}_c^i of \mathcal{I}_{φ_i} with $|\mathcal{I}_{\varphi_i} \setminus \mathcal{I}_c^i| < c$ and

$$\langle \lambda^i, v \rangle = 0 \quad \forall v \in \overline{H}^1(\Omega), \quad v|_{\Omega \setminus \mathcal{I}_c^i} = 0, \quad (84)$$

$$\langle (\lambda^i)^+, \varphi^i - \psi_2 \rangle = \langle (\lambda^i)^-, \varphi^i - \psi_1 \rangle = 0. \quad (85)$$

The notion of ' \mathcal{E} -almost' is motivated by the fact that the proof of the associated stationarity conditions is usually based on the application of Egorov's theorem, cf. e.g. [13].

It can be easily verified that the above weak stationarity concepts obey a hierarchical structure, cf. e.g. [84]. More precisely, every weak stationary point is almost weak stationary and every almost weak stationary point is \mathcal{E} -almost weak stationary. The converse is generally not true. However, if the inactive set \mathcal{I}_{φ_i} has a Lipschitz boundary, i.e. it possesses the $C^{0,1}$ -regularity property, cf. [5], then the concepts of weak stationarity and almost weak stationarity coincide. Moreover, if λ_i can be defined pointwise almost everywhere on Ω (e.g. if $\lambda_i \in L^1(\Omega)$), then the three concepts are equivalent.

We further note that the equality (83) is implied by the definition of weak stationarity due to equation (81). Nevertheless it has to be explicitly included for the weaker versions of weak stationarity for which it is no longer automatically satisfied.

The notion of weak stationarity is the weakest available dual stationarity concept in function spaces, as it provides no information on the signs of the multipliers $r_i (= \pi_i)$ and λ_i . Similar to the finite dimensional setting, cf. [127], the above stationarity conditions can be supplemented by a sign condition for the product of r_i and λ_i to form C-stationarity type systems, or paired with explicit conditions for signs of r_i and λ_i , individually, leading to the respective strong stationarity concepts.

Typical approaches to establish these stationarity concepts rely on the relaxation, regularization and/or penalization of the degeneracy of the lower-level problem. However, the literature on infinite dimensional MPECs is comparatively scarce. In [21, 106, 107], the authors use the conical derivative of the solution operator of the variational inequality to derive a stationarity system for the control problem, which one would classify now as strong stationarity. A different approach is introduced in [13], where the variational inequalities are approximated by variational equations and optimality conditions are derived by a passage to the limit in the approximation process. This technique typically yields a weaker stationarity system only. Further contributions to the topic include [14, 22, 57, 98, 138] most of which use regularization-penalization methods.

A first step towards the systematization and completion of stationarity concepts in function space was undertaken in [84], where the concept of ε -almost C-stationarity is introduced, paving the way for various contributions in the recent past. Here, we also mention [88] where an abstract first-order optimality system is derived by means of variational analysis. In [142], the MPEC is approximated by a sequence of non smooth problems similar to the virtual control approach from [101].

In the sequel, we sketch how a Yosida regularization technique with a subsequent passage to the limit with the Yosida parameter can be used to derive conditions of ε -almost C-stationarity type for the optimal control problem (P_Ψ) . For more details on the proofs of the results of this section we refer to [83].

For this purpose, we introduce the following sequence of double-well type potentials which will be used to approximate the double-obstacle potential in the lower-level problem. Here, γ denotes the subdifferential of the indicator function of $[\psi_1, \psi_2]$, i.e. $\gamma := \partial i_{[\psi_1, \psi_2]}$.

Definition 6 Let a mollifier $\zeta \in C^1(\mathbb{R})$ with $\text{supp } \zeta \subset [-1, 1]$, $\int_{\mathbb{R}} \zeta = 1$ and $0 \leq \zeta \leq 1$ a.e. on \mathbb{R} , and a function $\theta : \mathbb{R}^+ \rightarrow \mathbb{R}^+$, with $\theta(\alpha) > 0$ and $\frac{\theta(\alpha)}{\alpha} \rightarrow 0$ as $\alpha \rightarrow 0$, be given. For the Yosida approximation γ_α with parameter $\alpha > 0$ of γ define

$$\begin{aligned} \zeta_\alpha(s) &:= \frac{1}{\alpha} \zeta\left(\frac{s}{\alpha}\right), \quad \tilde{\gamma}_\alpha := \gamma_\alpha * \zeta_{\theta(\alpha)}, \quad \Psi_{0,\alpha}(s) := \int_0^s \tilde{\gamma}_\alpha(x) dx, \\ \Psi_{0,\alpha}(\varphi) &:= \int_{\Omega} (\Psi_{0,\alpha} \circ \varphi)(x) dx. \end{aligned}$$

Moreover, we set $\alpha_k := k^{-1}$, $\Psi_0^{(k)} := \Psi_{0,\alpha_k}$.

In the sequel, we approximate the problem (P_Ψ) by auxiliary problems $(P_\Psi^{(k)})$ where the double-obstacle Ψ_0 is replaced by $\Psi_0^{(k)}$. We then derive necessary first-order optimality conditions for the auxiliary problems and establish a stationarity system for (P_Ψ) by considering the limit process for $\alpha \rightarrow 0$.

We point out that this method requires the verification of the existence of globally optimal solutions to the auxiliary problems. Hereby, the arguments of Section 3.2 cannot be directly transferred to the smooth case since ρ is no longer guaranteed to be non-negative if we maintain the affine connection of the order parameter and the density given in (52). However, the line of argumentation can be saved by manually enforcing the non-negativity of the density function, i.e. $\rho(\varphi) := \max \left\{ \frac{\rho_1 + \rho_2}{2} + \frac{\rho_2 - \rho_1}{2} (\varphi + \overline{\varphi}_a), 0 \right\}$, with the help of the following theorem.

Theorem 5 Let $u \in L^2(\Omega; \mathbb{R}^n)^{K-1}$ be given and let $\{(\varphi^{(k)}, \mu^{(k)}, v^{(k)})\}_{k \in \mathbb{N}}$ be a sequence of solutions to the systems (53)–(55) with $\Psi_0 = \Psi_0^{(k)}$. Then

$$\left\| \max(-\varphi^{(k)} + \psi_1, 0) \right\|_{L^\infty} \rightarrow 0, \text{ as } k \rightarrow \infty.$$

Theorem 5 ensures that the order parameter of a solution to the system (53)–(55) for the double-well type potentials under consideration is always greater than $\psi_1 - \varepsilon$ for a small $\varepsilon > 0$ if k is sufficiently large. Consequently, the corresponding density is positive.

The next theorem verifies the consistency of Moreau–Yosida type approximations, i.e. the convergence of a sequence of solutions to the auxiliary problems to a solution of (P_Ψ) for $k \rightarrow \infty$.

Theorem 6 (Consistency of the regularization) Let the assumptions of Theorem 4 be fulfilled and let $\mathcal{J} : \bar{H}^1(\Omega)^K \times \bar{H}^1(\Omega)^K \times H_{0,\sigma}^1(\Omega; \mathbb{R}^n)^{K-1} \times L^2(\Omega; \mathbb{R}^n)^{K-1} \rightarrow \mathbb{R}$ be upper-semicontinuous.

Then a sequence $\{(\varphi^{(k)}, \mu^{(k)}, v^{(k)}, u^{(k)})\}_{k \in \mathbb{N}}$ of global solutions to $(P_{\Psi^{(k)}})$ in $\bar{H}^2(\Omega)^K \times \bar{H}^2(\Omega)^K \times H_{0,\sigma}^1(\Omega; \mathbb{R}^n)^{K-1} \times U_{ad}$ converges to a global solution of $(P_{\bar{\Psi}})$, provided that $\{ \mathcal{J}(\varphi^{(k)}, \mu^{(k)}, v^{(k)}, u^{(k)}) \}_{k \in \mathbb{N}}$ is assumed bounded, whenever U_{ad} is unbounded.

At this point, we turn our attention to the derivation of stationarity conditions for the optimal control problem. For the smooth potential functions, first-order optimality conditions can be directly derived using a classical result from Zowe and Kurcyusz, [150, Theorem 4.1] which leads to the following theorem.

Theorem 7 (First-order optimality conditions for smooth potentials) Let $\mathcal{J} : \bar{H}^1(\Omega)^K \times \bar{H}^1(\Omega)^K \times H_{0,\sigma}^1(\Omega; \mathbb{R}^n)^{K-1} \times L^2(\Omega; \mathbb{R}^n)^{K-1} \rightarrow \mathbb{R}$ be Fréchet differentiable and let $\bar{z} := (\bar{\varphi}, \bar{\mu}, \bar{v}, \bar{u})$ be a minimizer of the auxiliary problem $(P_{\bar{\Psi}}^{(k)})$.

Then there exist $(p, r, q) \in \bar{H}^1(\Omega)^K \times \bar{H}^1(\Omega)^{K-1} \times H_{0,\sigma}^1(\Omega; \mathbb{R}^n)^{K-1}$, with $p = (p_{-1}, \dots, p_{K-2})$, $r = (r_{-1}, \dots, r_{K-2})$, $q = (q_0, \dots, q_{K-2})$, such that

$$\begin{aligned} & -\frac{1}{\tau}(p_i - p_{i-1}) + m'(\varphi_i) \nabla \mu_{i+1} \cdot \nabla p_i - \operatorname{div}(p_i v_{i+1}) - \Delta r_{i-1} \\ & \quad + \Psi_0''(\varphi_i)^* r_{i-1} - \kappa r_{i+1} - \frac{1}{\tau} \rho'(\varphi_i) v_{i+1} \cdot (q_{i+1} - q_i) \\ & \quad - (\rho'(\varphi_i) v_{i+1} - \frac{\rho_2 - \rho_1}{2} m'(\varphi_i) \nabla \mu_{i+1}) (Dq_{i+1})^\top v_{i+2} \\ & \quad + 2\eta'(\varphi_i) \varepsilon(v_{i+1}) : Dq_i + \operatorname{div}(\mu_{i+1} q_i) = \frac{\partial \mathcal{J}}{\partial \varphi_i}(\bar{z}), \end{aligned} \quad (86)$$

$$\begin{aligned} & -r_{i-1} - \operatorname{div}(m(\varphi_{i-1}) \nabla p_{i-1}) - \operatorname{div}\left(\frac{\rho_2 - \rho_1}{2} m(\varphi_{i-1}) (Dq_i)^\top v_{i+1}\right) \\ & \quad - q_{i-1} \cdot \nabla \varphi_{i-1} = \frac{\partial \mathcal{J}}{\partial \mu_i}(\bar{z}), \end{aligned} \quad (87)$$

$$\begin{aligned} & -\frac{1}{\tau} \rho(\varphi_{j-1}) (q_j - q_{j-1}) - \rho(\varphi_{j-1}) (Dq_j)^\top v_{j+1} \\ & \quad - (Dq_{j-1}) (\rho(\varphi_{j-2}) v_{j-1} - \frac{\rho_2 - \rho_1}{2} m(\varphi_{j-2}) \nabla \mu_{j-1}) \\ & \quad - \operatorname{div}(2\eta(\varphi_{j-1}) \varepsilon(q_{j-1})) + p_{j-1} \nabla \varphi_{j-1} = \frac{\partial \mathcal{J}}{\partial v_j}(\bar{z}), \end{aligned} \quad (88)$$

$$\left(\frac{\partial \mathcal{J}}{\partial u_k}(\bar{z}) - q_{k-1} \right)_{k=1}^{K-1} \in [\mathbb{R}_+(U_{ad} - \bar{u})]^+, \quad (89)$$

for all $i = 0, \dots, K-1$ and $j = 1, \dots, K-1$. Here, $[\mathbb{R}_+(U_{ad} - \bar{u})]^+$ denotes the polar cone of the set $\{r(w - u) \mid w \in U_{ad}, r \in \mathbb{R}^+\}$. Furthermore, we use the convention that p_i, r_i, q_i are equal to 0 for $i \geq K-1$ along with q_{-1} and φ_i, μ_i, v_i for $i \geq K$.

In order to pass to the limit with respect to $k \rightarrow \infty$ it is necessary to ensure that the adjoint state (p, r, q) is bounded independently of the regularization parameter. This leads to the following theorem which states the adjoint system for the optimal control problem (P_Ψ) , cf. [83].

Theorem 8 (Stationarity conditions) *Suppose that the following assumptions are satisfied.*

- 1 \mathcal{J}' is a bounded mapping from $\bar{H}^1(\Omega)^K \times \bar{H}^1(\Omega)^K \times H_{0,\sigma}^1(\Omega; \mathbb{R}^n)^{K-1} \times U_{ad}$ into the space $(\bar{H}^1(\Omega)^K \times \bar{H}^1(\Omega)^K \times H_{0,\sigma}^1(\Omega; \mathbb{R}^n)^{K-1} \times L^2(\Omega; \mathbb{R}^n)^{K-1})^*$ and $\frac{\partial \mathcal{J}}{\partial u}$ satisfies the following weak lower-semicontinuity property

$$\left\langle \frac{\partial \mathcal{J}}{\partial u}(\hat{z}), \hat{u} \right\rangle \leq \liminf_{n \rightarrow \infty} \left\langle \frac{\partial \mathcal{J}}{\partial u}(\hat{z}^{(k)}), \hat{u}^{(k)} \right\rangle,$$

for $\hat{z}^{(k)} = (\hat{\phi}^{(k)}, \hat{\mu}^{(k)}, \hat{v}^{(k)}, \hat{u}^{(k)})$ converging weakly in

$$\bar{H}_{\partial_n}^2(\Omega)^K \times \bar{H}_{\partial_n}^2(\Omega)^K \times H_{0,\sigma}^1(\Omega; \mathbb{R}^n)^{K-1} \times U_{ad}$$

to $\hat{z} = (\hat{\phi}, \hat{\mu}, \hat{v}, \hat{u})$.

- 2 Let $(\varphi^{(k)}, \mu^{(k)}, v^{(k)}, u^{(k)}) \in \bar{H}_{\partial_n}^2(\Omega)^K \times \bar{H}_{\partial_n}^2(\Omega)^K \times H_{0,\sigma}^1(\Omega; \mathbb{R}^n)^{K-1} \times U_{ad}$ be a minimizer for $(P_{\Psi^{(k)}})$ and let further $(p^{(k)}, r^{(k)}, q^{(k)}) \in \bar{H}^1(\Omega)^K \times \bar{H}^1(\Omega)^K \times H_{0,\sigma}^1(\Omega; \mathbb{R}^n)^{K-1}$ be given as in Theorem 7.

Then there exists an element $(\varphi, \mu, v, u, p, r, q)$ and a subsequence denoted by $\{(\varphi^{(m)}, \mu^{(m)}, v^{(m)}, u^{(m)}, p^{(m)}, r^{(m)}, q^{(m)})\}_{m \in \mathbb{N}}$ with

$$\begin{aligned} \varphi^{(m)} &\rightarrow \varphi \text{ weakly in } \bar{H}_{\partial_n}^2(\Omega)^K, \quad \mu^{(m)} \rightarrow \mu \text{ weakly in } \bar{H}_{\partial_n}^2(\Omega)^{K-1}, \\ v^{(m)} &\rightarrow v \text{ weakly in } H^2(\Omega; \mathbb{R}^n)^{K-1}, \quad u^{(m)} \rightarrow u \text{ weakly in } L^2(\Omega; \mathbb{R}^n)^{K-1}, \\ p^{(m)} &\rightarrow p \text{ weakly in } \bar{H}^1(\Omega)^K, \quad r^{(m)} \rightarrow r \text{ weakly in } \bar{H}^1(\Omega)^{K-1}, \\ q^{(m)} &\rightarrow q \text{ weakly in } H_{0,\sigma}^1(\Omega; \mathbb{R}^n)^{K-1}, \quad \Psi_0^{(m)''}(\varphi_{i+1}^{(m)})^* r_i^{(m)} \rightarrow \lambda_i \text{ weakly in } \bar{H}^1(\Omega)^*, \end{aligned}$$

for all $i = -1, \dots, K-2$ which satisfies (86)-(89) where $\Psi_0''(\varphi_i)^* r_{i-1}$ is replaced by λ_{i-1} .

If the set U_{ad} is bounded, Theorem 8 holds also true for a sequence of stationary points for $(P_{\Psi^{(k)}})$. If it is unbounded, then the result can still be transferred to sequences of stationary points by assuming that the sequence $\{u^{(k)}\}_{k \in \mathbb{N}}$ is bounded in $L^2(\Omega; \mathbb{R}^n)^{K-1}$. Considering such sequences of stationary points only (rather than global solutions to the smooth, but yet non-convex auxiliary problems) favors numerical techniques as these typically can only guarantee stationary points.

The aforementioned multiplier conditions on r and λ are derived through a careful limiting analysis of the corresponding terms.

Theorem 9 (Limiting ε -almost C-stationarity) *Let $\Psi_0^{(m)}$, $m \in \mathbb{N}$ be the functionals of Definition 6, and let the tuples $(\varphi^{(m)}, \mu^{(m)}, v^{(m)}, u^{(m)}, p^{(m)}, r^{(m)}, q^{(m)})$, $(\varphi, \mu, v, u, p, r, q)$ and \mathcal{J} be as in Theorem 8. Moreover, let $\Lambda: \mathbb{R} \rightarrow \mathbb{R}$ be a Lipschitz function with $\Lambda(\psi_1) = \Lambda(\psi_2) = 0$. For*

$$a_i^{(m)} := \Psi_0^{(m)'}(\varphi_i^{(m)}), \quad \lambda_i^{(m)} := \Psi_0^{(m)''}(\varphi_i^{(m)})^* r_{i-1}^{(m)} \quad (90)$$

for $i = 0, \dots, K$, and for a_i denoting the limit of $a_i^{(m)}$, it holds that

$$(a_i, \Lambda(\varphi_i))_{L^2} = 0, \quad \langle \lambda_i, \Lambda(\varphi_i) \rangle = 0, \quad (91)$$

$$(a_i, r_{i-1})_{L^2} = 0, \quad \liminf (\lambda_i^{(m)}, r_{i-1}^{(m)})_{L^2} \geq 0. \quad (92)$$

Moreover, for every $\varepsilon > 0$ there exist a measurable subset M_i^ε of $M_i := \{x \in \Omega : \psi_1 < \varphi_i(x) < \psi_2\}$ with $|M_i \setminus M_i^\varepsilon| < \varepsilon$ and

$$\langle \lambda_i, v \rangle = 0 \quad \forall v \in \bar{H}^1(\Omega), \quad v|_{\Omega \setminus M_i^\varepsilon} = 0.$$

In combination with the adjoint system from Theorem 8, the last theorem states stationarity conditions corresponding to a function space version of limiting ε -almost C-stationarity type. For the underlying problem class, this is currently the most (and, to the best of our knowledge, only) selective stationarity system available.

3.4 Numerical solution methods

3.4.1 Adaptive mesh refinement techniques

A major challenge throughout the development of numerical solution algorithms for the optimal control of phase field models is the accurate reproduction of the corresponding interface. More precisely, the distinct characteristics of phase field models call for an appropriate adaptation of the underlying mesh, since solutions normally maintain a smooth structure on large parts of the domain, whereas most of the information is concentrated at the small interfacial layers. As the interfacial region is known to be characterized by $|\varphi| < 1$ a common heuristic approach is to refine the mesh locally based on the modulus of φ , see e.g. [6, 23, 99]. Since we have $|\nabla\varphi| \approx \frac{1}{\pi\varepsilon}$ at the center of the interfacial region, the value $|\nabla\varphi|$ can also be used as an indicator for the interface, see e.g. [68]. The first variant leads to a homogeneously refined mesh across the interface, while in the second case most refinement takes place around the zero level line of φ where $|\nabla\varphi|$ takes its maximum. We refer to [77], for a comparison of different refinement and marking strategies.

In [78], reliable and efficient residual based error estimation is proposed for the Cahn–Hilliard system with a relaxed non-smooth double-obstacle free energy. In [77], the former work is extended to the simulation of two-phase flow based on model ‘H’ and it is further extended to the simulation of variable density two-phase flow based on the model of [4] in [62], where additionally arbitrary polynomially bounded free energies are used. We note that based on results of [33] in [61] for a Cahn–Hilliard type model it is argued that an estimator based on the jumps of normal derivatives in general will result in well adapted meshes.

A-posteriori error estimation for the Cahn–Hilliard systems with non-smooth double obstacle free energy is proposed in [15, 16]. There, also residual based error estimation is proposed and reliability of the derived estimator is shown.

Such refinement strategies however ignore the contributions of the velocity field v (which is included for residual based methods) and, in the presence of the optimal control problem, the contribution of the adjoint variables to the total discretization error. This is why an adaptive error estimator which consists of dual-weighted primal residuals, primal-weighted dual residuals and complementarity errors is more favorable, cf. e.g. [17, 18].

While AFEM for PDE-constrained optimal control problems have been studied in great detail over the last decades, see, e.g., [79, 80, 140] for optimal control problems with control constraints, [20, 81] for state constraints, and [46, 70, 76] for optimal control problems governed by point-wise gradient constraints on the state, the literature on goal-oriented mesh adaptivity methods appears rather scarce with respect to MPECs in function spaces. However, in [30, 82] the method was successfully applied to the optimal control of elliptic variational inequalities.

The basic idea is to use the MPCC Lagrangian (76) and the associated saddle-point condition for optimal points to provide an estimation of the difference of the objective values at stationary points of the semi-discrete and of the fully discretized problem. When applying the method, e.g.,

to the optimal control problem (P_Ψ) it can be shown that

$$\begin{aligned} \mathcal{J}(\varphi_h, \mu_h, v_h, u_h) - \mathcal{J}(\varphi, \mu, v, u) &= \frac{1}{2} \left(\sum_{i=0}^{K-1} \langle a_h^i, \pi^i \rangle - \sum_{i=0}^{K-1} \langle a^i, \pi^i \rangle \right) \\ &+ \frac{1}{2} \left(\sum_{i=0}^{K-1} \langle (\lambda^i)^+, \varphi_h^i - \psi_2 \rangle - \sum_{i=0}^{K-1} \langle (\lambda_h^i)^+, \varphi^i - \psi_2 \rangle \right) \\ &+ \frac{1}{2} \left(\sum_{i=0}^{K-1} \langle (\lambda^i)^-, \varphi_h^i - \psi_1 \rangle - \sum_{i=0}^{K-1} \langle (\lambda_h^i)^-, \varphi^i - \psi_1 \rangle \right) \\ &+ \frac{1}{2} \nabla_x L(y_h, u_h, \Phi_h, \pi_h, \lambda_h^+, \lambda_h^-)((y_h, u_h, \Phi_h) - (y, u, \Phi)) \\ &+ O(\|(y_h, u_h, \Phi_h) - (y, u, \Phi)\|^3), \end{aligned} \quad (93)$$

where $(y, u, \Phi, \pi, \lambda^+, \lambda^-)$ is a stationary point of the optimal control problem (P_Ψ) and $(y_h, u_h, \Phi_h, \pi_h, \lambda_h^+, \lambda_h^-)$ satisfies a discretized stationarity system., cf. [75]. Hereby, we set $y := (\varphi, \mu, a, v)$ and $\Phi := (p, r, q)$. Moreover, O denotes the Landau symbol Big- O .

The penultimate term on the right-hand side of equation (93) assembles the weighted dual and primal residuals. Whereas the previous terms display the mismatch in the complementarity between the discretized solution and the original one.

In other words, the discretization error with respect to the objective function can be estimated by

$$\begin{aligned} \mathcal{J}(\varphi_h, \mu_h, v_h, u_h) - \mathcal{J}(\varphi, \mu, v, u) \\ \approx \sum_{i=0}^{K-1} (\eta_{CM1,i} + \eta_{CM2,i} + \eta_{CM3,i} + \eta_{CM4,i} + \eta_{CH1,i} \\ + \eta_{CH2,i} + \eta_{NS,i} + \eta_{AD\varphi,i} + \eta_{AD\mu,i} + \eta_{ADv,i}), \end{aligned} \quad (94)$$

where the complementarity error terms $\eta_{CM1,i}, \dots, \eta_{CM4,i}$, the weighted primal residuals $\eta_{CH1,i}, \eta_{CH2,i}, \eta_{NS,i}$ and the weighted dual residuals $\eta_{AD\varphi,i}, \eta_{AD\mu,i}, \eta_{ADv,i}$ are defined as in [75, Section 4]. We point out that the integral structure of these error terms allows a patchwise evaluation on the underlying mesh. Apart from the weights $\varphi_\delta^i, \mu_\delta^i$ and v_δ^i and $p_\delta^i, q_\delta^i, r_\delta^i$, respectively, the primal-dual-weighted error estimators only contain discrete quantities. In order to obtain a fully a-posteriori error estimator the weights are approximated involving a local higher-order approximation based on the respective discrete variables.

3.4.2 Numerical solution algorithms

As in our analytical investigations, the non-differentiability of the control-to-state operator also complicates the development of numerical solution algorithms for the optimal control of phase field models. As a consequence, there exist various approaches to design numerical solution algorithms. The different approaches can be typically linked to a specific derivation of the stationarity conditions and (like those) either rely on the relaxation, regularization and/or penalization of the degeneracy of the lower-level problem and a suitable adjustment of the corresponding (relaxation) parameter or on a direct characterization/calculation of some generalized derivative of the control-to-state operator, see e.g. [85, 90, 98, 128]. In this section, we exemplarily illustrate a regularizing algorithm which corresponds to the presented analytical approach.

For this purpose, we suppose that the stationarity conditions (86)-(89) are discretized in space based on Taylor-Hood finite elements which are known to be LBB-stable in case of the Navier-Stokes equation, cf., e.g., [65, 139]. More precisely, the phase field and the chemical potential are discretized via piecewise linear and globally continuous finite elements, whereas the discretization of the velocity field utilizes piecewise quadratic and globally continuous finite elements. For

more details on the chosen discretization approach we refer the reader to [75]. Furthermore, we consider the objective functional of tacking type given in (59).

We solve the resulting fully discrete optimization problem for a sequence $\alpha \rightarrow 0$ on a sequence of meshes $(\mathcal{T}^i)_{i=1}^K$, where we approximate Ψ_0 by the following expression

$$\Psi_{0,\alpha}(\varphi) := \frac{1}{2\alpha} (\max(0, \varphi - 1)^2 + \min(\varphi + 1)^2), \quad \alpha > 0.$$

If a solution to these regularized problems is successfully calculated by a steepest descent method employing the characterization of the derivative of \mathcal{J} in Theorem 7, then α is decreased until an approximate optimal control on the current sequence of grids is found that solves the original optimal control problem sufficiently well in the sense that it satisfies the complementarity conditions (91), (92) up to a given tolerance tol_c . Here, we define the multipliers a, λ based on the relation (90). The algorithm is enhanced by an outer adaptation loop which is based on the error estimator given in (94). The complete procedure is sketched in Algorithm 1.

Data: Initial data: $\varphi_{-1}, \varphi_0, v_0$ and $u_0 = 0$;

```

1 repeat
2   repeat
3     solve the regularized problem  $(P_{\Psi_\alpha})$  using a steepest descent method;
4     decrease  $\alpha$ ;
5   until complementarity conditions (91), (92) are satisfied up to a tolerance  $tol_c$ ;
6   calculate the error indicators and identify the sets  $\mathcal{M}_r, \mathcal{M}_c$  of cells to refine/coarsen;
7   adapt  $(\mathcal{T}^i)_{i=1}^K$  based on  $\mathcal{M}_r$  and  $\mathcal{M}_c$ ;
8 until  $\sum_{i=1}^K |\mathcal{T}^i| > \mathcal{A}_{\max}$ ;

```

Algorithm 1: The overall solution procedure

The mesh refinement of the grids $(\mathcal{T}^i)_{i=1}^K$ relies on the Dörfler marking procedure. More precisely, the error indicators from (94) are evaluated for all time steps i and for all cells $T \in \mathcal{T}^i$ individually and a set \mathcal{M}_r of cells to be refined is chosen as the set with the smallest cardinality which satisfies

$$\sum_{T \in \mathcal{M}_r} \eta_T \geq \theta^r \sum_{i=1}^K \sum_{T \in \mathcal{T}^i} \eta_T,$$

for a given parameter $0 < \theta^r < 1$. Due to the movement of the interface, we also select cells for coarsening if the calculated error indicator is smaller than a certain fraction of the mean error, i.e.

$$\mathcal{M}_c := \left\{ T \in (\mathcal{T}^i)_{i=1}^K \mid \eta_T \leq \frac{\theta^c}{\mathcal{A}} \sum_{i=1}^K \sum_{T \in \mathcal{T}^i} \eta_T \right\},$$

where $0 < \theta^c < 1$ is fixed and $\mathcal{A} := \sum_{i=1}^K |\mathcal{T}^i|$. The mesh refinement process is terminated if a desired total number of cells \mathcal{A}_{\max} is exceeded.

3.4.3 Numerical examples

Finally, the performance of Algorithm 1 for solving the phase field model (46) is illustrated. Hereby, we focus on the depiction of topological changes and geometric forms throughout the evolution process. In the first example, the aim is to split a single droplet into two separate square shaped regions. In the second example, a ring-shaped initial region should be deformed into a curved channel. For this purpose, 8 (first example) or 16 (second example) locally supported Ansatz functions of the control are employed, which are distributed over the two-dimensional domain.

The initial state, the desired state and the control for the first and second example are depicted in the first rows of Figure 7 and Figure 8, respectively.

The associated fluid parameters are given by $\rho_1 = 1000$, $\rho_2 = 100$, $\eta_1 = 10$, $\eta_2 = 1$, and $\sigma = 24.5 \cdot \frac{2}{\pi}$ and are taken from a benchmark problem for rising bubble dynamics in [97]. Furthermore, a gravitational acceleration $g = 0.981$ in the vertical direction is incorporated and $\varepsilon = 0.04$ as well as $m(\varphi) \equiv \frac{1}{12500}$ are set. The time horizon is $T = 1.0$, and the time step size is $\tau = 0.00125$.

For the marking procedure the parameter values $\theta^r = 0.7$ and $\theta^c = 0.01$ are fixed. Furthermore, the stopping criteria use the tolerance $tol_c = 1e-3$ for the complementarity conditions and the maximum amount of cells $\mathcal{A}_{max} = 8e6$ for the adaptation process, which relates to $1e4$ cells in average per time instance.

In Figure 7, the computed evolution of the order parameter is presented. As expected, the algorithm easily handles the split-up of the droplet. However, notice that phase field models can not approach sharp corners, due to their inherent regularization property. This causes an ineradicable mismatch of the final and the desired state.

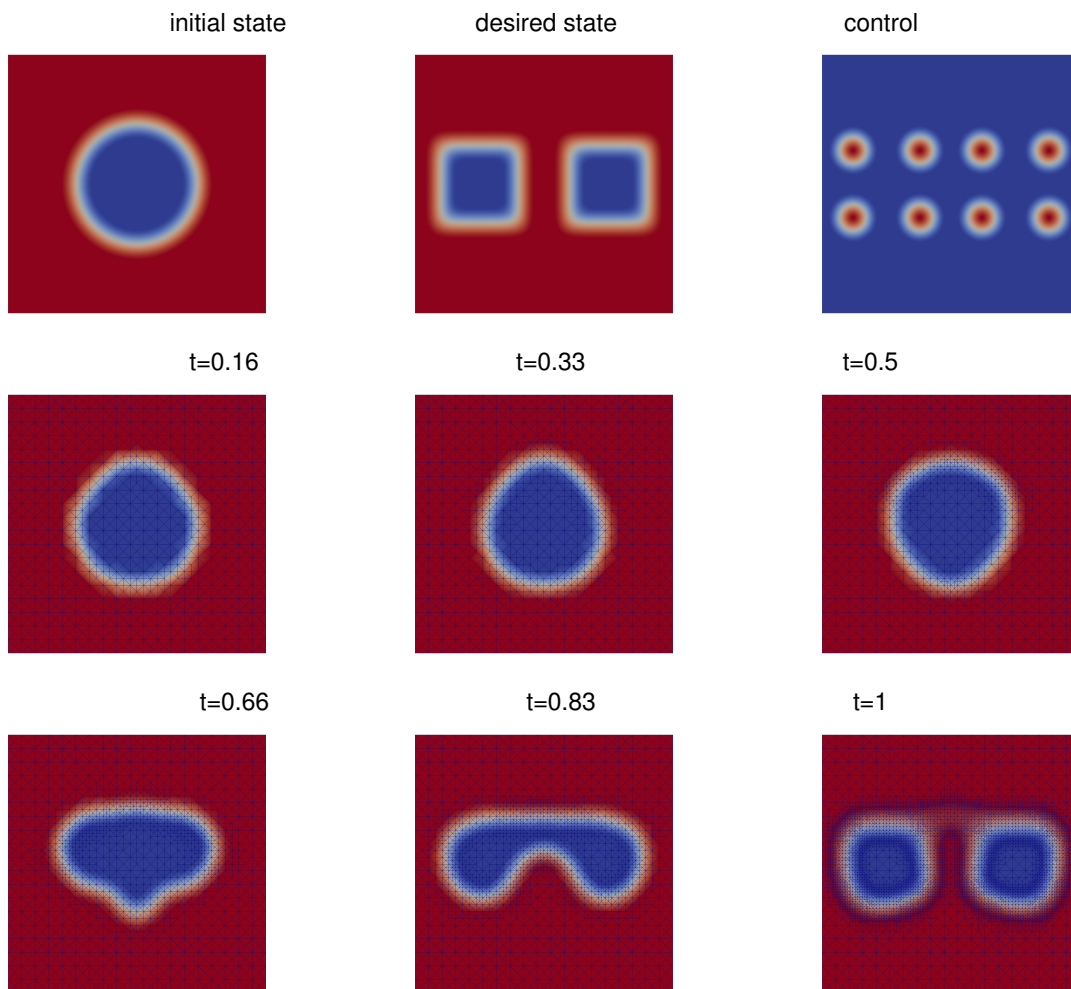


Figure 7: The initial state, the desired state, the control and the order parameter at different times for the first example.

In contrast, the calculated final state of the second example matches the desired state more closely; see 8. Here we see that the ring-shaped initial region is deformed in such a way that the upper part of the ring is pushed towards the top of the domain and the lower part is pushed

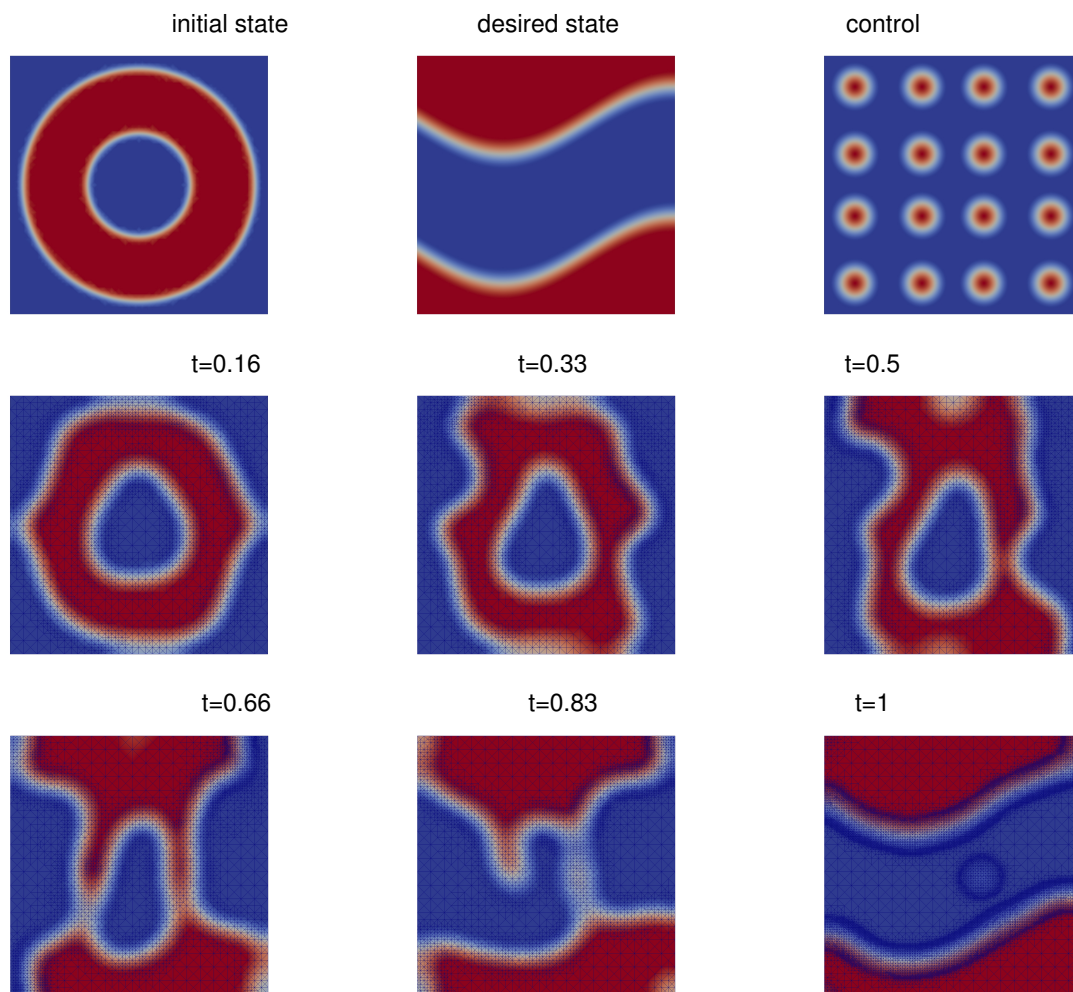


Figure 8: The initial state, the desired state, the control and the order parameter at different times for the second example.

towards the bottom. As a result the phase splits into two separate regions towards the end of the evolution.

In both examples one observes a fine resolution of the interfacial boundaries similar to conventional adaptation techniques based on the gradient of φ . However, additionally some refinements on the bulk phases, which are related, e.g., to the error associated with the velocity field are witnessed. Moreover, the goal-oriented error indicator incorporates the structure of the optimization problem which leads to comparatively more refinements at the end of the evolution process. This is illustrated in Figure 9, where the distribution of cells over the simulation time for the dual-weighted residuals method and a conventional adaptive method based on the order parameter φ are compared for the second example.

References

- [1] Abels, H., Breit, D.: Weak Solutions for a Non-Newtonian Diffuse Interface Model with Different Densities. arXiv:1509.05663v1 (2015). URL <http://arxiv.org/abs/1509.05663>
- [2] Abels, H., Depner, D., Garcke, H.: Existence of weak solutions for a diffuse interface model for two-phase flows of incompressible fluids with different densities. *J. Math. Fluid Mech.*

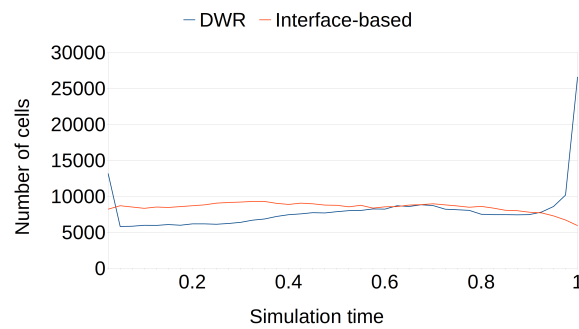


Figure 9: The number of cells at each time step for the goal-oriented method and for an adaptation based on the order parameter φ .

- 15**(3), 453–480 (2013). DOI 10.1007/s00021-012-0118-x. URL <http://dx.doi.org/10.1007/s00021-012-0118-x>
- [3] Abels, H., Depner, D., Garcke, H.: On an incompressible Navier-Stokes/Cahn-Hilliard system with degenerate mobility. *Ann. Inst. H. Poincaré Anal. Non Linéaire* **30**(6), 1175–1190 (2013). DOI 10.1016/j.anihpc.2013.01.002. URL <https://doi.org/10.1016/j.anihpc.2013.01.002>
- [4] Abels, H., Garcke, H., Grün, G.: Thermodynamically consistent, frame indifferent diffuse interface models for incompressible two-phase flows with different densities. *Mathematical Models and Methods in Applied Sciences* **22**(3), 1150,013(40) (2012)
- [5] Adams, R.A., Fournier, J.J.F.: Sobolev spaces, *Pure and Applied Mathematics (Amsterdam)*, vol. 140, second edn. Elsevier/Academic Press, Amsterdam (2003)
- [6] Aland, S., Voigt, A.: Benchmark computations of diffuse interface models for two-dimensional bubble dynamics. *International Journal for Numerical Methods in Fluids* **69**, 747–761 (2012)
- [7] Alikakos, N.D., Bates, P.W., Chen, X.: Convergence of the Cahn-Hilliard equation to the Hele-Shaw model. *Arch. Rational Mech. Anal.* **128**(2), 165–205 (1994). DOI 10.1007/BF00375025. URL <https://doi.org/10.1007/BF00375025>
- [8] Angenent, S., Gurtin, M.E.: Multiphase thermomechanics with interfacial structure. II. Evolution of an isothermal interface. *Arch. Rational Mech. Anal.* **108**(4), 323–391 (1989). DOI 10.1007/BF01041068. URL <https://doi.org/10.1007/BF01041068>
- [9] Antil, H., Hintermüller, M., Nochetto, R., Surowiec, T., Wegner, D.: Finite horizon model predictive control of electrowetting on dielectric with pinning. *Interfaces Free Bound.* **19**(1), 1–30 (2017). DOI 10.4171/IFB/375. URL <https://doi.org/10.4171/IFB/375>
- [10] Antil, H., Nochetto, R., Sodr e, P.: Optimal control of a free boundary problem with surface tension effects: A priori error analysis. *arXiv preprint arXiv:1402.5709* (2014)
- [11] Antil, H., Nochetto, R.H., Sodr e, P.: Optimal control of a free boundary problem: analysis with second-order sufficient conditions. *SIAM J. Control Optim.* **52**(5), 2771–2799 (2014). DOI 10.1137/120893306. URL <http://dx.doi.org/10.1137/120893306>
- [12] Aubin, J.P.: Applied functional analysis. John Wiley & Sons, New York-Chichester-Brisbane (1979). Translated from the French by Carole Labrousse, With exercises by Bernard Cornet and Jean-Michel Lasry
- [13] Barbu, V.: Optimal control of variational inequalities, *Research Notes in Mathematics*, vol. 100. Pitman (Advanced Publishing Program), Boston, MA (1984)

- [14] Barbu, V.: Analysis and control of nonlinear infinite-dimensional systems, *Mathematics in Science and Engineering*, vol. 190. Academic Press, Inc., Boston, MA (1993)
- [15] Bañas, L., Nürnberg, R.: Adaptive finite element methods for Cahn–Hilliard equations. *Journal of Computational and Applied Mathematics* **218**, 2–11 (2008)
- [16] Bañas, L., Nürnberg, R.: A posteriori estimates for the Cahn–Hilliard equation. *Mathematical Modelling and Numerical Analysis* **43**(5), 1003–1026 (2009)
- [17] Becker, R., Kapp, H., Rannacher, R.: Adaptive finite element methods for optimal control of partial differential equations: basic concept. *SIAM J. Control Optim.* **39**(1), 113–132 (electronic) (2000). DOI 10.1137/S0363012999351097. URL <http://dx.doi.org/10.1137/S0363012999351097>
- [18] Becker, R., Kapp, H., Rannacher, R.: Adaptive finite element methods for optimization problems. In: Numerical analysis 1999 (Dundee), *Chapman & Hall/CRC Res. Notes Math.*, vol. 420, pp. 21–42. Chapman & Hall/CRC, Boca Raton, FL (2000)
- [19] Bellettini, G., Paolini, M.: Anisotropic motion by mean curvature in the context of Finsler geometry. *Hokkaido Math. J.* **25**(3), 537–566 (1996). DOI 10.14492/hokmj/1351516749. URL <https://doi.org/10.14492/hokmj/1351516749>
- [20] Benedix, O., Vexler, B.: A posteriori error estimation and adaptivity for elliptic optimal control problems with state constraints. *Comput. Optim. Appl.* **44**(1), 3–25 (2009). DOI 10.1007/s10589-008-9200-y. URL <http://dx.doi.org/10.1007/s10589-008-9200-y>
- [21] Bergounioux, M.: Optimal control of an obstacle problem. *Appl. Math. Optim.* **36**(2), 147–172 (1997). DOI 10.1007/s002459900058. URL <http://dx.doi.org/10.1007/s002459900058>
- [22] Bergounioux, M., Dietrich, H.: Optimal control of problems governed by obstacle type variational inequalities: a dual regularization-penalization approach. *J. Convex Anal.* **5**(2), 329–351 (1998)
- [23] Blank, L., Butz, M., Garcke, H.: Solving the Cahn–Hilliard variational inequality with a semi-smooth Newton method. *ESAIM: Control, Optimisation and Calculus of Variations* **17**(4), 931–954 (2011)
- [24] Blank, L., Farshbaf-Shaker, M., Garcke, H., Rupprecht, C., Styles, V.: Multi-material phase field approach to structural topology optimization. In: G. Leugering, P. Benner, S. Engell, A. Griewank, H. Harbrecht, M. Hinze, R. Rannacher, S. Ulbrich (eds.) *Trends in PDE Constrained Optimization, International Series of Numerical Mathematics*, vol. 165. Birkhäuser Verlag (2015)
- [25] Blowey, J.F., Elliott, C.M.: The Cahn–Hilliard gradient theory for phase separation with non-smooth free energy. I. Mathematical analysis. *European J. Appl. Math.* **2**(3), 233–280 (1991). DOI 10.1017/S095679250000053X. URL <https://doi.org/10.1017/S095679250000053X>
- [26] Boyer, F.: A theoretical and numerical model for the study of incompressible mixture flows. *Computers & fluids* **31**(1), 41–68 (2002)
- [27] Boyer, F., Lapuerta, C., Minjeaud, S., Piar, B., Quintard, M.: Cahn–Hilliard/Navier–Stokes model for the simulation of three-phase flows. *Transport in Porous Media* **82**(3), 463–483 (2010)
- [28] Bronsard, L., Kohn, R.V.: Motion by mean curvature as the singular limit of Ginzburg–Landau dynamics. *J. Differential Equations* **90**(2), 211–237 (1991). DOI 10.1016/0022-0396(91)90147-2. URL [https://doi.org/10.1016/0022-0396\(91\)90147-2](https://doi.org/10.1016/0022-0396(91)90147-2)

- [29] Browder, F.E.: Nonlinear variational inequalities and maximal monotone mappings in banach spaces. *Mathematische Annalen* **183**(3), 213–231 (1969). DOI 10.1007/BF01351381. URL <http://dx.doi.org/10.1007/BF01351381>
- [30] C. Brett C. M. Elliott, M.H., Löbhard, C.: Mesh adaptivity in optimal control of elliptic variational inequalities with point-tracking of the state. *Interfaces Free Bound.* **17**(1), 21–53 (2015). DOI 10.4171/IFB/332. URL <http://dx.doi.org/10.4171/IFB/332>
- [31] Caffarelli, L., Salsa, S.: A geometric approach to free boundary problems, *Graduate Studies in Mathematics*, vol. 68. American Mathematical Society, Providence, RI (2005). DOI 10.1090/gsm/068. URL <https://doi.org/10.1090/gsm/068>
- [32] Cahn, J.W., Hilliard, J.E.: Free energy of a nonuniform system. I. Interfacial free energy. *The Journal of chemical physics* **28**(2), 258–267 (1958)
- [33] Carstensen, C.: Quasi-interpolation and a-posteriori error analysis in finite element methods. *Mathematical Modelling and Numerical Analysis* **33**(6), 1187–1202 (1999)
- [34] Chen, X.: Generation and propagation of interfaces for reaction-diffusion equations. *J. Differential Equations* **96**(1), 116–141 (1992). DOI 10.1016/0022-0396(92)90146-E. URL [https://doi.org/10.1016/0022-0396\(92\)90146-E](https://doi.org/10.1016/0022-0396(92)90146-E)
- [35] Chen, X.: Global asymptotic limit of solutions of the Cahn-Hilliard equation. *J. Differential Geom.* **44**(2), 262–311 (1996). URL <http://projecteuclid.org/euclid.jdg/1214458973>
- [36] Chen, X., Elliott, C.M.: Asymptotics for a parabolic double obstacle problem. *Proc. Roy. Soc. London Ser. A* **444**(1922), 429–445 (1994). DOI 10.1098/rspa.1994.0030. URL <https://doi.org/10.1098/rspa.1994.0030>
- [37] Cho, S.K., Moon, H., Kim, C.J.: Creating, transporting, cutting, and merging liquid droplets by electrowetting-based actuation for digital microfluidic circuits. *Microelectromechanical Systems, Journal of* **12**(1), 70–80 (2003). DOI 10.1109/JMEMS.2002.807467
- [38] Cohen, D.S., Murray, J.D.: A generalized diffusion model for growth and dispersal in a population. *J. Math. Biol.* **12**(2), 237–249 (1981). DOI 10.1007/BF00276132. URL <https://doi.org/10.1007/BF00276132>
- [39] Colli, P., Farshbaf-Shaker, M.H., Gilardi, G., Sprekels, J.: Optimal boundary control of a viscous Cahn-Hilliard system with dynamic boundary condition and double obstacle potentials. *SIAM J. Control Optim.* **53**(4), 2696–2721 (2015). DOI 10.1137/140984749. URL <http://dx.doi.org/10.1137/140984749>
- [40] Colli, P., Gilardi, G., Sprekels, J.: A boundary control problem for the viscous cahn–hilliard equation with dynamic boundary conditions. *Applied Mathematics & Optimization* **73**(2), 195–225 (2016). DOI 10.1007/s00245-015-9299-z. URL <http://dx.doi.org/10.1007/s00245-015-9299-z>
- [41] Crank, J.: Free and moving boundary problems. The Clarendon Press, Oxford University Press, New York (1987)
- [42] Croft, W., Elliott, C.M., Ladds, G., Stinner, B., Venkataraman, C., Weston, C.: Parameter identification problems in the modelling of cell motility. arXiv preprint arXiv:1311.7602 (2013). URL <http://arxiv.org/pdf/1311.7602.pdf>
- [43] Dal, M.G., et al.: An introduction to γ -convergence. *Progress in Nonlinear Differential Equations and their Applications* **8** (1993)
- [44] De Mottoni, P., Schatzman, M.: Geometrical evolution of developed interfaces. *Transactions of the American Mathematical Society* **347**(5), 1533–1589 (1995)

- [45] Deckelnick, K., Elliott, C.M., Styles, V.: Optimal control of the propagation of a graph in inhomogeneous media. *SIAM J. Control Optim.* **48**(3), 1335–1352 (2009)
- [46] Deckelnick, K., Günther, A., Hinze, M.: Finite element approximation of elliptic control problems with constraints on the gradient. *Numer. Math.* **111**(3), 335–350 (2009). DOI 10.1007/s00211-008-0185-3. URL <http://dx.doi.org/10.1007/s00211-008-0185-3>
- [47] Delfour, M.C., Zolésio, J.P.: Shapes and geometries, *Advances in Design and Control*, vol. 22, second edn. Society for Industrial and Applied Mathematics (SIAM), Philadelphia, PA (2011). DOI 10.1137/1.9780898719826. URL <http://dx.doi.org/10.1137/1.9780898719826>. Metrics, analysis, differential calculus, and optimization
- [48] Ding, H., Spelt, P.D., Shu, C.: Diffuse interface model for incompressible two-phase flows with large density ratios. *Journal of Computational Physics* **226**(2), 2078–2095 (2007)
- [49] Ekeland, I., Témam, R.: Convex analysis and variational problems, *Classics in Applied Mathematics*, vol. 28, english edn. Society for Industrial and Applied Mathematics (SIAM), Philadelphia, PA (1999). DOI 10.1137/1.9781611971088. URL <http://dx.doi.org/10.1137/1.9781611971088>. Translated from the French
- [50] Elliott, C., Stinner, B., Styles, V., Welford, R.: Numerical computation of advection and diffusion on evolving diffuse interfaces. *IMA Journal of Numerical Analysis* **31**(3), 786–812 (2011)
- [51] Elliott, C.M., Garcke, H.: On the Cahn-Hilliard equation with degenerate mobility. *SIAM J. Math. Anal.* **27**(2), 404–423 (1996). DOI 10.1137/S0036141094267662. URL <https://doi.org/10.1137/S0036141094267662>
- [52] Elliott, C.M., Songmu, Z.: On the Cahn-Hilliard equation. *Arch. Rational Mech. Anal.* **96**(4), 339–357 (1986). DOI 10.1007/BF00251803. URL <http://dx.doi.org/10.1007/BF00251803>
- [53] Ern, A., Guermond, J.L.: Theory and practice of finite elements, *Applied Mathematical Sciences*, vol. 159. Springer-Verlag, New York (2004). DOI 10.1007/978-1-4757-4355-5. URL <http://dx.doi.org/10.1007/978-1-4757-4355-5>
- [54] Evans, L.C., Soner, H.M., Souganidis, P.E.: Phase transitions and generalized motion by mean curvature. *Comm. Pure Appl. Math.* **45**(9), 1097–1123 (1992). DOI 10.1002/cpa.3160450903. URL <https://doi.org/10.1002/cpa.3160450903>
- [55] Fife, P.C.: Models for phase separation and their mathematics. *Electron. J. Differential Equations* pp. No. 48, 26 (2000)
- [56] Friedman, A.: Variational principles and free-boundary problems. *Pure and Applied Mathematics*. John Wiley & Sons, Inc., New York (1982). A Wiley-Interscience Publication
- [57] Friedman, A.: Optimal control for variational inequalities. *SIAM J. Control Optim.* **24**(3), 439–451 (1986). DOI 10.1137/0324025. URL <http://dx.doi.org/10.1137/0324025>
- [58] Frigeri, S., Gal, C.G., Grasselli, M., Sprekels, J.: Two-dimensional nonlocal Cahn-Hilliard-Navier-Stokes systems with variable viscosity, degenerate mobility and singular potential. *Nonlinearity* **32**(2), 678–727 (2019). DOI 10.1088/1361-6544/aaedd0. URL <https://doi.org/10.1088/1361-6544/aaedd0>
- [59] Frigeri, S., Rocca, E., Sprekels, J.: Optimal distributed control of a nonlocal Cahn-Hilliard/Navier-Stokes system in two dimensions. *SIAM J. Control Optim.* **54**(1), 221–250 (2016). DOI 10.1137/140994800. URL <http://dx.doi.org/10.1137/140994800>

- [60] Garcia, C.E., Prett, D.M., Morari, M.: Model predictive control: Theory and practice—a survey. *Automatica* **25**(3), 335–348 (1989). DOI 10.1016/0005-1098(89)90002-2. URL [http://dx.doi.org/10.1016/0005-1098\(89\)90002-2](http://dx.doi.org/10.1016/0005-1098(89)90002-2)
- [61] Garcke, H., Hecht, C., Hinze, M., Kahle, C.: Numerical approximation of phase field based shape and topology optimization for fluids. *SIAM Journal on Scientific Computing* **37**(4), 1846–1871 (2015)
- [62] Garcke, H., Hinze, M., Kahle, C.: A stable and linear time discretization for a thermodynamically consistent model for two-phase incompressible flow. *Applied Numerical Mathematics* **99**, 151–171 (2016)
- [63] Garcke, H., Lam, K.F., Stinner, B.: Diffuse interface modelling of soluble surfactants in two-phase flow. *Communications in Mathematical Sciences* **12**(8), 1475–1522 (2014)
- [64] Giga, Y.: Surface evolution equations, *Monographs in Mathematics*, vol. 99. Birkhäuser Verlag, Basel (2006). A level set approach
- [65] Girault, V., Raviart, P.A.: Finite element methods for Navier-Stokes equations, *Springer Series in Computational Mathematics*, vol. 5. Springer-Verlag, Berlin (1986). DOI 10.1007/978-3-642-61623-5. URL <http://dx.doi.org/10.1007/978-3-642-61623-5>. Theory and algorithms
- [66] Gong, J., Fan, S.K., Kim, C.: Portable digital microfluidics platform with active but disposable lab-on-chip. In: Micro Electro Mechanical Systems, 2004. 17th IEEE International Conference on. (MEMS), pp. 355–358 (2004). DOI 10.1109/MEMS.2004.1290595
- [67] Grün, G.: On convergent schemes for diffuse interface models for two-phase flow of incompressible fluids with general mass densities. *SIAM Journal on Numerical Analysis* **51**(6), 3036–3061 (2013)
- [68] Grün, G., Klingbeil, F.: Two-phase flow with mass density contrast: Stable schemes for a thermodynamic consistent and frame indifferent diffuse interface model. *Journal of Computational Physics* **257**(A), 708–725 (2014)
- [69] Guillén-González, F., Tierra, G.: Splitting schemes for a Navier–Stokes–Cahn–Hilliard model for two fluids with different densities. *Journal of Computational Mathematics* **32**(6), 643–664 (2014)
- [70] Günther, A., Hinze, M.: Elliptic control problems with gradient constraints—variational discrete versus piecewise constant controls. *Comput. Optim. Appl.* **49**(3), 549–566 (2011). DOI 10.1007/s10589-009-9308-8. URL <http://dx.doi.org/10.1007/s10589-009-9308-8>
- [71] Gurtin, M.E., Polignone, D., Viñals, J.: Two-phase binary fluids and immiscible fluids described by an order parameter. *Math. Models Methods Appl. Sci.* **6**(6), 815–831 (1996). DOI 10.1142/S0218202596000341. URL <https://doi.org/10.1142/S0218202596000341>
- [72] Heikenfeld, J., Zhou, K., Kreit, E., Raj, B., Yang, S., Sun, B., Milarcik, A., Clapp, L., Schwartz, R.: Electrofluidic displays using Young-Laplace transposition of brilliant pigment dispersions. *Nat Photon* **3**(5), 292–296 (2009)
- [73] Héron, B.: Quelques propriétés des applications de trace dans des espaces de champs de vecteurs à divergence nulle. *Comm. Partial Differential Equations* **6**(12), 1301–1334 (1981). DOI 10.1080/03605308108820212. URL <http://dx.doi.org/10.1080/03605308108820212>
- [74] Hildebrandt, S.: Free boundary problems for minimal surfaces and related questions. *Comm. Pure Appl. Math.* **39**(S, suppl.), S111–S138 (1986). DOI 10.1002/cpa.3160390708. URL <https://doi.org/10.1002/cpa.3160390708>. *Frontiers of the mathematical sciences: 1985* (New York, 1985)

- [75] Hintermüller, M., Hinze, H., Kahle, C., Keil, T.: A goal-oriented dual-weighted adaptive finite elements approach for the optimal control of a Cahn-Hilliard-Navier-Stokes system. in preparation (2016)
- [76] Hintermüller, M., Hinze, M., Hoppe, R.H.: Weak-duality based adaptive finite element methods for pde-constrained optimization with pointwise gradient state-constraints. *J. Comput. Math* **30**(2), 101–123 (2012)
- [77] Hintermüller, M., Hinze, M., Kahle, C.: An adaptive finite element Moreau–Yosida-based solver for a coupled Cahn–Hilliard/Navier–Stokes system. *Journal of Computational Physics* **235**, 810–827 (2013)
- [78] Hintermüller, M., Hinze, M., Tber, M.H.: An adaptive finite-element Moreau-Yosida-based solver for a non-smooth Cahn-Hilliard problem. *Optim. Methods Softw.* **26**(4-5), 777–811 (2011). DOI 10.1080/10556788.2010.549230. URL <http://dx.doi.org/10.1080/10556788.2010.549230>
- [79] Hintermüller, M., Hoppe, R.H., Iliash, Y., Kieweg, M.: An a posteriori error analysis of adaptive finite element methods for distributed elliptic control problems with control constraints. *ESAIM: Control, Optimisation and Calculus of Variations* **14**(3), 540–560 (2008)
- [80] Hintermüller, M., Hoppe, R.H.W.: Goal-oriented adaptivity in control constrained optimal control of partial differential equations. *SIAM J. Control Optim.* **47**(4), 1721–1743 (2008). DOI 10.1137/070683891. URL <http://dx.doi.org/10.1137/070683891>
- [81] Hintermüller, M., Hoppe, R.H.W.: Goal-oriented adaptivity in pointwise state constrained optimal control of partial differential equations. *SIAM J. Control Optim.* **48**(8), 5468–5487 (2010). DOI 10.1137/090761823. URL <http://dx.doi.org/10.1137/090761823>
- [82] Hintermüller, M., Hoppe, R.H.W., Löbhard, C.: Dual-weighted goal-oriented adaptive finite elements for optimal control of elliptic variational inequalities. *ESAIM Control Optim. Calc. Var.* **20**(2), 524–546 (2014). DOI 10.1051/cocv/2013074. URL <http://dx.doi.org/10.1051/cocv/2013074>
- [83] Hintermüller, M., Keil, T., Wegner, D.: Optimal control of a semidiscrete Cahn-Hilliard-Navier-Stokes system with nonmatched fluid densities. *SIAM J. Control Optim.* **55**(3), 1954–1989 (2017). DOI 10.1137/15M1025128. URL <http://dx.doi.org/10.1137/15M1025128>
- [84] Hintermüller, M., Kopacka, I.: Mathematical programs with complementarity constraints in function space: C - and strong stationarity and a path-following algorithm. *SIAM J. Optim.* **20**(2), 868–902 (2009). DOI 10.1137/080720681. URL <http://dx.doi.org/10.1137/080720681>
- [85] Hintermüller, M., Kopacka, I.: A smooth penalty approach and a nonlinear multi-grid algorithm for elliptic MPECs. *Comput. Optim. Appl.* **50**(1), 111–145 (2011). DOI 10.1007/s10589-009-9307-9. URL <https://doi.org/10.1007/s10589-009-9307-9>
- [86] Hintermüller, M., Laurain, A.: A shape and topology optimization technique for solving a class of linear complementarity problems in function space. *Comput. Optim. Appl.* **46**(3), 535–569 (2010). DOI 10.1007/s10589-008-9201-x. URL <http://dx.doi.org/10.1007/s10589-008-9201-x>
- [87] Hintermüller, M., Laurain, A.: Optimal shape design subject to elliptic variational inequalities. *SIAM J. Control Optim.* **49**(3), 1015–1047 (2011). DOI 10.1137/080745134. URL <http://dx.doi.org/10.1137/080745134>

- [88] Hintermüller, M., Mordukhovich, B.S., Surowiec, T.M.: Several approaches for the derivation of stationarity conditions for elliptic MPECs with upper-level control constraints. *Math. Program.* **146**(1-2, Ser. A), 555–582 (2014). DOI 10.1007/s10107-013-0704-6. URL <http://dx.doi.org/10.1007/s10107-013-0704-6>
- [89] Hintermüller, M., Ring, W.: A level set approach for the solution of a state-constrained optimal control problem. *Numerische Mathematik* **98**(1), 135–166 (2004). DOI 10.1007/s00211-004-0531-z. URL <http://dx.doi.org/10.1007/s00211-004-0531-z>
- [90] Hintermüller, M., Surowiec, T.: A bundle-free implicit programming approach for a class of elliptic MPECs in function space. *Mathematical Programming* **160**(1), 271–305 (2016). DOI 10.1007/s10107-016-0983-9. URL <http://dx.doi.org/10.1007/s10107-016-0983-9>
- [91] Hintermüller, M., Wegner, D.: Distributed optimal control of the Cahn-Hilliard system including the case of a double-obstacle homogeneous free energy density. *SIAM J. Control Optim.* **50**(1), 388–418 (2012). DOI 10.1137/110824152. URL <http://dx.doi.org/10.1137/110824152>
- [92] Hintermüller, M., Wegner, D.: Optimal control of a semidiscrete Cahn-Hilliard-Navier-Stokes system. *SIAM J. Control Optim.* **52**(1), 747–772 (2014). DOI 10.1137/120865628. URL <http://dx.doi.org/10.1137/120865628>
- [93] Hintermüller, M., Wegner, D.: Distributed and boundary control problems for the semidiscrete Cahn-Hilliard/Navier-Stokes system with nonsmooth Ginzburg-Landau energies. In: U. Langer, H. Albrecher, H. Engl, R. Hoppe, K. Kunisch, H. Niederreiter, C. Schmeisser (eds.) *Topological Optimization and Optimal Transport, Radon Series on Computational and Applied Mathematics*, vol. 17. De Gruyter (2017)
- [94] Hinze, M., Ziegenbalg, S.: Optimal control of the free boundary in a two-phase Stefan problem. *J. Comput. Phys.* **223**(2), 657–684 (2007). DOI 10.1016/j.jcp.2006.09.030. URL <http://dx.doi.org/10.1016/j.jcp.2006.09.030>
- [95] Hinze, M., Ziegenbalg, S.: Optimal control of the free boundary in a two-phase Stefan problem with flow driven by convection. *ZAMM Z. Angew. Math. Mech.* **87**(6), 430–448 (2007). DOI 10.1002/zamm.200610326. URL <http://dx.doi.org/10.1002/zamm.200610326>
- [96] Hohenberg, P.C., Halperin, B.I.: Theory of dynamic critical phenomena. *Reviews of Modern Physics* **49**(3), 435 (1977)
- [97] Hysing, S., Turek, S., Kuzmin, D., Parolini, N., Burman, E., Ganesan, S., Tobiska, L.: Quantitative benchmark computations of two-dimensional bubble dynamics. *International Journal for Numerical Methods in Fluids* **60**(11), 1259–1288 (2009). DOI 10.1002/flid.1934. URL <http://onlinelibrary.wiley.com/doi/10.1002/flid.1934/abstract>
- [98] Ito, K., Kunisch, K.: Optimal control of elliptic variational inequalities. *Appl. Math. Optim.* **41**(3), 343–364 (2000). DOI 10.1007/s002459911017. URL <http://dx.doi.org/10.1007/s002459911017>
- [99] Kay, D., Styles, V., Welford, R.: Finite element approximation of a Cahn-Hilliard-Navier-Stokes system. *Interfaces and Free Boundaries* **10**(1), 15–43 (2008). URL http://www.ems-ph.org/journals/show_issue.php?issn=1463-9963&vol=10&iss=1
- [100] Kinderlehrer, D., Stampacchia, G.: An introduction to variational inequalities and their applications, *Classics in Applied Mathematics*, vol. 31. Society for Industrial and Applied Math-

- ematics (SIAM), Philadelphia, PA (2000). DOI 10.1137/1.9780898719451. URL <http://dx.doi.org/10.1137/1.9780898719451>. Reprint of the 1980 original
- [101] Krumbiegel, K., Rösch, A.: A virtual control concept for state constrained optimal control problems. *Comput. Optim. Appl.* **43**(2), 213–233 (2009). DOI 10.1007/s10589-007-9130-0. URL <http://dx.doi.org/10.1007/s10589-007-9130-0>
- [102] Laurain, A., Walker, S.W.: Droplet footprint control. *SIAM Journal on Control and Optimization* **53**(2), 771–799 (2015). DOI 10.1137/140979721. URL <http://dx.doi.org/10.1137/140979721>
- [103] Ling, K., Tao, W.Q.: A sharp-interface model coupling VOSET and IBM for simulations on melting and solidification. *Comput. & Fluids* **178**, 113–131 (2019). DOI 10.1016/j.compfluid.2018.08.027. URL <https://doi.org/10.1016/j.compfluid.2018.08.027>
- [104] Lowengrub, J., Truskinovsky, L.: Quasi-incompressible Cahn-Hilliard fluids and topological transitions. *R. Soc. Lond. Proc. Ser. A Math. Phys. Eng. Sci.* **454**(1978), 2617–2654 (1998). DOI 10.1098/rspa.1998.0273. URL <http://dx.doi.org/10.1098/rspa.1998.0273>
- [105] Luo, Z.Q., Pang, J.S., Ralph, D.: *Mathematical programs with equilibrium constraints*. Cambridge University Press, Cambridge (1996). DOI 10.1017/CBO9780511983658. URL <http://dx.doi.org/10.1017/CBO9780511983658>
- [106] Mignot, F.: Contrôle dans les inéquations variationnelles elliptiques. *J. Functional Analysis* **22**(2), 130–185 (1976)
- [107] Mignot, F., Puel, J.P.: Optimal control in some variational inequalities. *SIAM J. Control Optim.* **22**(3), 466–476 (1984). DOI 10.1137/0322028. URL <http://dx.doi.org/10.1137/0322028>
- [108] Minty, G.J.: On a “monotonicity” method for the solution of non-linear equations in Banach spaces. *Proc. Nat. Acad. Sci. U.S.A.* **50**, 1038–1041 (1963)
- [109] Modica, L.: The gradient theory of phase transitions and the minimal interface criterion. *Arch. Rational Mech. Anal.* **98**(2), 123–142 (1987). DOI 10.1007/BF00251230. URL <https://doi.org/10.1007/BF00251230>
- [110] Moubachir, M., Zolésio, J.P.: *Moving shape analysis and control, Pure and Applied Mathematics (Boca Raton)*, vol. 277. Chapman & Hall/CRC, Boca Raton, FL (2006). DOI 10.1201/9781420003246. URL <http://dx.doi.org/10.1201/9781420003246>. Applications to fluid structure interactions
- [111] Nielsen, C.P., Bruus, H.: Sharp-interface model of electrodeposition and ramified growth. *Phys. Rev. E* (3) **92**(4), 042303, 15 (2015). DOI 10.1103/PhysRevE.92.042302. URL <https://doi.org/10.1103/PhysRevE.92.042302>
- [112] Nochetto, R.H., Paolini, M., Verdi, C.: Optimal interface error estimates for the mean curvature flow. *Ann. Scuola Norm. Sup. Pisa Cl. Sci. (4)* **21**(2), 193–212 (1994). URL http://www.numdam.org/item?id=ASNSP_1994_4_21_2_193_0
- [113] Nochetto, R.H., Verdi, C.: Combined effect of explicit time-stepping and quadrature for curvature driven flows. *Numer. Math.* **74**(1), 105–136 (1996). DOI 10.1007/s002110050210. URL <https://doi.org/10.1007/s002110050210>
- [114] Novick-Cohen, A., Segel, L.A.: Nonlinear aspects of the Cahn-Hilliard equation. *Phys. D* **10**(3), 277–298 (1984). DOI 10.1016/0167-2789(84)90180-5. URL [https://doi.org/10.1016/0167-2789\(84\)90180-5](https://doi.org/10.1016/0167-2789(84)90180-5)
- [115] Oono, Y., Puri, S.: Study of phase-separation dynamics by use of cell dynamical systems. *I. Modeling. Physical Review A* **38**(1), 434–463 (1988)

- [116] Oono, Y., Puri, S.: Study of phase-separation dynamics by use of cell dynamical systems. II. Two-dimensional demonstrations. *Physical Review A* **38**(3), 1542 (1988)
- [117] Outrata, J., Kočvara, M., Zowe, J.: Nonsmooth approach to optimization problems with equilibrium constraints, *Nonconvex Optimization and its Applications*, vol. 28. Kluwer Academic Publishers, Dordrecht (1998). DOI 10.1007/978-1-4757-2825-5. URL <http://dx.doi.org/10.1007/978-1-4757-2825-5>. Theory, applications and numerical results
- [118] Pego, R.L.: Front migration in the nonlinear Cahn-Hilliard equation. *Proc. Roy. Soc. London Ser. A* **422**(1863), 261–278 (1989)
- [119] Prüss, J., Racke, R., Zheng, S.: Maximal regularity and asymptotic behavior of solutions for the Cahn-Hilliard equation with dynamic boundary conditions. *Ann. Mat. Pura Appl.* (4) **185**(4), 627–648 (2006). DOI 10.1007/s10231-005-0175-3. URL <https://doi.org/10.1007/s10231-005-0175-3>
- [120] Rockafellar, R.T.: On the maximal monotonicity of subdifferential mappings. *Pacific J. Math.* **33**, 209–216 (1970)
- [121] Rockafellar, R.T.: On the maximality of sums of nonlinear monotone operators. *Trans. Amer. Math. Soc.* **149**, 75–88 (1970)
- [122] Rockafellar, R.T.: Conjugate duality and optimization. Society for Industrial and Applied Mathematics, Philadelphia, Pa. (1974). Lectures given at the Johns Hopkins University, Baltimore, Md., June, 1973, Conference Board of the Mathematical Sciences Regional Conference Series in Applied Mathematics, No. 16
- [123] Rubenštejn, L.I.: The Stefan problem. American Mathematical Society, Providence, R.I. (1971). Translated from the Russian by A. D. Solomon, *Translations of Mathematical Monographs*, Vol. 27
- [124] Rubinstein, J., Sternberg, P., Keller, J.B.: Fast reaction, slow diffusion, and curve shortening. *SIAM J. Appl. Math.* **49**(1), 116–133 (1989). DOI 10.1137/0149007. URL <https://doi.org/10.1137/0149007>
- [125] Saguez, C.: Optimal control of free boundary problems. In: System modelling and optimization (Budapest, 1985), *Lecture Notes in Control and Inform. Sci.*, vol. 84, pp. 776–788. Springer, Berlin (1986). DOI 10.1007/BFb0043905. URL <http://dx.doi.org/10.1007/BFb0043905>
- [126] Satoh, W., Loughran, M., Suzuki, H.: Microfluidic transport based on direct electrowetting. *Journal of Applied Physics* **96**(1), 835–841 (2004)
- [127] Scheel, H., Scholtes, S.: Mathematical programs with complementarity constraints: stationarity, optimality, and sensitivity. *Math. Oper. Res.* **25**(1), 1–22 (2000). DOI 10.1287/moor.25.1.1.15213. URL <http://dx.doi.org/10.1287/moor.25.1.1.15213>
- [128] Schiela, A., Wachsmuth, D.: Convergence analysis of smoothing methods for optimal control of stationary variational inequalities with control constraints. *ESAIM Math. Model. Numer. Anal.* **47**(3), 771–787 (2013). DOI 10.1051/m2an/2012049. URL <https://doi.org/10.1051/m2an/2012049>
- [129] Sethian, J.A.: Level set methods and fast marching methods, *Cambridge Monographs on Applied and Computational Mathematics*, vol. 3, second edn. Cambridge University Press, Cambridge (1999). Evolving interfaces in computational geometry, fluid mechanics, computer vision, and materials science
- [130] Shapiro, B., Moon, H., Garrell, R.L., Kim, C.J.: Equilibrium behavior of sessile drops under surface tension, applied external fields, and material variations. *Journal of Applied Physics* **93**(9), 5794–5811 (2003)

- [131] Smolders, C., Van Aartsen, J., Steenbergen, A.: Liquid-liquid phase separation in concentrated solutions of non-crystallizable polymers by spinodal decomposition. *Kolloid-Zeitschrift und Zeitschrift für Polymere* **243**(1), 14–20 (1971)
- [132] Stauffer, D.: Application of the generalized Landau ansatz to second order phase transitions. *Zeitschrift für Physik A Hadrons and nuclei* **221**(2), 122–133 (1969)
- [133] Stoth, B.E.E.: Convergence of the Cahn-Hilliard equation to the Mullins-Sekerka problem in spherical symmetry. *J. Differential Equations* **125**(1), 154–183 (1996). DOI 10.1006/jdeq.1996.0028. URL <https://doi.org/10.1006/jdeq.1996.0028>
- [134] Sturm, K., Hintermüller, M., Hömberg, D.: Distortion compensation as a shape optimisation problem for a sharp interface model. *Comput. Optim. Appl.* **64**(2), 557–588 (2016). DOI 10.1007/s10589-015-9816-7. URL <https://doi.org/10.1007/s10589-015-9816-7>
- [135] Tachim Medjo, T.: Optimal control of a Cahn-Hilliard-Navier-Stokes model with state constraints. *J. Convex Anal.* **22**(4), 1135–1172 (2015)
- [136] Tayler, A.B.: *Mathematical models in applied mechanics*. Oxford Applied Mathematics and Computing Science Series. The Clarendon Press, Oxford University Press, New York (1986)
- [137] Temam, R.: *Navier-Stokes equations. Theory and numerical analysis*. North-Holland Publishing Co., Amsterdam-New York-Oxford (1977). *Studies in Mathematics and its Applications*, Vol. 2
- [138] Tiba, D.: Optimal control of nonsmooth distributed parameter systems, *Lecture Notes in Mathematics*, vol. 1459. Springer-Verlag, Berlin (1990). DOI 10.1007/BFb0085564. URL <http://dx.doi.org/10.1007/BFb0085564>
- [139] Verfürth, R.: A posteriori error analysis of space-time finite element discretizations of the time-dependent Stokes equations. *Calcolo* **47**(3), 149–167 (2010). DOI 10.1007/s10092-010-0018-5. URL <http://dx.doi.org/10.1007/s10092-010-0018-5>
- [140] Vexler, B., Wollner, W.: Adaptive finite elements for elliptic optimization problems with control constraints. *SIAM J. Control Optim.* **47**(1), 509–534 (2008). DOI 10.1137/070683416. URL <http://dx.doi.org/10.1137/070683416>
- [141] Visintin, A.: Models of phase transitions, *Progress in Nonlinear Differential Equations and their Applications*, vol. 28. Birkhäuser Boston, Inc., Boston, MA (1996). DOI 10.1007/978-1-4612-4078-5. URL <https://doi.org/10.1007/978-1-4612-4078-5>
- [142] Wachsmuth, G.: Towards M-stationarity for optimal control of the obstacle problem with control constraints. *SIAM J. Control Optim.* **54**(2), 964–986 (2016). DOI 10.1137/140980582. URL <http://dx.doi.org/10.1137/140980582>
- [143] Walker, S.W., Bonito, A., Nochetto, R.H.: Mixed finite element method for electrowetting on dielectric with contact line pinning. *Interfaces Free Bound.* **12**(1), 85–119 (2010). DOI 10.4171/IFB/228. URL <http://dx.doi.org/10.4171/IFB/228>
- [144] Walker, S.W., Shapiro, B., Nochetto, R.H.: Electrowetting with contact line pinning: Computational modeling and comparisons with experiments. *Physics of Fluids (1994-present)* **21**(10), 102,103 (2009)
- [145] Wang, Q.F., Nakagiri, S.I.: Weak solutions of Cahn-Hilliard equations having forcing terms and optimal control problems. *Sūrikaiseikikenkyūsho Kōkyūroku* (1128), 172–180 (2000). *Mathematical models in functional equations (Japanese)* (Kyoto, 1999)

- [146] Wheeler, A., Moon, H., Kim, C.J., Loo, J.A., Garrell, R.L.: Electrowetting-based microfluidics for analysis of peptides and proteins by matrix-assisted laser desorption/ionization mass spectrometry. *Anal. Chem.* **76**(16), 4833–4838 (2004)
- [147] Yong, J.M., Zheng, S.M.: Feedback stabilization and optimal control for the Cahn-Hilliard equation. *Nonlinear Anal.* **17**(5), 431–444 (1991). DOI 10.1016/0362-546X(91)90138-Q. URL [http://dx.doi.org/10.1016/0362-546X\(91\)90138-Q](http://dx.doi.org/10.1016/0362-546X(91)90138-Q)
- [148] Zeidler, E.: *Nonlinear functional analysis and its applications. II/B.* Springer-Verlag, New York (1990). DOI 10.1007/978-1-4612-0985-0. URL <http://dx.doi.org/10.1007/978-1-4612-0985-0>. *Nonlinear monotone operators*, Translated from the German by the author and Leo F. Boron
- [149] Zhao, Q.: A sharp-interface model and its numerical approximation for solid-state dewetting with axisymmetric geometry. *J. Comput. Appl. Math.* **361**, 144–156 (2019). DOI 10.1016/j.cam.2019.04.008. URL <https://doi.org/10.1016/j.cam.2019.04.008>
- [150] Zowe, J., Kurcyusz, S.: Regularity and stability for the mathematical programming problem in Banach spaces. *Appl. Math. Optim.* **5**(1), 49–62 (1979). DOI 10.1007/BF01442543. URL <http://dx.doi.org/10.1007/BF01442543>